



Doc n°: IA-RP-2000-4225-CNE

Issue: 1.0

Date: 2017-09-27

Sheet: 1 Of: 63



# **IASI QUARTERLY PERFORMANCE REPORT**

**FROM 2015/03/01 TO 2015/05/31**

-----

**BY IASI TEC (TECHNICAL EXPERTISE CENTER)**



**FOR IASI FM2 ON METOP A**

		Doc n°: IA-RP-2000-4225-CNE Issue: 1.0 Date: 2017-09-27 Sheet: 2 Of: 63
--	---	--

## ANALYSE DOCUMENTAIRE

### Bordereau d'indexation

<b>Classe (Confidentialité) :</b> NC		<b>Code Consultation :</b>	
<b>Mots clés d'auteur :</b> IASI TEC quarterly synthesis report			
<b>OBJET :</b>  <div style="text-align: center;">IASI TEC periodic report</div>			
<b>TITRE :</b>  <div style="text-align: center;">IASI quarterly performance report</div>			
<b>Auteur(s) :</b>  <div style="text-align: center;">           Claire Maraldi, Elsa Jacquette et Denis Jouglet (CNES)            avec le support de J-C Calvel (AKKA Technologies, marché ACIS 128780 )         </div>			
<b>RESUME :</b>  Quarterly report issued by the IASI TEC team to show trends and layout from the "long term synthesis" TEC function for flags and observables quality indicators			
<b>Document(s) rattaché(s) :</b> Ce document vit seul		<b>Localisation physique du document :</b> Salle IASI TEC	
<b>Volume :</b>  <div style="text-align: center;">1</div>	<b>Nombre de pages total :</b>  <div style="text-align: center;">63</div> <div style="margin-top: 10px;">           dont - liminaires : 7            annexes : 0         </div>	<b>Nombre d'annexes :</b>  <div style="text-align: center;">0</div>	<b>LANGUE :</b>  <div style="text-align: center;">English</div>
<b>Document géré en Configuration :</b>  <div style="text-align: center;">Non</div>		<b>A DATER DU :</b>	<b>RESPONSABLE :</b>
<b>Contrat :</b> Néant			
<b>SYSTEME HOTE : (logiciel + référence fichier) :</b>  <div style="text-align: center;">OpenOffice Writer 3.2</div>			

		Doc n°: IA-RP-2000-4225-CNE Issue: 1.0 Date: 2017-09-27 Sheet: 3 Of: 63
---	---	--

<b>DIFFUSION</b>
------------------



On CNES web site : <http://smc.cnes.fr/IASI>  
Instrument characteristics / In-orbit performances monitoring

<b>DOCUMENT MODEL CHANGE RECORD</b>
-------------------------------------

Version	Date	Paragraphs	Description
1.0	05/03/11		Creation of the model
2.0	01/01/15	4.3.2.5 4.8	Cube corner Speed Quality (CSQ) monitoring IASI-A inter-calibration with CRIS and AIRS



<b>DOCUMENT CHANGE RECORD</b>
-------------------------------

Version	Date	Paragraphs	Description
1.0	2017-09-27		Creation of the document

		Doc n°: IA-RP-2000-4225-CNE Issue: 1.0 Date: 2017-09-27 Sheet: 4 Of: 63
--	---	--

## Table of contents

<b>1 INTRODUCTION.....</b>	<b>9</b>
<b>2 RELATED DOCUMENTS.....</b>	<b>9</b>
2.1 APPLICABLE DOCUMENTS.....	9
2.2 REFERENCE DOCUMENTS.....	9
<b>3 SIGNIFICANT EVENTS.....</b>	<b>10</b>
3.1 EXTERNAL CALIBRATION.....	10
3.2 ON BOARD CONFIGURATION.....	10
3.3 GROUND CONFIGURATIONS UPDATES FOR LEVEL 1 PROCESSING.....	11
3.4 DATA BASES UPDATE FOR THE USERS.....	11
3.5 ON GROUND HW/SW EVOLUTION.....	12
3.6 DECONTAMINATION.....	12
3.7 INSTRUMENT.....	13
3.7.1 External events.....	13
3.7.2 Operation leading to mission outage.....	13
3.7.3 Anomaly leading to mission outage.....	13
<b>4 PERFORMANCE MONITORING.....</b>	<b>14</b>
4.1 PERFORMANCE MONITORING.....	14
4.2 PERFORMANCE SYNOPSIS.....	15
4.3 LEVEL 0 DATA QUALITY (L0).....	16
4.3.1 Overall quality.....	16
4.3.2 Main flag and quality indicator parameters.....	18
4.3.3 Second level flags and quality indicators.....	27
4.3.4 Conclusion.....	27
4.4 LEVEL 1 DATA QUALITY (L1).....	27
4.4.1 Overall quality.....	27
4.4.2 Main flag and quality indicator parameters.....	28
4.4.3 Conclusion.....	31
4.5 SOUNDER RADIOMETRIC PERFORMANCES.....	32
4.5.1 Radiometric Noise.....	32
4.5.2 Radiometric Calibration.....	33
4.5.3 Delay of detection chains.....	37
4.5.4 Optical Transmission.....	38
4.5.5 Interferometric Contrast.....	39
4.5.6 Interferogram baseline.....	40
4.5.7 Detection Chain.....	41
4.5.8 Conclusion.....	41
4.6 SOUNDER SPECTRAL PERFORMANCES.....	42
4.6.1 Monitoring of the ISRF inputs.....	42
4.6.2 Spectral calibration assessment.....	44
4.6.3 Ghost evolution monitoring.....	46
4.6.4 Conclusion.....	48
4.7 GEOMETRIC PERFORMANCES.....	49
4.7.1 Sounder / IIS co-registration monitoring.....	49
4.7.2 IIS / AVHRR co-registration.....	50

		Doc n°: IA-RP-2000-4225-CNE Issue: 1.0 Date: 2017-09-27 Sheet: 5 Of: 63
--	--	--

4.7.3 Conclusion.....	52
4.8 IASI-A INTER-CALIBRATION WITH CRIS AND AIRS.....	53
4.8.1 IASI-A inter-calibration with CRIS.....	53
4.8.2 IASI-A inter-calibration with AIRS.....	55
4.9 IIS RADIOMETRIC PERFORMANCES.....	57
4.9.1 IIS Radiometric Noise Monitoring.....	57
4.9.2 IIS Radiometric Calibration Monitoring.....	58
4.9.3 Conclusion.....	60
<b>5 IASI TEC SOFTWARE AND INTERFACES.....</b>	<b>61</b>
5.1 IASI TEC EVOLUTION.....	61
5.2 SIC EVOLUTION.....	61
5.3 EUMETCAST INTERFACE.....	62
5.4 FTP INTERFACE.....	62
<b>6 CONCLUSION AND OPERATIONS FORESEEN.....</b>	<b>63</b>
6.1 SUMMARY.....	63
6.2 SHORT-TERM EVENTS.....	63
6.3 OPERATIONS FORESEEN.....	63

## Figures and tables

Table 1: External Calibration TEC Requests.....	10
Table 2: DPS and MAS configuration TEC Requests.....	10
Table 3: DPS and MAS previous configuration.....	10
Table 4: IASI L1 Auxiliary File Configuration on the Operational EPS Ground Segment.....	11
Table 5: IASI L1 auxiliary file previous configuration.....	11
Table 6: IASI Data Bases for the users.....	11
Table 7: previous IASI Data Bases.....	12
Table 8: IASI L1 PPF Configuration on the Operational EPS Ground Segment.....	12
Table 9: Previous IASI L1 PPF.....	12
Table 10: Decontamination TEC Requests.....	12
Table 11: Previous decontamination.....	12
Table 12: Overview of METOP manoeuvres in the reporting period.....	13
Table 13: PL-SOL.....	13
Table 14: Scheduled interruptions.....	13
Table 15: Major anomalies.....	13
Table 16: Minor anomalies.....	13
Table 17: Functional status legend .....	14
Table 18: IASI product components functional status .....	15
Figure 1 : IASI L0 data quality orbit average (per pixel and CCD).....	16
Figure 2 : IASI L0 data quality spatial distribution (per pixel).....	17
Figure 3 : Temporal evolution of spikes anomaly ratio in % for all pixels (orbit average).....	18
Figure 4 : Geographical distribution of spikes occurrences in % for band 3 and all pixels.....	19
Figure 5 : Temporal evolution of NZPD determination anomaly ratio in % for all pixels (orbit average).....	20
Figure 6 : IASI NZPD determination quality flag spatial distribution (per pixel).....	21
Figure 7 : NZPD inter-pixel for all pixels and CCD calculated with respect to pixel 1 (orbit average).....	22
Figure 8 : IASI L0 over/under-flows orbit average of all pixels.....	23







		Doc n°: IA-RP-2000-4225-CNE Issue: 1.0 Date: 2017-09-27 Sheet: 6 Of: 63
--	--	--

Figure 9 : IASI Overflows and Underflows spatial distribution (per pixel).....	24
Figure 10 : Max of NZPD quality index for all pixels and CCD - BB.....	25
Figure 11 : Max of NZPD quality index for all pixels and CCD - CS.....	25
Figure 12 : Number of CSQ.....	26
Figure 14 : IASI product overall quality spatial distribution (per pixel).....	28
Figure 15 : GQisQualIndex average (L1 data quality index for IASI sounder).....	29
Figure 16 : GQisQualIndexIIS average (L1 data quality index for IASI Integrated Imager).....	29
Figure 17 : GQisQualIndexSpect average (L1 data index for spectral calibration quality).....	30
Figure 18 : GQisQualIndexRad average (L1 data index for radiometric calibration quality).....	30
Figure 19 : GQisQualIndexLoc average (L1 data index for ground localisation quality).....	31
Figure 20 : MDptPixQual average (L1 quality index for IASI integrated imager, fraction of not dead pixels).....	31
Figure 21 : Instrument noise evolution between start and end of the period.....	32
Figure 22 : Scan mirror reflectivity evolution.....	33
Figure 23 : Radiometric calibration error due to scan mirror reflectivity dependency with viewing angle Maximum effect on SN1 for different scene temperature. Done with the period May 2014 / May 2015.....	34
Figure 24 : Black Body Temperature.....	35
Figure 25 : Focal Plane Temperature.....	36
Figure 26 : Monitoring of detection chain maximum delays for all bands.....	37
Figure 27 : Ratio of calibration coefficient slopes as a function of wave number and time after the last decontamination.....	38
Figure 28 : Contrast Monitoring.....	39
Figure 29 : Monitoring of interferogram baseline.....	40
Figure 30 : Monitoring of detection chain margins.....	41
Figure 31 : GFaxAxeY average (Y filtered coordinates of sounder interferometric axis).....	42
Figure 32 : GFaxAxeZ average (Z filtered coordinates of sounder interferometric axis).....	43
Figure 33 : Cube Corner offset variation.....	43
Figure 34 : Optical bench Temperature.....	44
Figure 35 : Spectral shift error between L1C IASI and simulated L1C with A4/OP + ECMWF.....	45
Figure 36 : Inter pixel spectral shift error for L1C IASI.....	46
Figure 37 : Ghost amplitude as a function of wave number for different time (Top: pixel 2, bottom: pixel 4).....	48
Figure 38 : Temporal evolution of the IIS/sounder co-registration for each sounder pixel. The offsets are reported in radian, Y and Z define an orthogonal referential linked to IIS.....	50
Figure 39 : Column offset (black) guess vs. column offset averaged over all lines (LN) as a function of the scan position (SP=SN), and orbit number (across track IIS/AVHRR offset).....	51
Figure 40 : Line offset guess (black) vs. line offset averaged over all lines (LN) as a function of the scan position (SP=SN), and the orbit number (along track IIS/AVHRR offset).....	51
Figure 45 : Temporal evolution of the noise between start and end of the period.....	57
Figure 46 : Slope and offset coefficients matrix.....	58
Figure 47 : Relative evolution in % of average of slope (red curve) and offset (black curve) coefficients.....	59
Figure 48 : IIS Focal Plane Temperature.....	60
Table 19: IASI TEC at CNES Toulouse.....	61
Table 20: SIC at CNES Toulouse.....	61
Table 21: EUMETCAST configuration at CNES Toulouse.....	62

		Doc n°: IA-RP-2000-4225-CNE Issue: 1.0 Date: 2017-09-27 Sheet: 7 Of: 63
---	---	--



**LIST OF ACRONYMS**

4A/OP	Automatized Atmospheric Absorptions Atlas/ Operational
APO	Other Parameters OPS
AR	Anomaly Report
ASE	Acquisition Start End
AVHRR	Advanced Very High Resolution Radiometer
BB	Black Body
BRD	BoaRD configuration
CCFD	Cube Corner Functional Device
CCD	Cube Corner Direction
CCM	Cube Corner Mechanism
CD	Cube corner Compensation Device
CHART	Component Health Assessment and Reporting Tool
CGS	Core Ground Segment at EUMETSAT
CNES	Centre National d'Etudes Spatiales
CS	Cold Space
DA	Applicable document
DPS	Data Processing Subsystem
ECMWF	European Centre for Medium Range Weather Forecasts
EM	Engineering Model
EPS	EUMETSAT Polar System
EUMETSAT	European organisation for exploitation of METeorological SATellites
FM2 / FM3	Flight Model n°2 or 3
FOV	Field Of View
GRD	GRound configuration
IASI	Infrared Atmospheric Sounding Interferometer
IIS	Integrated Imaging Subsystem
IPSF	Instrument Point Spread Function
ISRF	Instrument Spectral Response Function
LFD	Locking Filtering Device
LN	Line Number
LSB	Least Significant Bit
METOP	METeorological OPERational satellite
MPF	Mission Planning Facility
NedT	Noise equivalent difference Temperature
NDVI	Normalized Difference Vegetation Index
NZPD	Number of Zero Path Difference
ODB	Operational Data Base
OPS	Operational Software
PC	Principal Component
PDD	Position Data Diagnostic

		Doc n°: IA-RP-2000-4225-CNE Issue: 1.0 Date: 2017-09-27 Sheet: 8 Of: 63
--	---	--

PDU	Product Dissemination Unit
PL SOL	PayLoad Switch Off-Line
PN	Pixel Number
PTSI	Parameter Table Status Identifier
RMS	Root Mean Square
RD	Reference Document
SAA	South Atlantic Anomaly
SEU	Single Event Upset
TEC	IASI Technical Centre of Expertise (located in CNES, Toulouse)
TIGR	Thermodynamic Initial Guess Retrieval data set
VDS	Verification Data Selection
ZPD	Zero Path Difference



		Doc n°: IA-RP-2000-4225-CNE Issue: 1.0 Date: 2017-09-27 Sheet: 9 Of: 63
--	---	--

## 1 INTRODUCTION

The IASI TEC is based at CNES Toulouse and is responsible for the monitoring of the IASI system performances, covering both instrument and level 1 processing sub-systems.

This document describes the activities and results obtained at the IASI TEC for instrument FM2 on METOP-A during the following period:

- Start Time: 2015/03/01                      Orbit: 43392
- End Time: 2015/05/31                      Orbit: 44698
- Duration: 3 months

Note that IASI ended the Calibration / Validation (commissioning) phase on July 2007.



## 2 RELATED DOCUMENTS

### 2.1 *APPLICABLE DOCUMENTS*

N°	Reference	Titre
DA.1	IA-SP-0000-3242-CNE	Spécification de suivi de la performance en vol de IASI sur METOP-A
DA.2	IA-DF-0000-4195-CNES	Spécification de l'outil d'inter-étalonnage SIC

### 2.2 *REFERENCE DOCUMENTS*

N°	Reference	Titre
RD.1	EUM/OPS-EPS/REP/08/0565	IASI annual in-flight review 1 <sup>st</sup> February 2007 - 31 <sup>st</sup> August 2008
RD.2	EUM/OPS-EPS/REP/09/0223	IASI annual in-flight performance report 2009
RD.3	EUM/OPS-EPS/REP/10/0020	IASI annual in-flight performance report 2010
RD.4	EUM/OPS-EPS/REP/11/0059	IASI annual in-flight performance report 2011
RD.5	EUM/OPS-EPS/REP/12/0620	IASI annual in-flight performance report 2012
RD.6	EUM/OPS-EPS/REP/14/744897	Metop-A IASI annual in-flight performance report 2013
RD.7	IA-RP-2000-4190-CNE	IASI in-flight cube corner compensation device stop performance report

		Doc n°: IA-RP-2000-4225-CNE Issue: 1.0 Date: 2017-09-27 Sheet: 10 Of: 63
--	--	---

### 3 SIGNIFICANT EVENTS

The following tables present a timeline of the various requests sent by TEC and the external IASI activities.

Those events are typically the configuration changes, programming requests, software update, but also any external operation or activity such as mission interruption, manoeuvre, dissemination problem, ...

#### 3.1 EXTERNAL CALIBRATION

Table 1 shows the External Calibration within the time period reported here. Note that the VDS files that come with each request are not described here.

Execution	TEC ref. <sup>(1)</sup>	Description	Activities
17/03/2014 from 5h15 to 9h11 orb. 43622 to 43624	RM-93	Monthly_MPF <sup>(2)</sup>  Targets: Earth 15, Blackbody, 2 <sup>nd</sup> Deep Space, Mirror Backside	For routine monitoring (IIS and IASI NeDT, scan mirror reflectivity, ghost,...)
15/04/2014 from 5h15 to 9h11 orb. 44034 to 44036	RM-94		
14/05/2014 from 5h15 to 9h11 orb. 44446 to 44448	RM-95		

Table 1: External Calibration TEC Requests

<sup>(1)</sup> TEC convention: R for Routine, M for Monthly and L for moon avoidance, followed by a chronological number

<sup>(2)</sup> An external calibration could be the result of:

- a TEC request or
- a “MPF” uploaded directly by EUMETSAT in full accordance with TEC. The reference “Monthly\_MPF” is based on the March 2008 TEC External Calibration request. The MPF for moon avoidance is based on the December 2008 TEC External Calibration request: “ICAL\_OCF\_xx\_M02\_20081216060000Z\_20090616060000Z\_20081209100934Z\_IASI\_EXTCALIBRA.dts”

#### 3.2 ON BOARD CONFIGURATION

Table 2 presents the on-board processing configuration updates that had been made within the time period reported here:

PTSI	IASI on board parameter files	Delivery by TEC	activated on	TEC ref.	affected parameters of a DPS TOP configuration update



Table 2: DPS and MAS configuration TEC Requests

For information, Table 3 shows the delivery applicable at the beginning of the period:

PTSI	IASI on board parameter files	Delivery by TEC	activated on	TEC ref.	affected parameters of a DPS TOP configuration update
<b>14</b> 2.0	IDPS_OBP_xx_M02_20130822131701Z_20140222131701Z_20130822125747Z_IASI_DPSPARAMOD.tar	22/08/2013 13h00	28/08/2013 10h08 orbit 35584	R_56	Update of reduced spectra, Modification of on-board thresholds (ArcImagMeanRMSCutOff and ZpdQualIndexCutOff) to be in line with the IASI-B filtering strategy

Table 3: DPS and MAS previous configuration

The associated ground configuration table (BRD file), necessary to handle coherent configuration at system level, is presented in the next section. These associated configuration table are necessary for L1 processing.

		Doc n°: IA-RP-2000-4225-CNE Issue: 1.0 Date: 2017-09-27 Sheet: 11 Of: 63
--	---	---

### 3.3 GROUND CONFIGURATIONS UPDATES FOR LEVEL 1 PROCESSING

Table 4 presents the on-ground processing configuration updates that had been made within the time period reported here:

IDef	IASI L1 auxiliary files	Delivery by TEC	Upload on GS1	Content
<b>59</b> <b>31</b>	IASI_BRD_xx_M02_20150522000000Z _xxxxxxxxxxxxxxZ_20150521083338Z _IAST_0000000014 IASI_GRD_xx_M02_20150522000000Z _xxxxxxxxxxxxxxZ_20150521083343Z _IAST_0000000031	21/05/2015 08h33		Update of Scan Mirror Reflectivity

Table 4: IASI L1 Auxiliary File Configuration on the Operational EPS Ground Segment

For information, Table 5 shows the delivery applicable at the beginning of the period:

IDef	IASI L1 auxiliary files	Delivery by TEC	Upload on GS1	Content
<b>58</b> <b>30</b> <b>14</b>	IASI_BRD_xx_M02_20140527150000Z _xxxxxxxxxxxxxxZ_20140527124036Z _IAST_0000000014 IASI_GRD_xx_M02_20140527150000Z_xxxx _xxxxxxxxxxZ_20140527124041Z_IAST_0000 000030 IASI_ODB_xx_M02_20130417080000Z _xxxxxxxxxxxxxxZ_20130417074829Z _IAST_0000000014	27/05/2014 12h40  17/04/2013	BRD & GRD activated on 17/06/2014 06:53 orbit 39745	Update of Scan Mirror Reflectivity (+ IdefOffsetSondIISModel )

Table 5: IASI L1 auxiliary file previous configuration



### 3.4 DATA BASES UPDATE FOR THE USERS

The Noise Covariance Matrix (NCM) and Spectral data base (SDB) are specific data bases for the users. They are updated according to the main ground level 1 evolutions.

Table 6 presents the updates of the NCM and SDB that had been made within the time period reported here:

IDef	Users Data-Base	Delivery by TEC	TEC ref.	Comments

Table 6: IASI Data Bases for the users

		Doc n°: IA-RP-2000-4225-CNE Issue: 1.0 Date: 2017-09-27 Sheet: 12 Of: 63
--	---	---

For information, Table 7 shows the delivery applicable at the beginning of the period:

IDef	Users Data-Base	Delivery by TEC	TEC ref.	Comments
5	IASI_NCM_xx_M02_20141028000000Z_20141028000000Z_20141027140151Z_IA_ST_SPECTRESPO	27/10/2014	R_COV_5	Covariance matrix from L0 noise on BB (2014/09/24external calibration)
14	IASI_SDB_xx_M02_20130923140000Z_20130923140000Z_20130923124758Z_IASIST_IASISPECDB	23/09/2013	R_57	User database associated to ODB IDefSDB 14

Table 7: previous IASI Data Bases

### 3.5 ON GROUND HW/SW EVOLUTION

Table 8 presents the updates of PPF L1 software within the time period reported here:

IASI L1 PPF software version	Delivery by TEC	Date introduced on GS1	Comments
7.2	04/2015	27/05/2015 for sensing time 11:38 <sup>UTC</sup> Orbit 44635	SVM files's management

Table 8: IASI L1 PPF Configuration on the Operational EPS Ground Segment

For information, Table 9 shows the software version applicable at the beginning of the period:

IASI L1 PPF software version	Delivery by TEC	Date introduced on GS1	Comments
7.1	07/2014	22/07/2014 for sensing time 08:11 <sup>UTC</sup> Orbit 40243	<ul style="list-style-type: none"> <li>- Bad error handling in SD_BAS_OperateurLoc (coordinates transformation Earth &lt;-&gt; METOP) ;</li> <li>- Update of IASI L1 Product Header (improvement of COUNT_DEGRADED_INST and _PROC counters).</li> </ul>

Table 9: Previous IASI L1 PPF

### 3.6 DECONTAMINATION

Table 10 presents decontaminations that have been made or requested within the time period reported here:



Last due date	Date of decontamination	Description

Table 10: Decontamination TEC Requests

For information, Table 11 shows the previous decontamination:

Last due date	Date of decontamination	Description
In 2015	From 8 to 13/09/2014	

Table 11: Previous decontamination

		Doc n°: IA-RP-2000-4225-CNE Issue: 1.0 Date: 2017-09-27 Sheet: 13 Of: 63
--	---	---

### 3.7 INSTRUMENT

#### 3.7.1 External events

This category is for those activities/events that are external to IASI but still have an impact. It is broken down into classes of *PL-SOL* and *OOP* manoeuvre.

##### 3.7.1.1 Manoeuvres

Date	Type <sup>(*)</sup>	Description	IP flag	OoP mission Outage
2015/04/28	IP	IP manoeuvre #35 (orbit 44223)		

Table 12: Overview of METOP manoeuvres in the reporting period

(<sup>\*</sup>): IP for In-Plane manoeuvres (IASI stays in NOP) and OoP for Out of plane manoeuvres (IASI is put in Heater 2)

##### 3.7.1.2 PL-SOL

Table 13 presents the PL-SOL events that have occurred within the time period reported here:

Dates	Orbits	Description

Table 13: PL-SOL

#### 3.7.2 Operation leading to mission outage

This chapter presents the intervention on IASI needing routine interruption that have occurred within the time period reported here.

Dates	Orbits	type	IASI mode	Description
2015/04/09 to 13	43949-44008			IASI Instrument Management System switch to B side

Table 14: Scheduled interruptions

#### 3.7.3 Anomaly leading to mission outage

Table 15 and Table 16 present the major and minor anomalies internal to IASI that have occurred within the time period reported here.

Note that, in this section minor anomalies are all identified and without any impact on the mission, and major anomalies only affect IASI instrument, and no other sub-systems of the spacecraft.



Dates	Orbits	Anomaly type <sup>(*)</sup>	IASI mode	Description
2015/04/23	44223	Auto-Recovery		DMC Checksum error

Table 15: Major anomalies

(<sup>\*</sup>): SEU (LAS, CCM or DPS) anomalies or SET anomalies

Day	Orbits	error n°	Severity	Anomaly type	LN	SN	Description

Table 16: Minor anomalies

		Doc n°: IA-RP-2000-4225-CNE Issue: 1.0 Date: 2017-09-27 Sheet: 14 Of: 63
--	---	---

## 4 PERFORMANCE MONITORING

### 4.1 *PERFORMANCE MONITORING*

In order to ensure that the IASI system is permanently running in good conditions, the CNES (IASI TEC) and EUMETSAT (CGS) are monitoring products at various temporal levels : at line, PDUs and DUMP (full orbit).

The on-board and ground processing performance algorithms issue more than one hundred quality indicators, called flags and simple parameters. Those are alarms for any bad functioning or local performance degradation.

According to the results, the TEC is also in charge of delivering new on-board or ground parameters to EUMETSAT when it is necessary. EUMETSAT is then in charge of uploading them on-board or as an input of the level 1 processing chain. During the whole instrument life, these parameter adjustments are necessary in order to take into account instrument evolution in the processing and finally to maintain a good data quality.

The Table 17 is the colour code used for the status report.

Status Colour	Meaning
GREEN	$\geq 95\%$ of good spectra
YELLOW	$< 95\%$ of good spectra
RED	Production interrupted
BLANK	No Status Reported



*Table 17: Functional status legend*

## 4.2 PERFORMANCE SYNOPSIS

Table 18 provides a synthetic view of all the indicators evaluated for L0/L1 data and their current status.

Section	Component	Description	Status	Comments
<a href="#">4.3</a>	L0	<b>Level-0 Data Quality</b> <ul style="list-style-type: none"> <li>Overall quality</li> <li>Main flag and quality indicator parameters</li> <li>Spikes monitoring</li> <li>Reduce- ZPD monitoring</li> <li>Overflows/Underflows monitoringd Spectra monitoring</li> <li>Second level flag and quality indicators</li> </ul>	GREEN	On-board processing
<a href="#">4.4</a>	L1	<b>Level-1 Data Quality</b> <ul style="list-style-type: none"> <li>Overall</li> <li>Main flag and quality indicator parameters</li> </ul>	GREEN	On ground processing
<a href="#">4.5</a>	L1	<b>Sounder radiometric performances</b> <ul style="list-style-type: none"> <li>Radiometric noise</li> <li>Radiometric calibration</li> <li>Acquisition chain delay</li> <li>Optical transmission</li> <li>- Ice</li> <li>Prediction of decontamination date</li> <li>Interferometric contrast</li> <li>Interferogram baseline</li> <li>Detection chain</li> </ul>	GREEN	
<a href="#">4.6</a>	L1	<b>Sounder spectral performances</b> <ul style="list-style-type: none"> <li>Dimensional stability</li> <li>- Position of axis</li> <li>- Cube Corner constant offset</li> <li>- Cube Corner velocity</li> <li>- Optical bench temperature</li> <li>Spectral calibration</li> <li>Ghost evolution</li> </ul>	GREEN	
<a href="#">4.7</a>	L1	<b>Geometric performances</b> <ul style="list-style-type: none"> <li>Sounder/IIS co-registration</li> <li>IIS/AVHRR co registration</li> </ul>	GREEN	
<a href="#">4.8</a>	L1	<b>IASI-A inter-calibration</b> <ul style="list-style-type: none"> <li>IASI-A inter-calibration with CRIS</li> <li>IASI-A inter-calibration with AIRS</li> </ul>	GREEN	
<a href="#">4.9</a>	L1	<b>IIS radiometric performances</b> <ul style="list-style-type: none"> <li>IIS radiometric noise monitoring</li> <li>IIS radiometric calibration monitoring</li> </ul>	GREEN	

Table 18: IASI product components functional status

		Doc n°: IA-RP-2000-4225-CNE Issue: 1.0 Date: 2017-09-27 Sheet: 16 Of: 63
--	---	---

### 4.3 LEVEL 0 DATA QUALITY (L0)

#### 4.3.1 Overall quality

The IASI L0 data quality (orbit average) through IASI engineering products is shown in Figure 1.

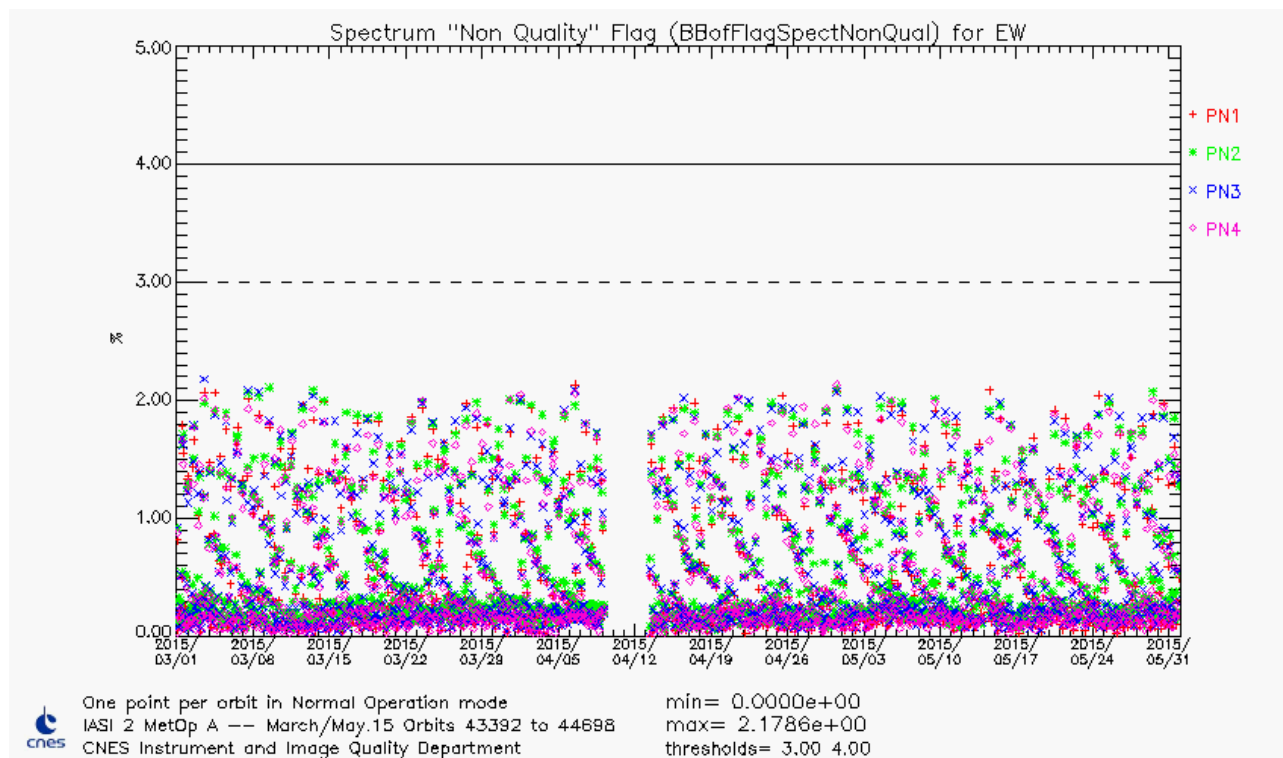


Figure 1 : IASI L0 data quality orbit average (per pixel and CCD)

The geographical distribution of the overall L0 (board) quality flag for the 4 pixels is shown in Figure 2.



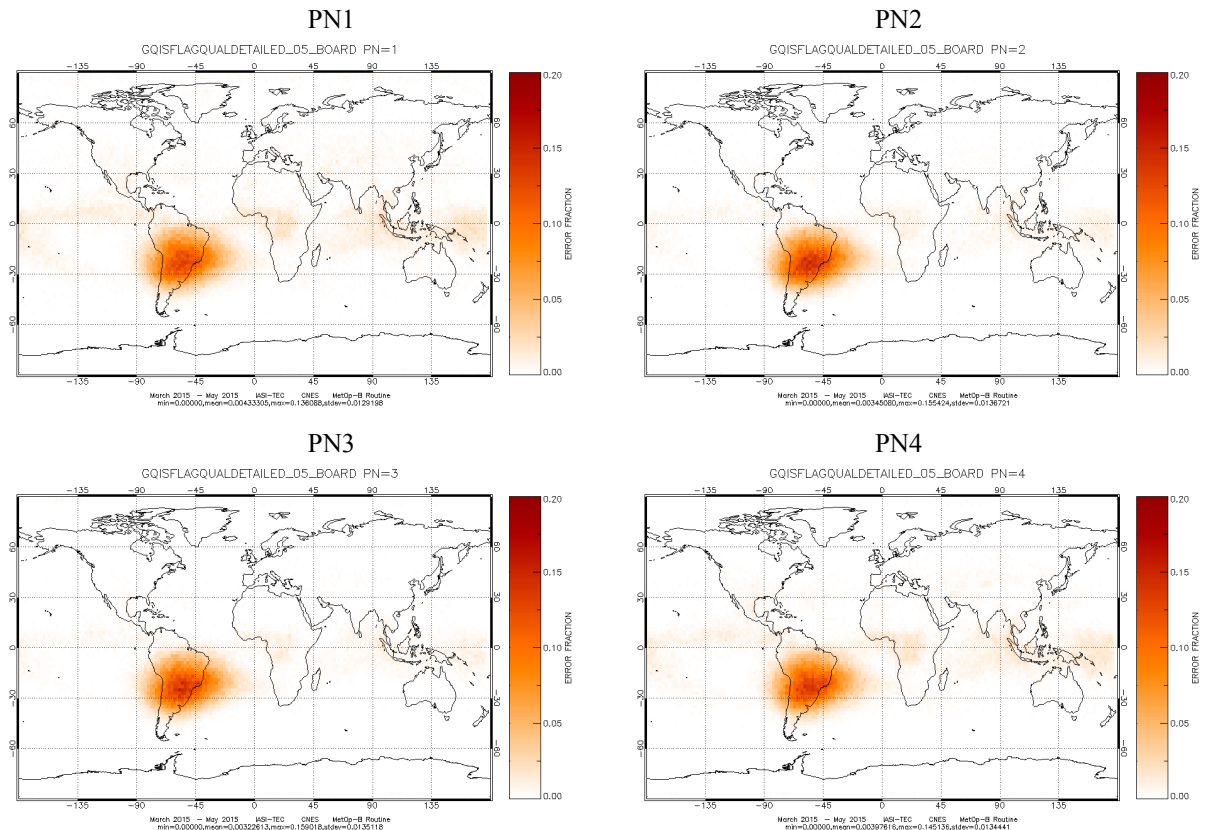




Figure 2 : IASI L0 data quality spatial distribution (per pixel)

The IASI L0 quality and on-board processing are nominal.

		Doc n°: IA-RP-2000-4225-CNE Issue: 1.0 Date: 2017-09-27 Sheet: 18 Of: 63
--	--	---

### 4.3.2 Main flag and quality indicator parameters

The main contributors to the rejected spectra by on-board processing are: spikes (proton interaction on detectors), failure of NZPD algorithm determination and over/underflows (measured data exceeding on-board coding tables capacity). They are analysed in details hereafter.

#### 4.3.2.1 Spikes monitoring

Spikes occur when a proton hits a detector. This very high energetic particle disrupts the measure of the interferogram and then corrupts the spectrum.

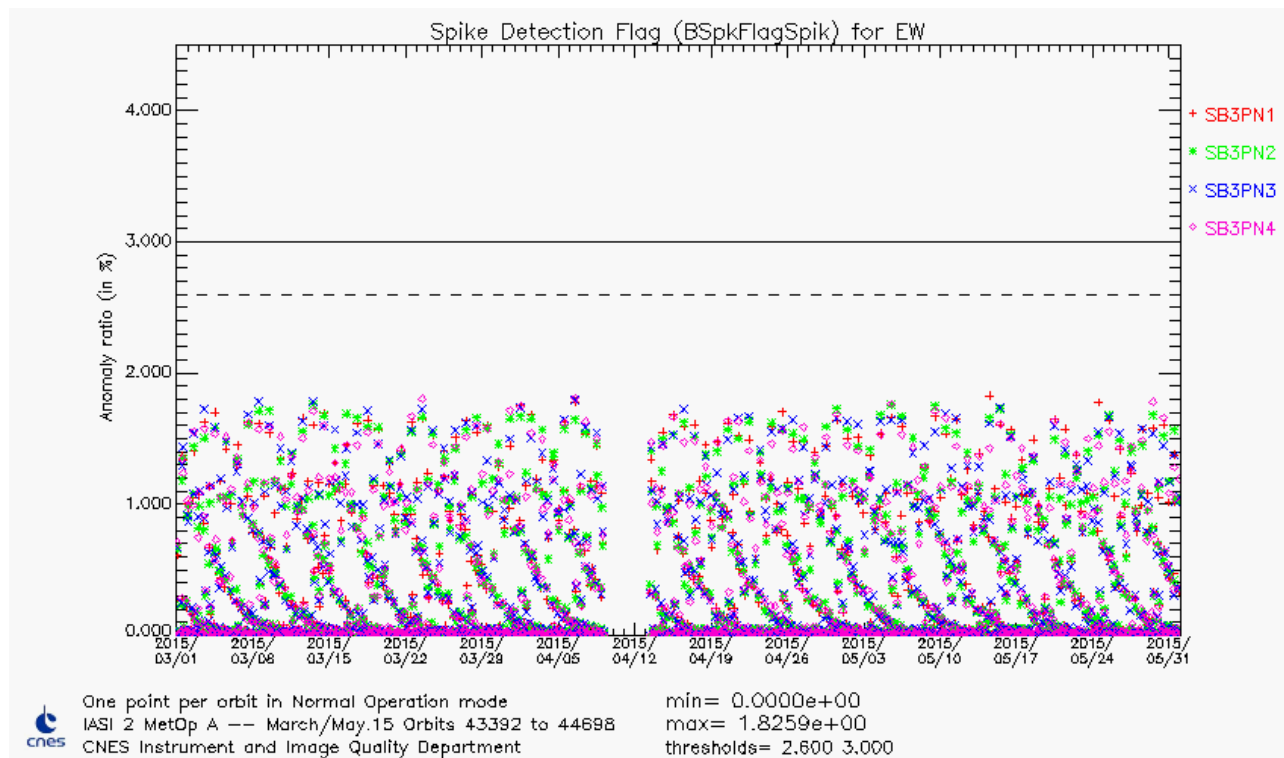


Figure 3 : Temporal evolution of spikes anomaly ratio in % for all pixels (orbit average)

An example of the geographical distribution of spikes occurrences on band 3 for the 4 pixels is shown in Figure 4.



Doc n°: IA-RP-2000-4225-CNE

Issue: 1.0

Date: 2017-09-27

Sheet: 19 Of: 63

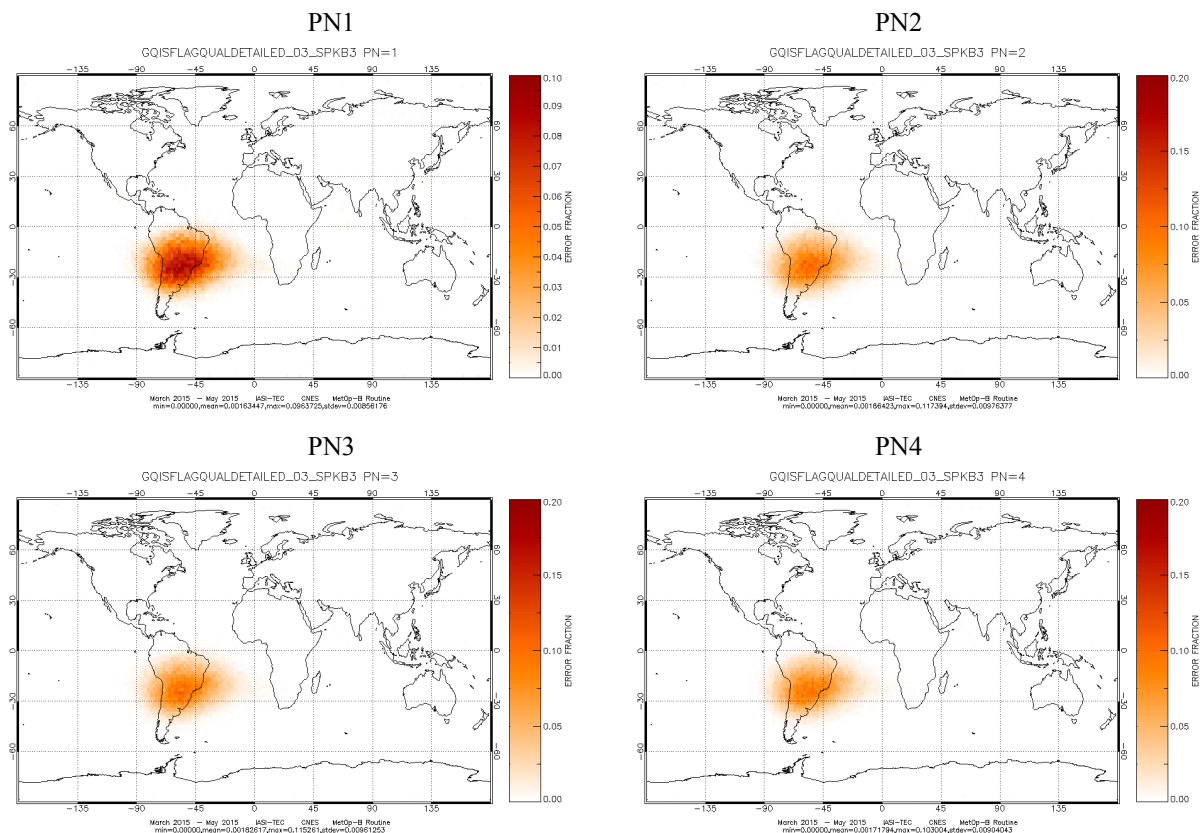




Figure 4 : Geographical distribution of spikes occurrences in % for band 3 and all pixels

Spikes are mainly located in the regions of Earth where the magnetic field doesn't protect the satellite from the energetic particles: the poles and the SAA (South Atlantic anomaly).

Spike anomaly ratio is nominal for the reported period.

		Doc n°: IA-RP-2000-4225-CNE Issue: 1.0 Date: 2017-09-27 Sheet: 20 Of: 63
--	--	---

#### 4.3.2.2 ZPD monitoring

The ZPD (“Zero Path Difference”) is the position of the central fringe of the interferogram. The NZPD is the number of the sample detected as the ZPD. On IASI, it is determined by a software. This is a special feature of IASI in comparison to other instruments for which NZPD determination is done by hardware.

NZPD variations are governed by two phenomenons:

1. ASE fluctuations which have the same effect on each pixel and can produce NZPD variation of 30-40 samples over month. This is the first order phenomena.
2. Mechanical deformation of the interferometer or evolution of detection chain delays. These phenomenons affect the 4 pixels in different way. However this phenomenon has a second order effect in comparison to the first one.

**We monitor both NZPD determination quality flag and interpixel homogeneity. We expect stability.**

BZPDFlagNZPDNonQualEW: Temporal evolution of NZPD determination quality flag for earth view

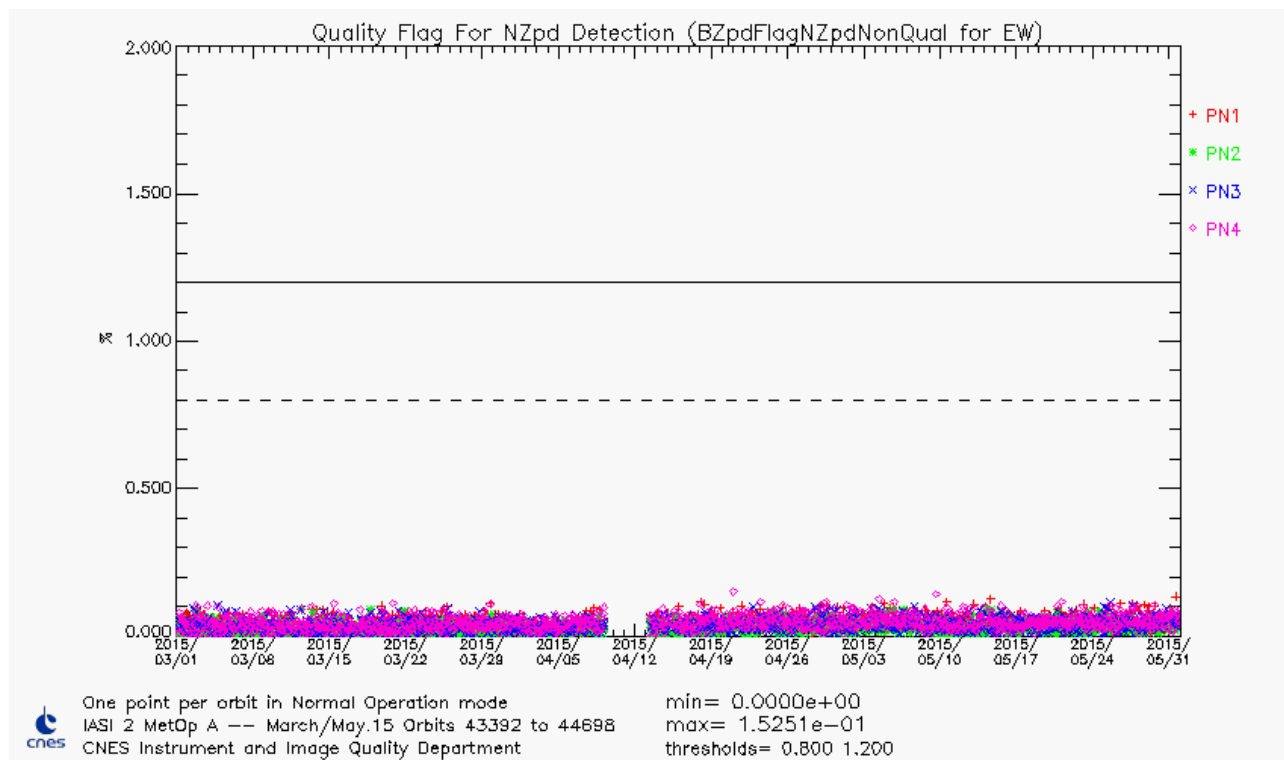


Figure 5 : Temporal evolution of NZPD determination anomaly ratio in % for all pixels (orbit average)

NZPD determination anomaly ratio is nominal for the reported period.

The geographical distribution of the NZPD determination quality flag for the 4 pixels is shown in Figure 6.

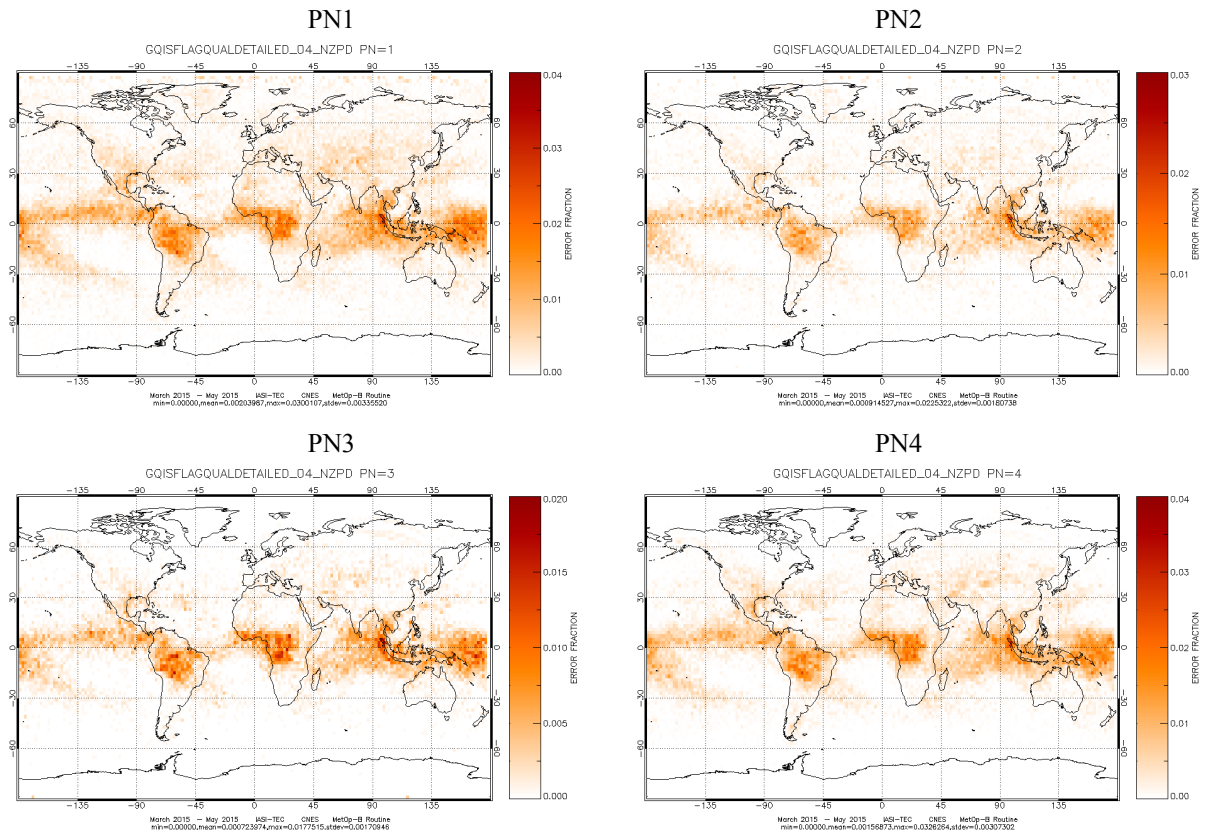


Figure 6 : IASI NZPD determination quality flag spatial distribution (per pixel)

The NZPD determination fails over some clouds that have a temperature that induces no energy in the central fringe of the interferogram.

### NZPD inter-pixel homogeneity monitoring

This monitoring is necessary in order to follow potential deformation of the interferometer or evolution of detection chain delay.

The NZPD inter-pixel homogeneity is nominal over the reported period. Consequently, these parameters are perfectly stable and in-line with the specification.

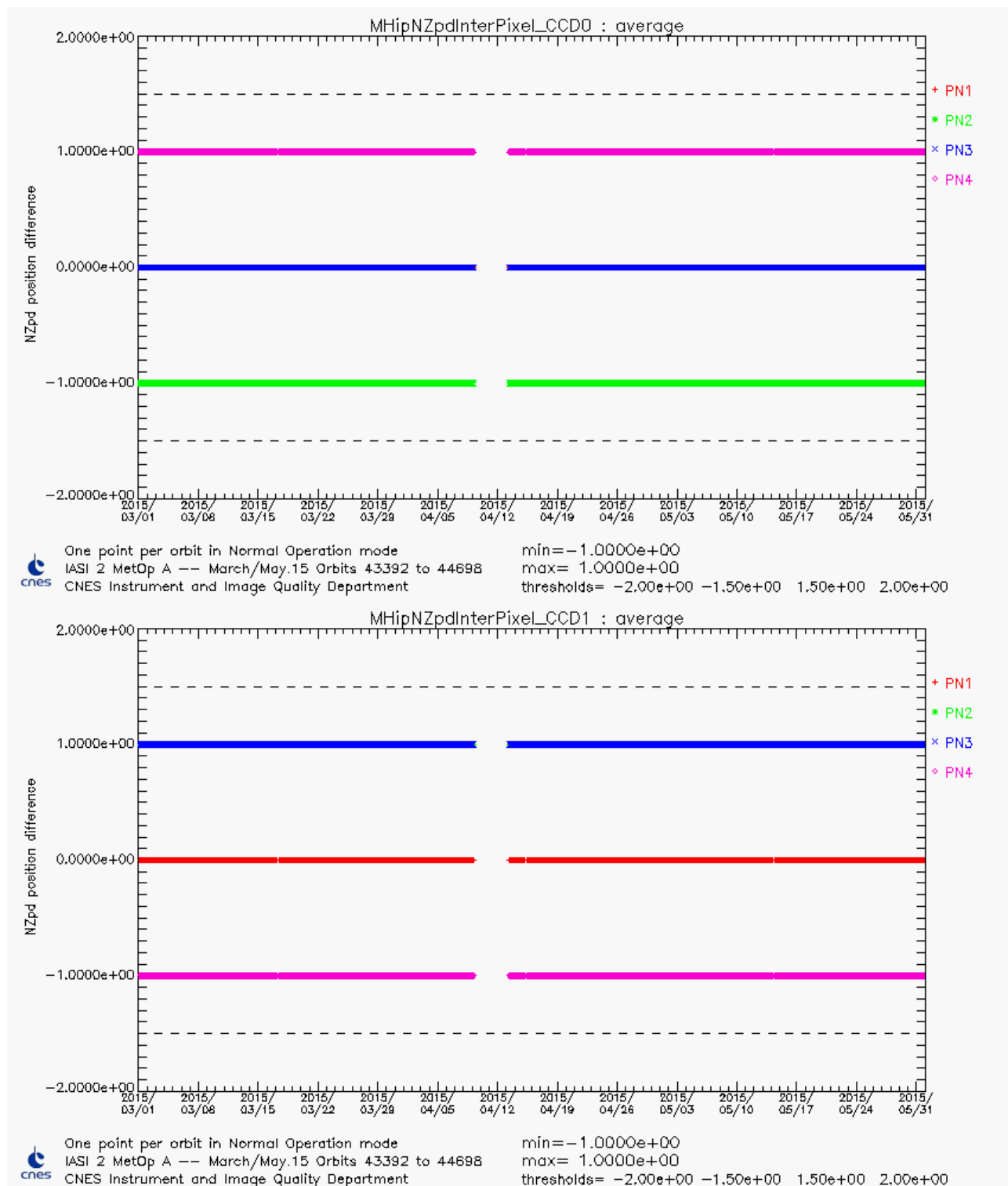




Figure 7 : NZPD inter-pixel for all pixels and CCD calculated with respect to pixel 1 (orbit average)

		Doc n°: IA-RP-2000-4225-CNE Issue: 1.0 Date: 2017-09-27 Sheet: 23 Of: 63
--	--	---

#### 4.3.2.3 Overflows / Underflows monitoring

The total number of bits available for a spectrum to be transmitted to the ground is limited. For that reason, we have defined coding tables to encode each measured spectrum. These tables have been designed by using “extreme spectrum” corresponding to known drastic atmospheric conditions. The coding step is also set to not introduce additional noise into the spectrum. However for very extreme atmospheric conditions (sunglint in B3, very high stratospheric temperature...) a measurement can exceed on-board coding tables’ capacity and causes an over/underflow.

Over/underflows occurrences are monitored and stability is expected. As long as they remain to low levels, the coding table is not changed. Note that changing the coding tables requires compromises. Indeed, increasing the encoding capacity can be achieved by two different ways. A first solution consists in an increase of the coding step without changing the number of bits. However, that leads to an increase of the digitalization noise. Then, a second solution consists in keeping the coding step constant while increasing the number of bits available for a particular band. But, the total amount of bits available for the entire spectrum is limited and constant. So, that requires to decrease the encoding capacity in another spectral band.

Time series of Overflows and Underflows (orbit average) are shown in following figure for all pixels.

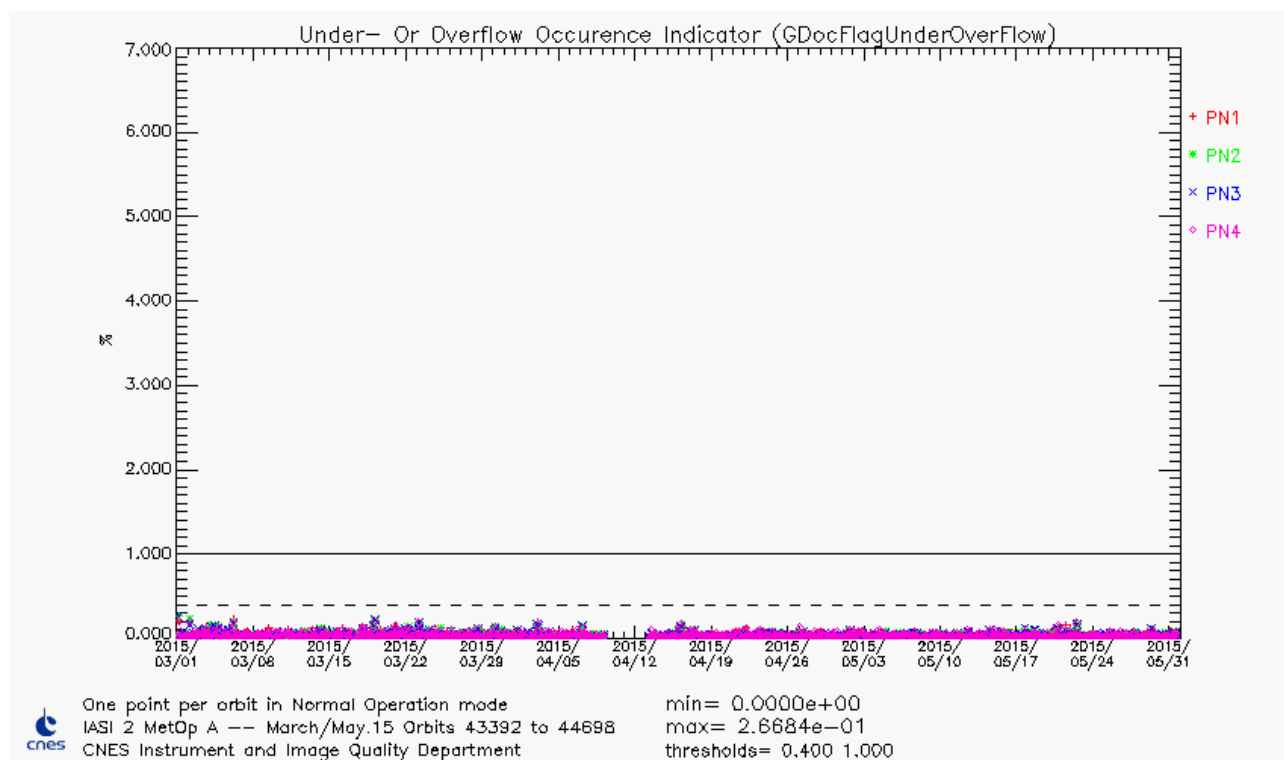




Figure 8 : IASI L0 over/under-flows orbit average of all pixels

Over/underflows ratio is nominal for the reported period.

The geographical distribution of the Overflows and Underflows for the 4 pixels is shown in Figure 9.

		Doc n°: IA-RP-2000-4225-CNE Issue: 1.0 Date: 2017-09-27 Sheet: 24 Of: 63
---	---	---

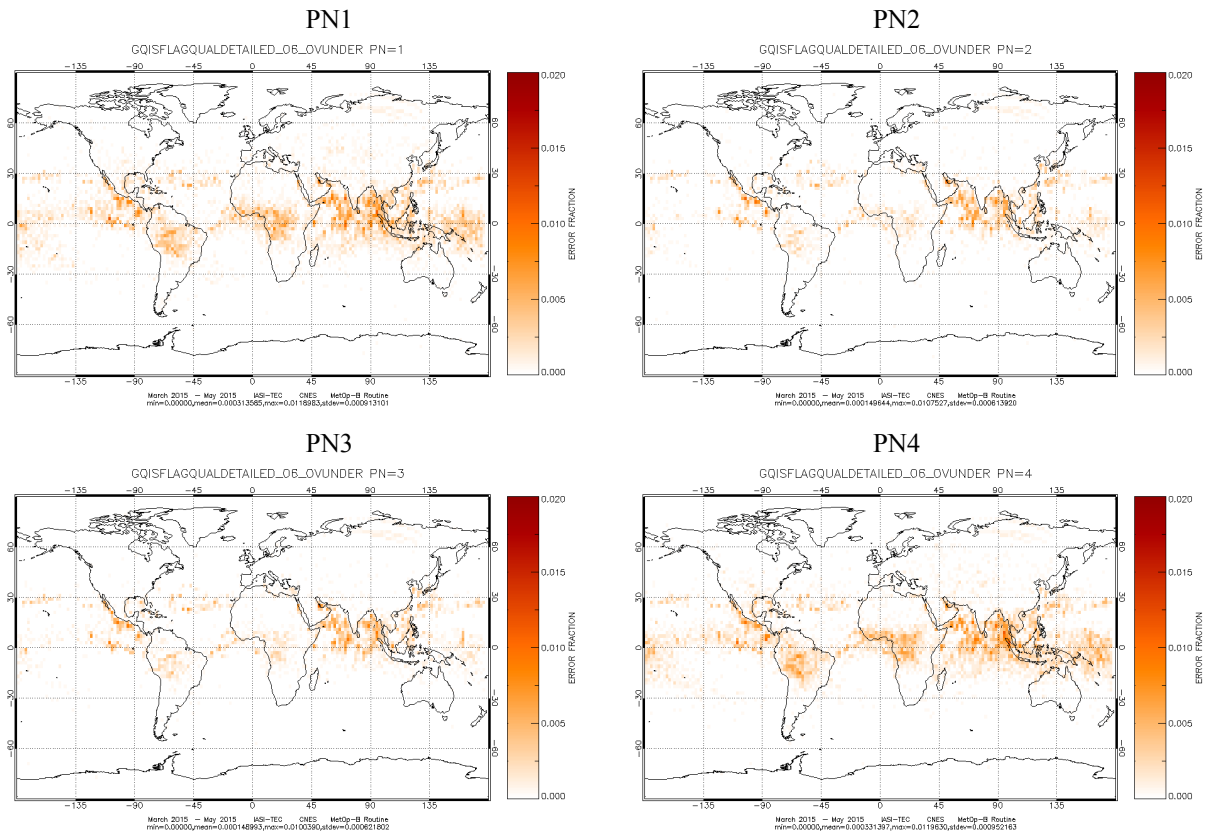


Figure 9 : IASI Overflows and Underflows spatial distribution (per pixel)

#### 4.3.2.4 Reduced Spectra monitoring

On-board Reduced Spectra is one of the most important parameter to monitor. It ensures that on-board spectra still have a good radiometric calibration when on-board configuration reduced spectra are reloaded. This is the case, for instance, after an instrument mode change.

Reduced spectra are slightly evolving with respect to potential deformation of the interferometer (optical bench).

In order to prevent from a large difference between current and on-board configuration reduced spectra, we apply the DPS processing on the verification interferograms using the reduced spectra from the on-board configuration (TOP) instead of the filtered reduced spectra computed on-board with the current calibration views. These reduced spectra from the on-board configuration are used as initialisation each time there is mode change. If they are too far from the reality, no spectra can be computed on-board after a mode change. We monitor the evolution of ZPD determination quality index for calibration views (BZpdNzpdQualIndexBB and CS) obtained by this DPS processing at TEC, results of this monitoring are given hereafter.



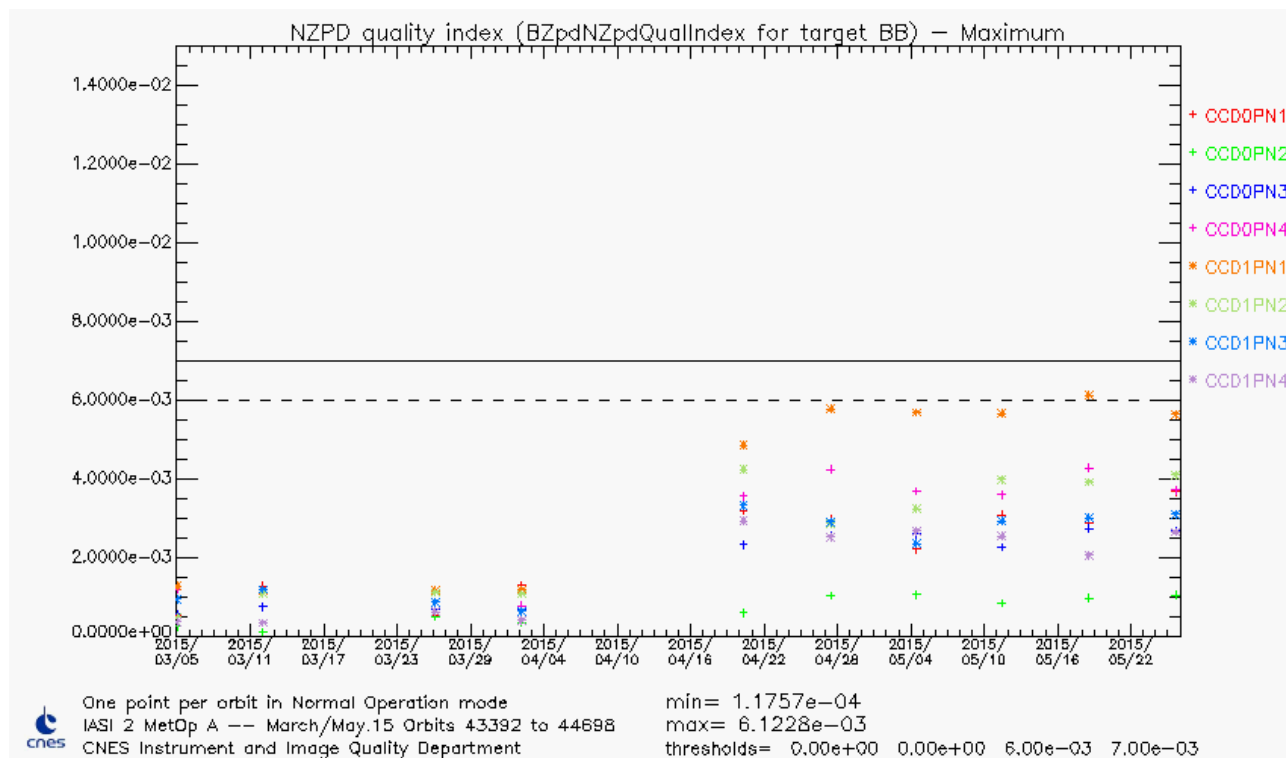


Figure 10 : Max of NZPD quality index for all pixels and CCD - BB

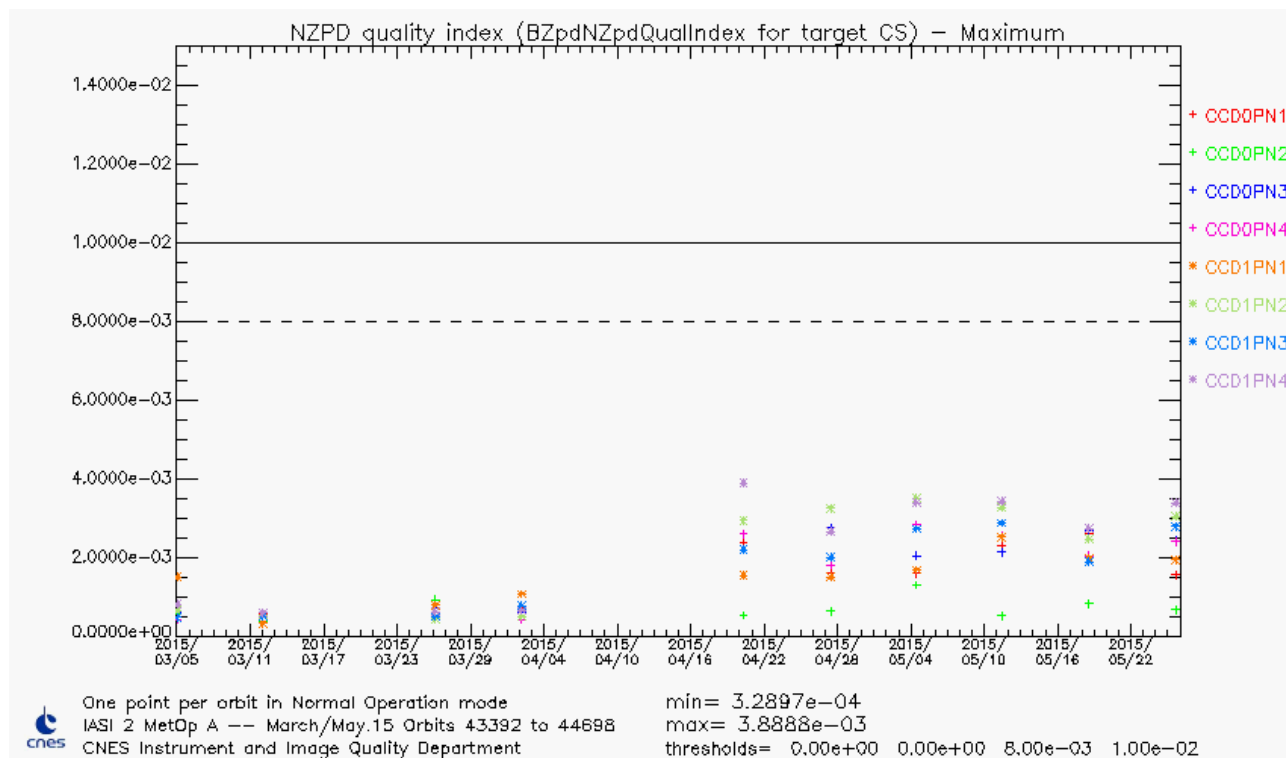




Figure 11 : Max of NZPD quality index for all pixels and CCD - CS

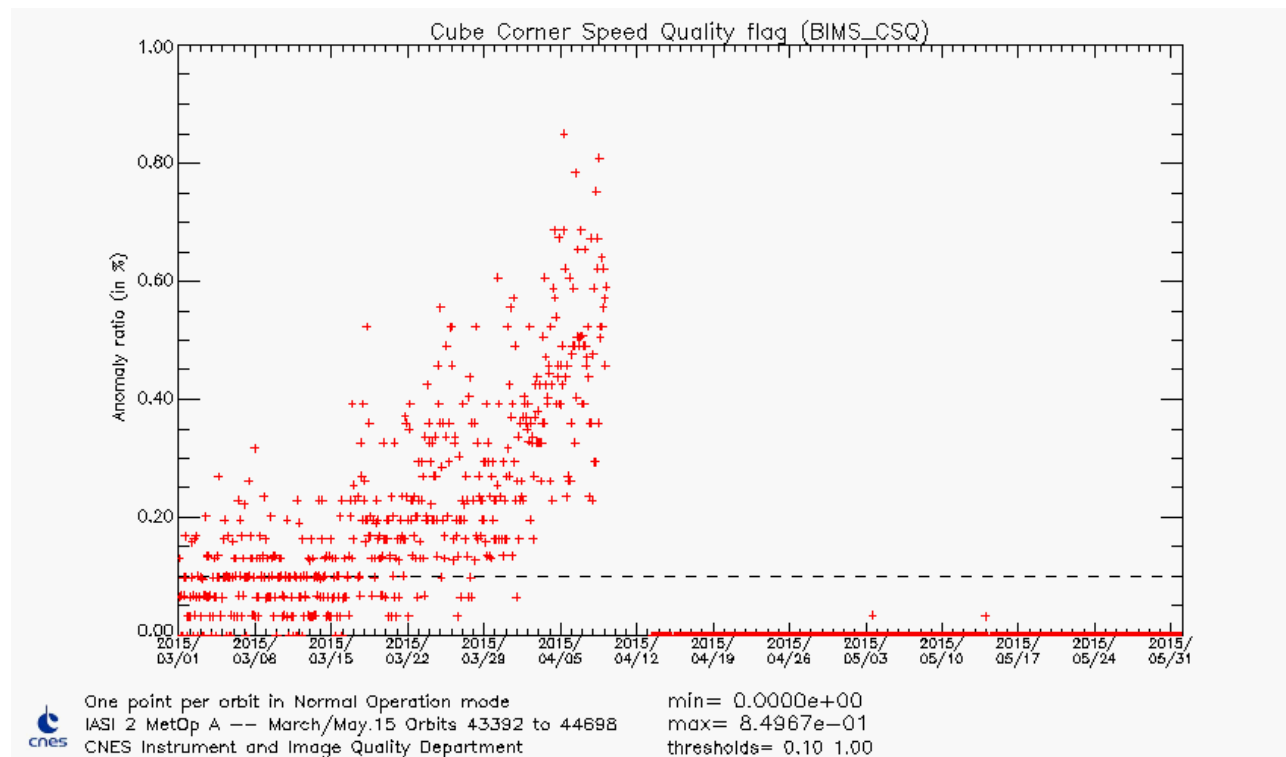
As soon as average BZPDNZPDQualIndexBB and CS remain below 0.01 on-board reduced spectra are robust to an instrument mode change.

The maximum of NZpdQualIndex for BB is increasing since the switch to IMS the redundant side. The last update of the on-board reduced spectra was performed in August 2013, the reduced spectra will be updated in summer 2015 in order to stay under the on board threshold.

		Doc n°: IA-RP-2000-4225-CNE Issue: 1.0 Date: 2017-09-27 Sheet: 26 Of: 63
--	--	---

#### 4.3.2.5 Cube corner Speed Quality (CSQ) monitoring

From verification products (BB & CS):



From engineering products (EW):

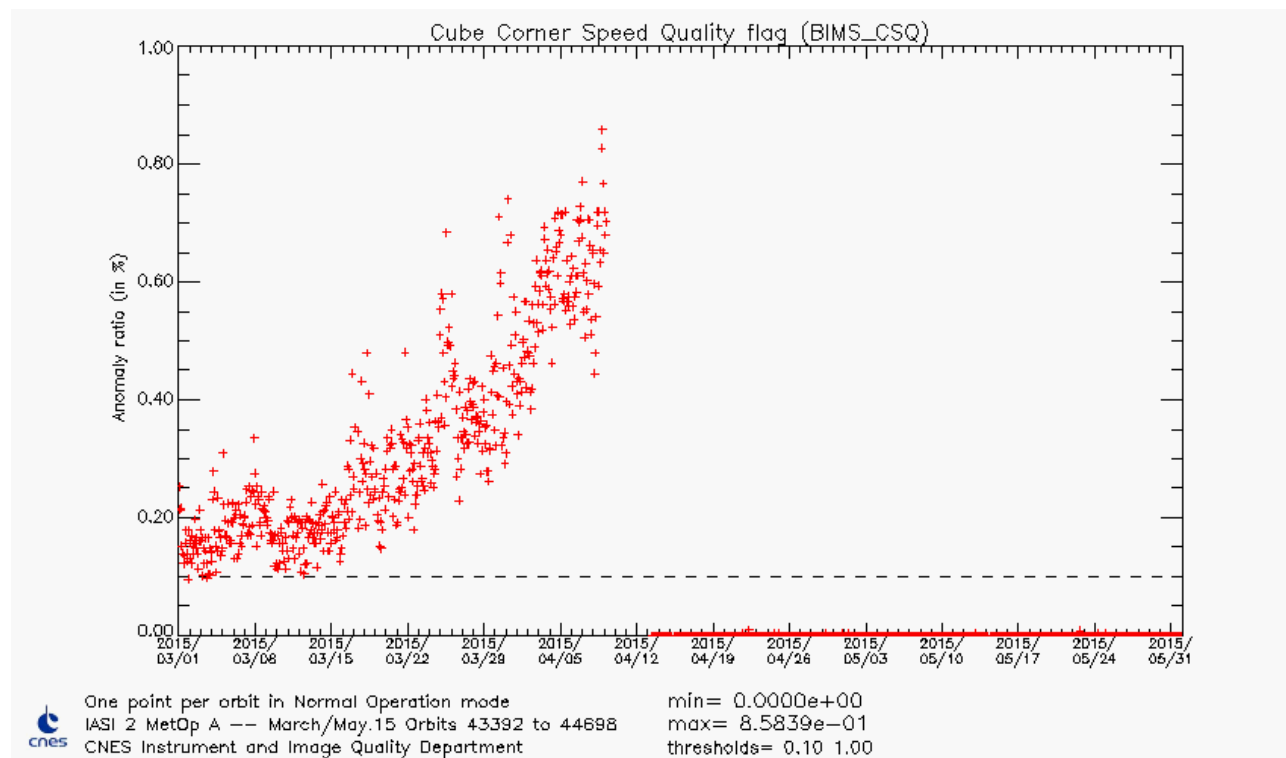




Figure 12 : Number of CSQ

Since autumn 2014, the number of CSQ had increased. This issue has been analysed by CNES and EUMETSAT and it was decided to switch to the IMS B-side from 9 to 13<sup>th</sup> April 2015. Since IASI-A is on IMS redundant side, the CSQ rate came back to normal values.

		Doc n°: IA-RP-2000-4225-CNE Issue: 1.0 Date: 2017-09-27 Sheet: 27 Of: 63
--	--	---

### 4.3.3 Second level flags and quality indicators

L0 Flag and quality indicators are stable, apart from the raising of CSQ flags.

### 4.3.4 Conclusion

L0 Flag and quality indicators are stable.

## 4.4 LEVEL 1 DATA QUALITY (L1)

### 4.4.1 Overall quality

The IASI overall quality is shown as the orbit averages of the quality indicator for the individual pixels in the next figure.

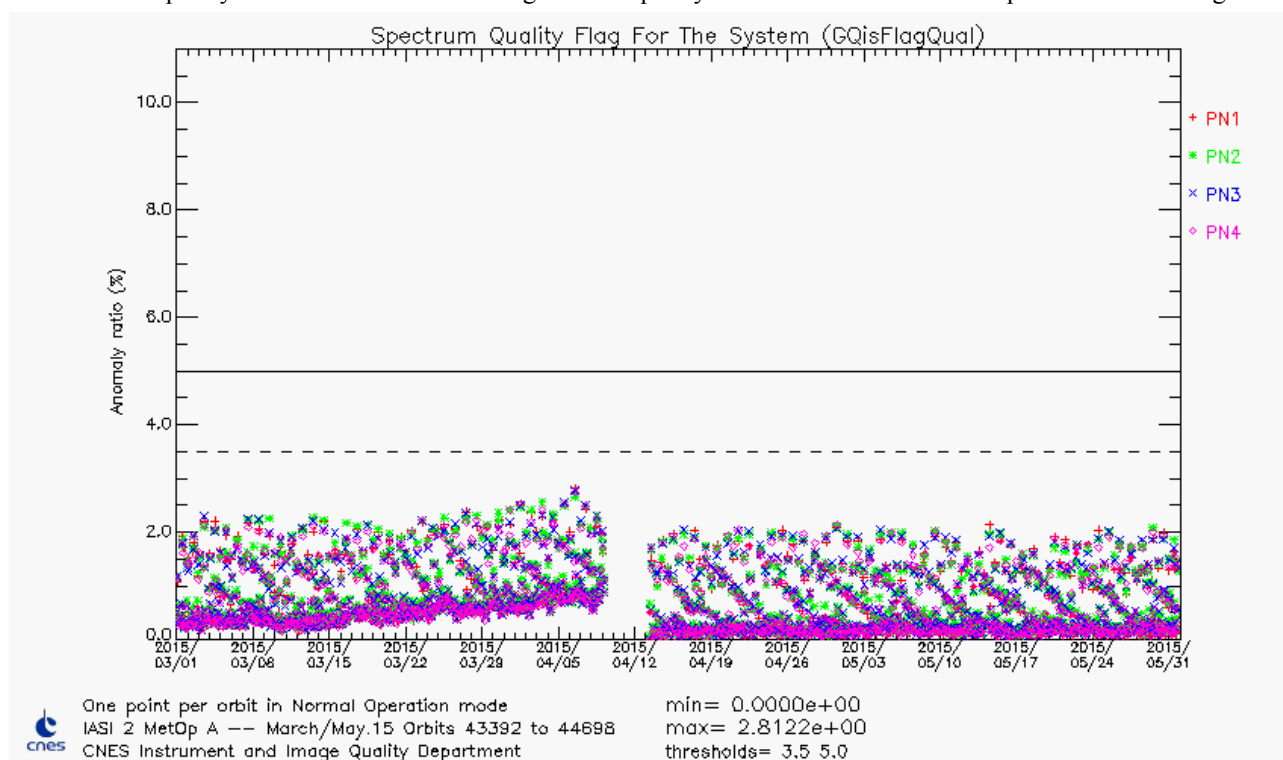




Figure 13 : IASI L1 data quality orbit average (% of bad by PN)

One should note that, over the period covered by the present document, the averaged data rejection ratio is less than 1%. We clearly see that data quality is better on the bands B1 and B2 in comparison to band B3 (which is the most affected by spikes).

The geographical distribution of the IASI product overall quality for the 4 pixels is shown in Figure 14.

		Doc n°: IA-RP-2000-4225-CNE Issue: 1.0 Date: 2017-09-27 Sheet: 28 Of: 63
--	--	---

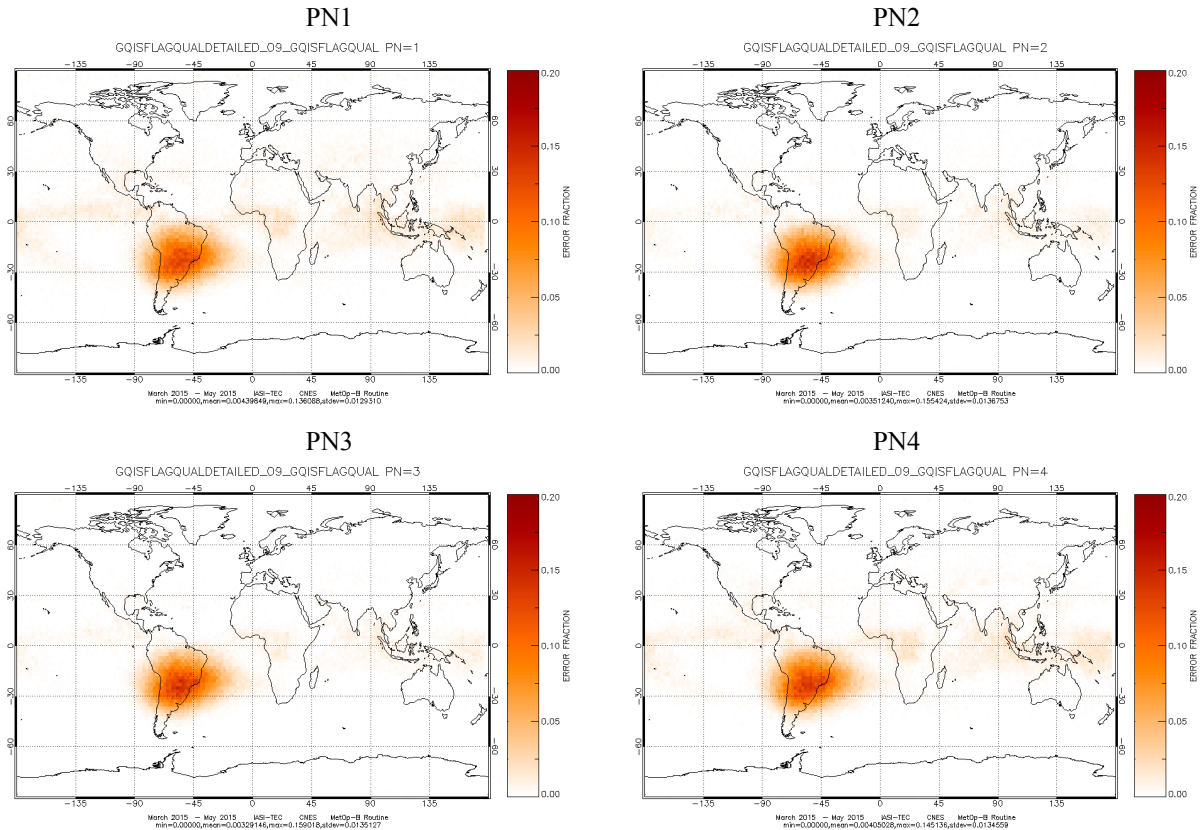


Figure 14 : IASI product overall quality spatial distribution (per pixel)

The main contributors are the spikes (mainly in band 3, which is the band the most sensitive to the spikes).

#### 4.4.2 Main flag and quality indicator parameters

All the quality indexes that follow are general L1 quality indexes of sounder products.

GQisQualIndex – average – is the average general quality index of the sounder products.

GQisQualIndexIIS is the IASI integrated imager (IIS) images quality index.

GQisQualIndexSpect is the spectral quality index of the sounder products.

GQisQualIndexRad is the radiometric quality index of the sounder products.

GqisQualIndexLoc is the ground localisation quality index of the sounder products.

MDptPixQual is a quality index for IASI integrated imager (IIS) that represents a fraction of not dead pixels.

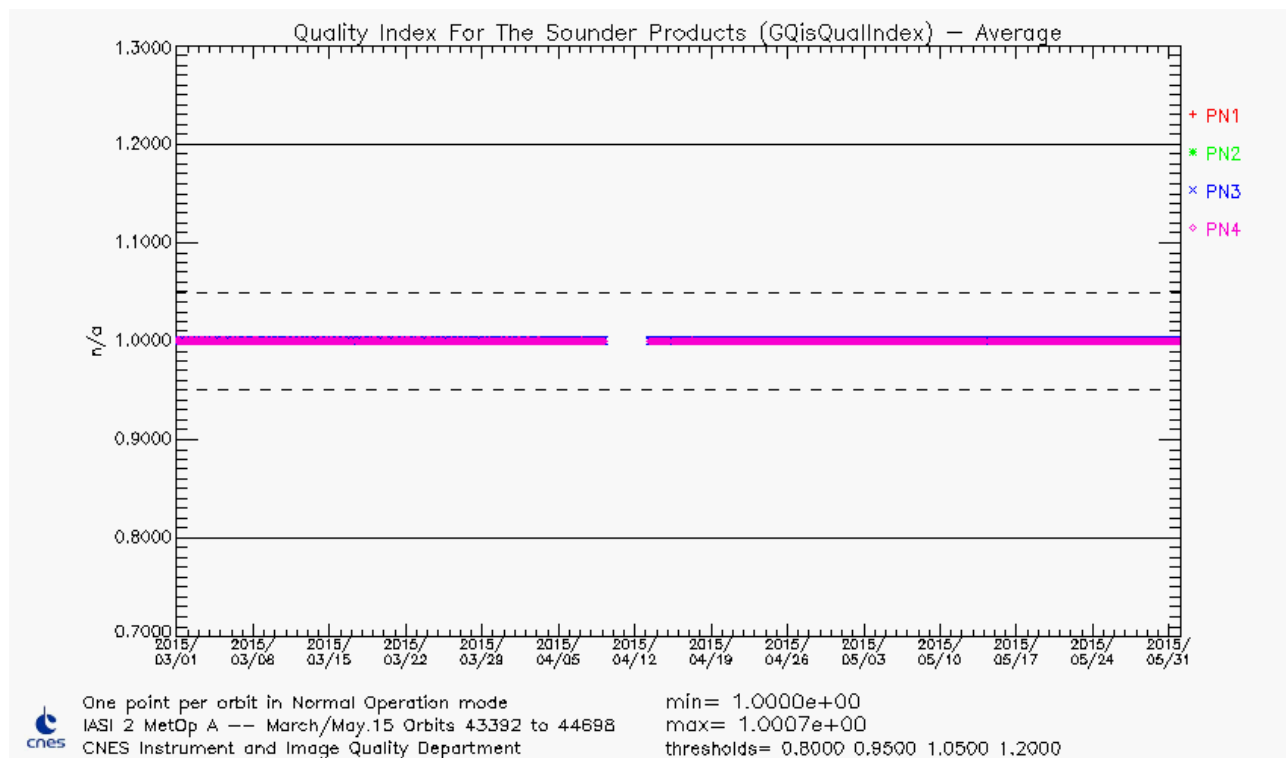


Figure 15 : GQisQualIndex average (L1 data quality index for IASI sounder)

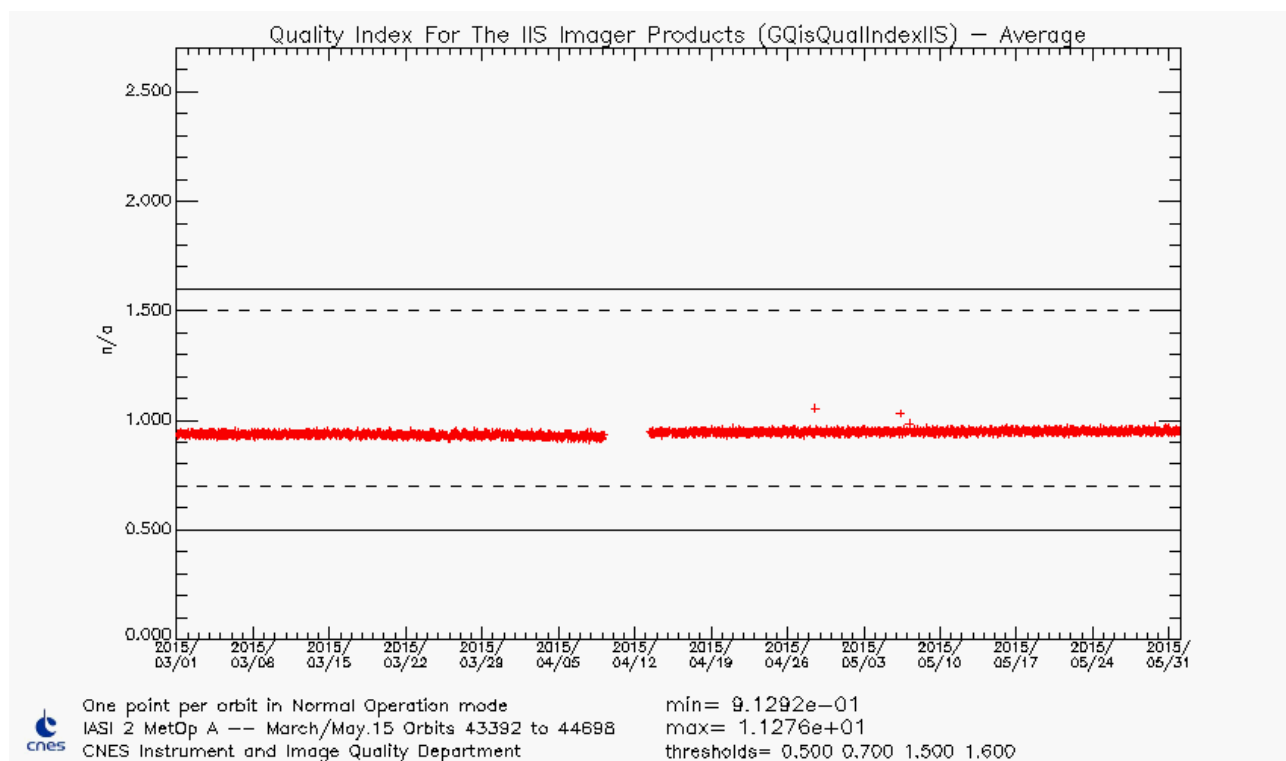


Figure 16 : GQisQualIndexIIS average (L1 data quality index for IASI Integrated Imager)

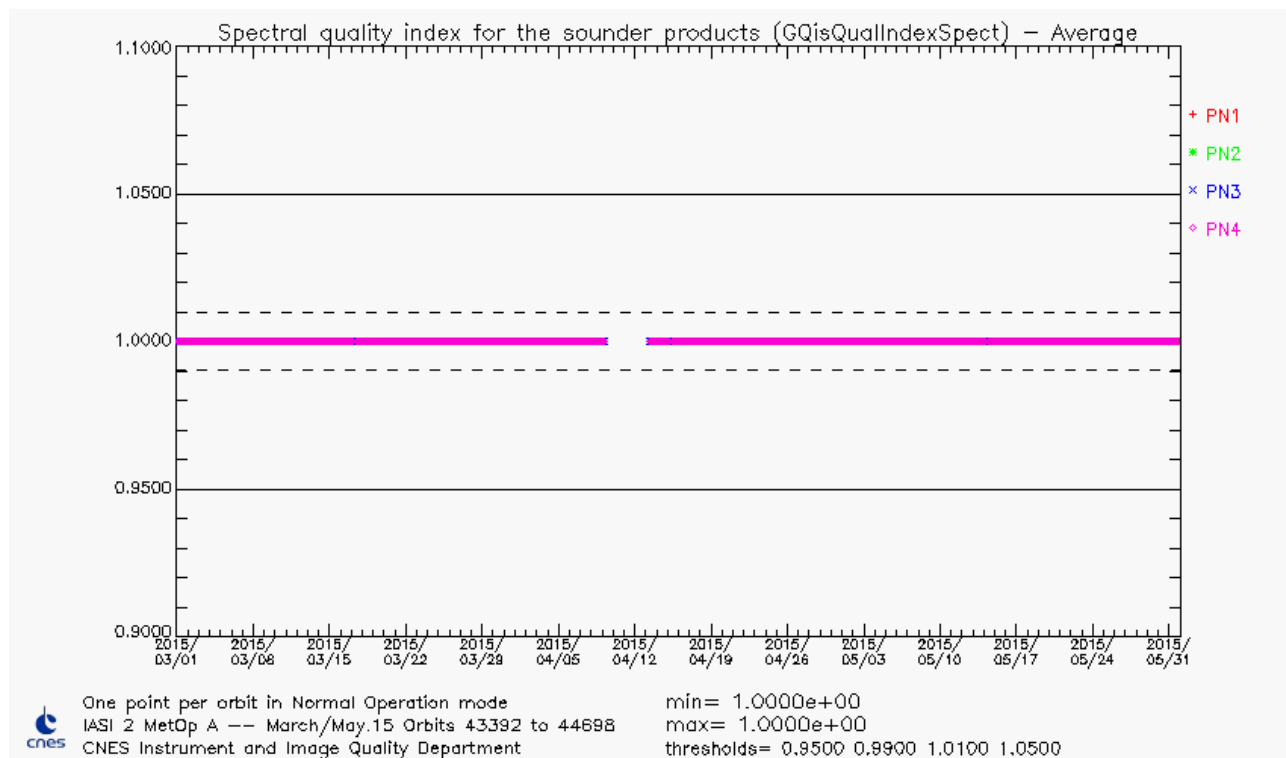


Figure 17 : GQisQualIndexSpect average (L1 data index for spectral calibration quality)

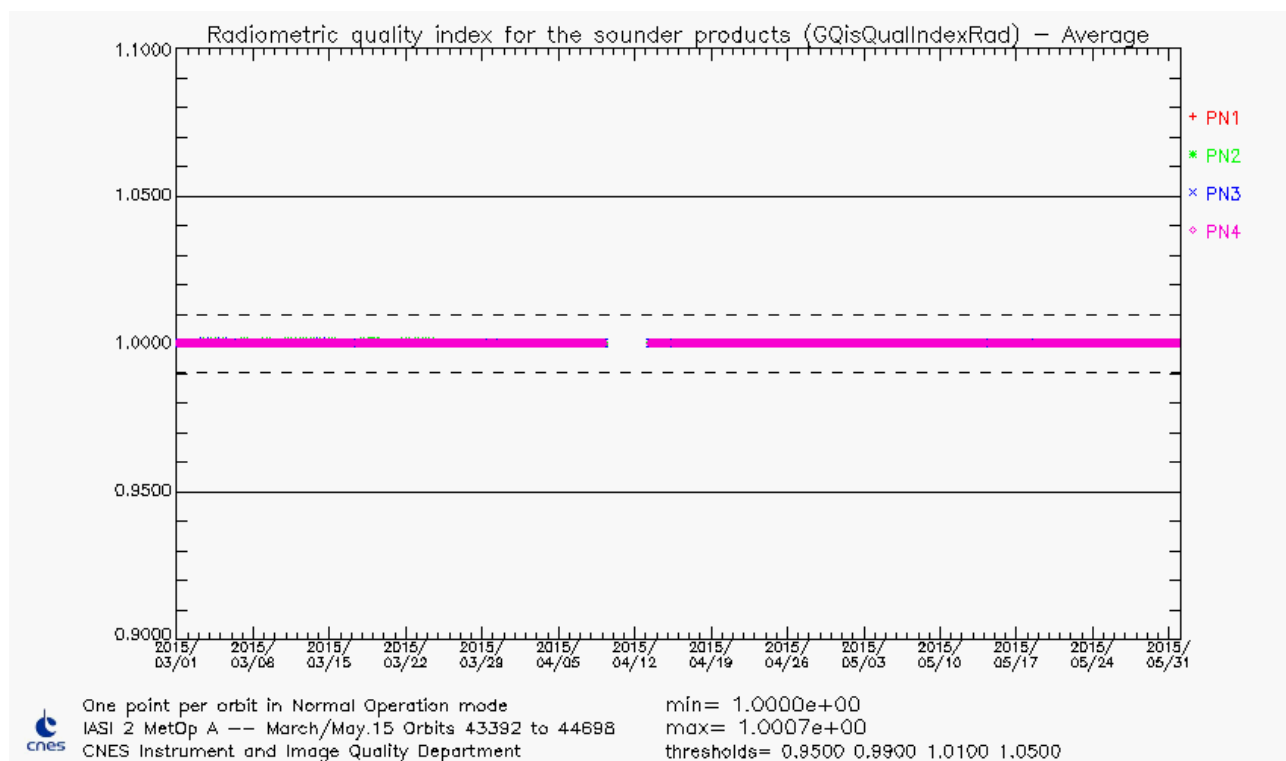




Figure 18 : GQisQualIndexRad average (L1 data index for radiometric calibration quality)

		Doc n°: IA-RP-2000-4225-CNE Issue: 1.0 Date: 2017-09-27 Sheet: 31 Of: 63
---	---	---

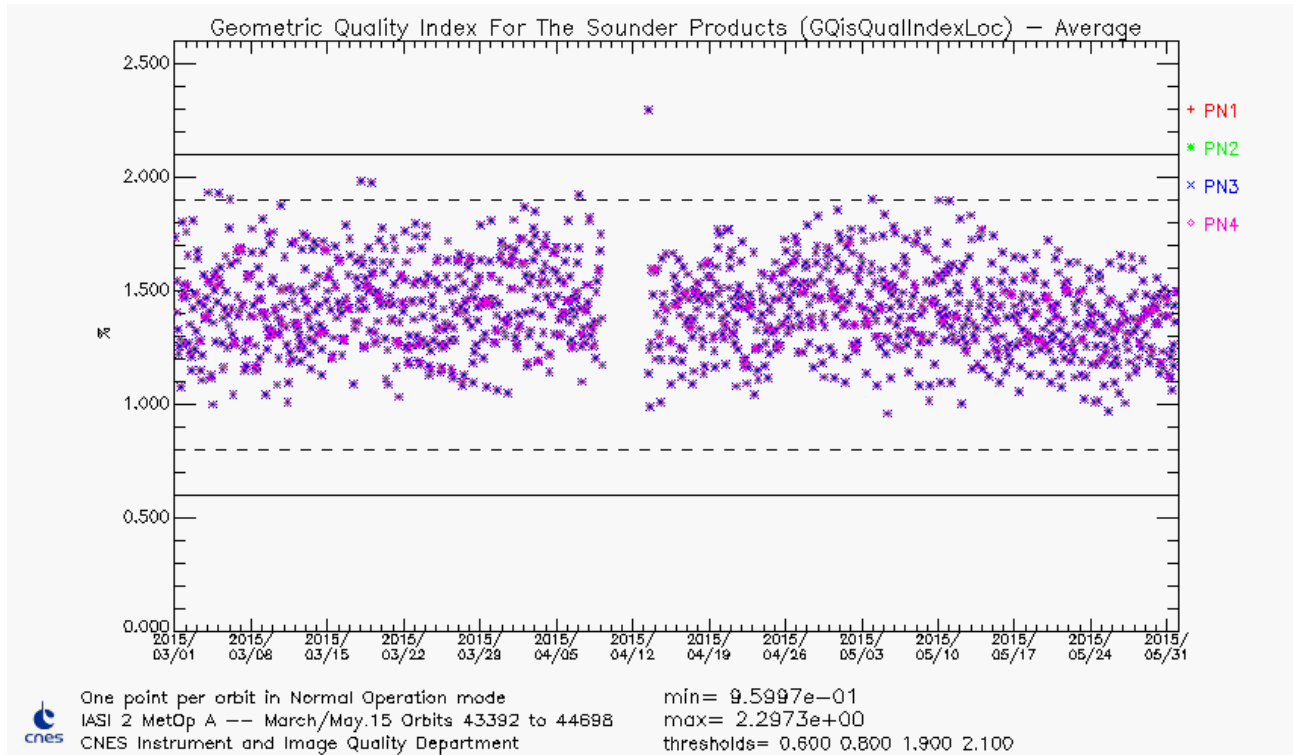


Figure 19 : GQisQualIndexLoc average (L1 data index for ground localisation quality)

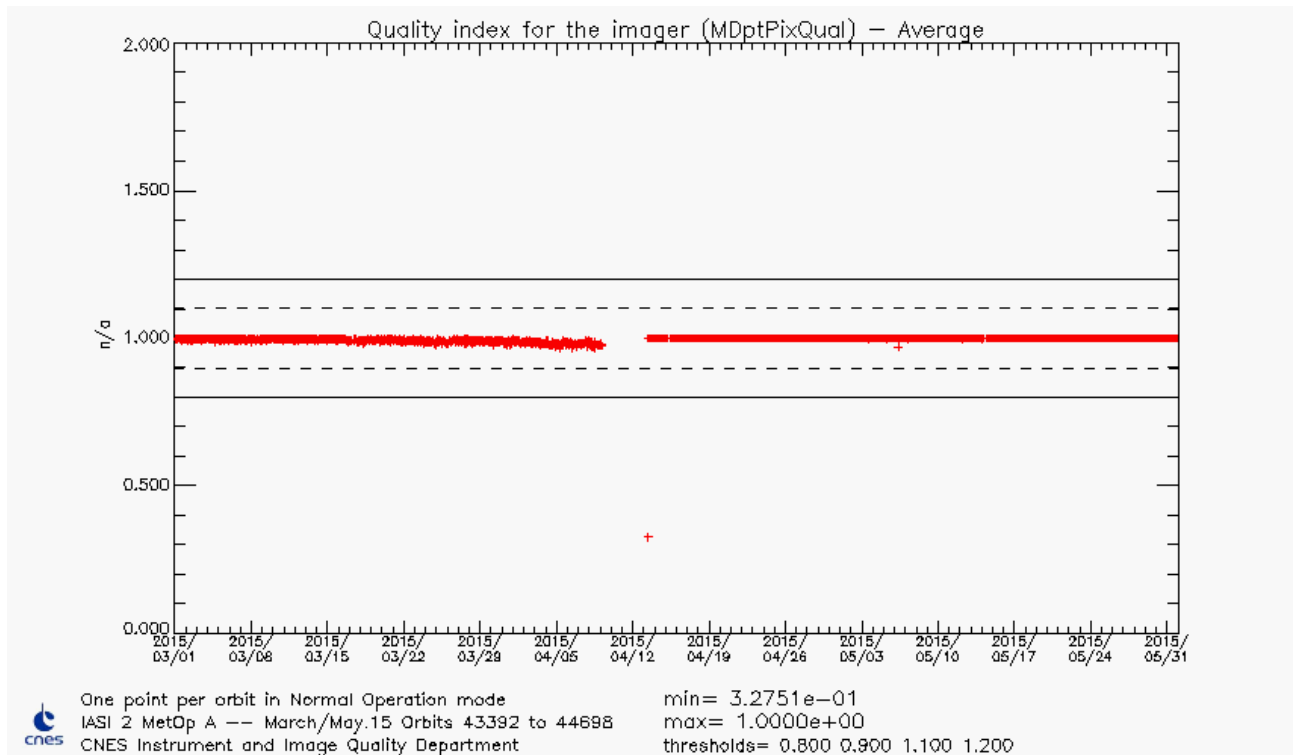


Figure 20 : MDptPixQual average (L1 quality index for IASI integrated imager; fraction of not dead pixels)

#### 4.4.3 Conclusion

L1 Flag and quality indicators are stable and meet the specifications.

## 4.5 SOUNDER RADIOMETRIC PERFORMANCES

### 4.5.1 Radiometric Noise

Monitoring the radiometric noise allows to monitor the long term degradation of the instrument as well as to look for punctual anomaly of IASI or other component of METOP.

#### Monthly L0 noise estimation (CE)

This monthly estimation is performed during routine External Calibration on BB views.

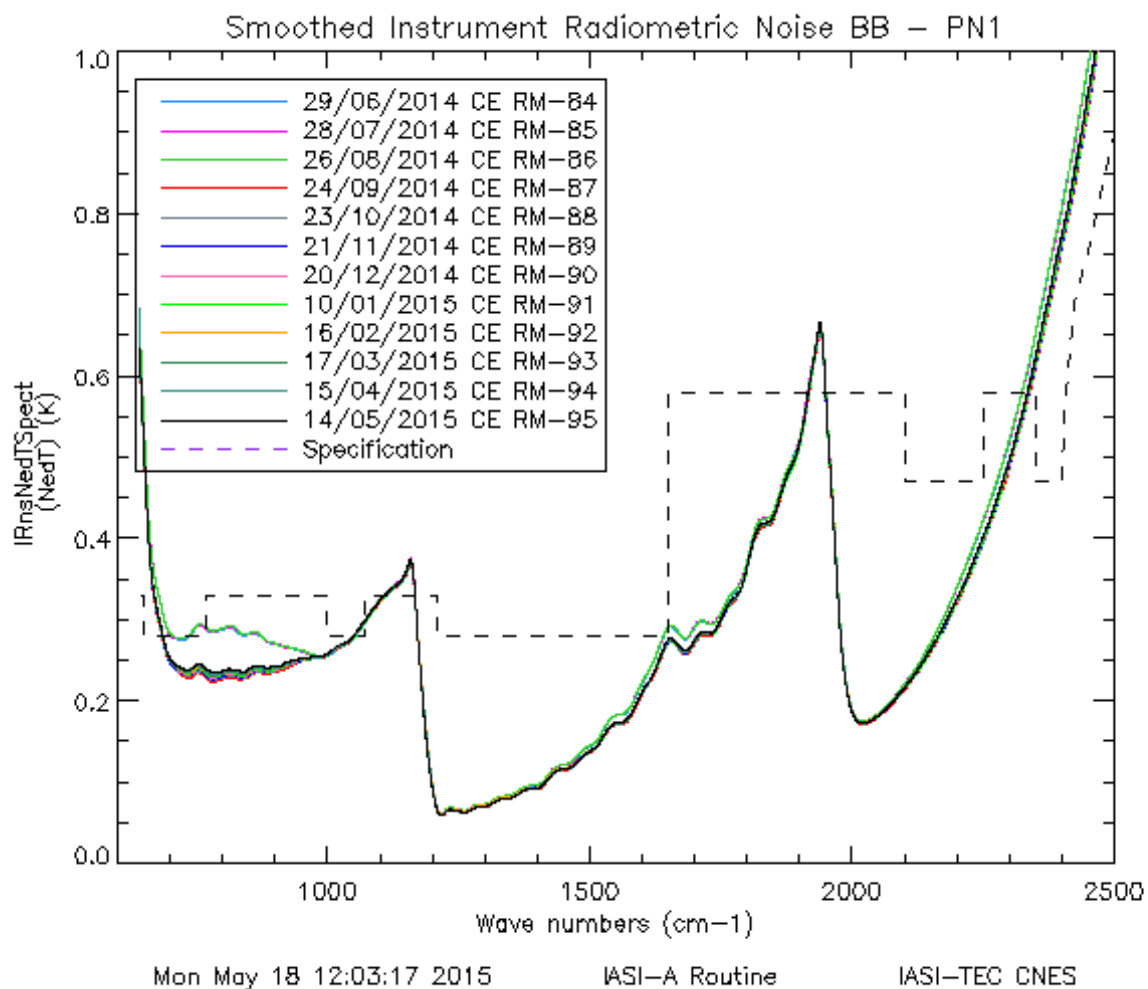


Figure 21 : Instrument noise evolution between start and end of the period

The instrument noise is very stable apart from ice effect between 700 and 1000  $\text{cm}^{-1}$ . This point will be developed in section 4.5.4.1.



#### 4.5.2 Radiometric Calibration

The radiometric calibration allows to convert an instrumental measurement into a physical value. The radiometric calibration is used to convert an interferogram into an absolute energy flux by taking into account instrument discrepancies. Even if the calibration has been studied on ground, it has to be continuously monitored in-flight in order to follow any potential degradation of the instrument (optics, detectors ...).

Approach: Radiometric fine characterization has been done during on-ground testing and Cal/Val. All parameters likely to cause a failure in radiometric calibration process have been identified and are continuously monitored. As long as they remain stable, there is no problem with radiometric calibration.

##### Evolution of scanning mirror reflectivity

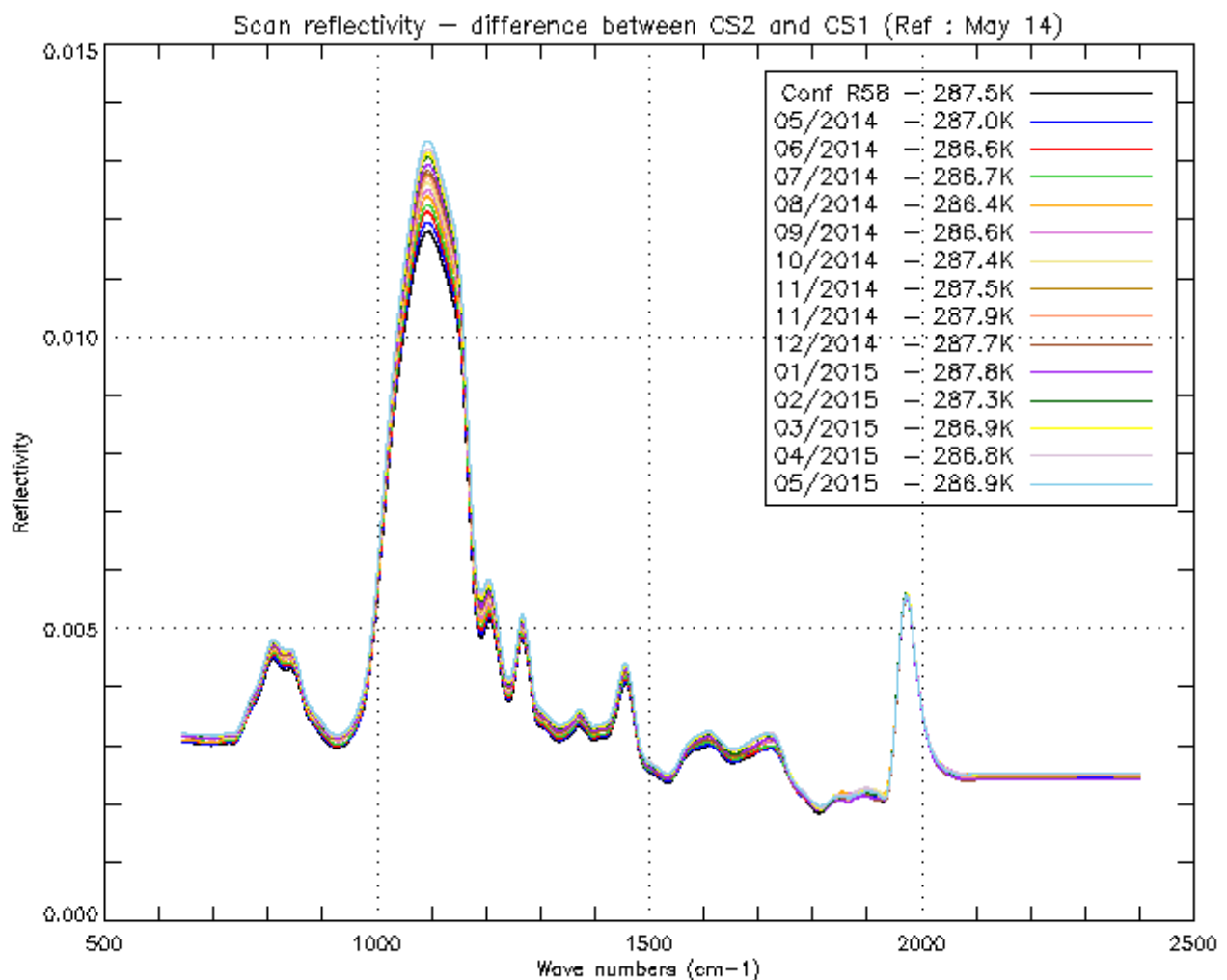
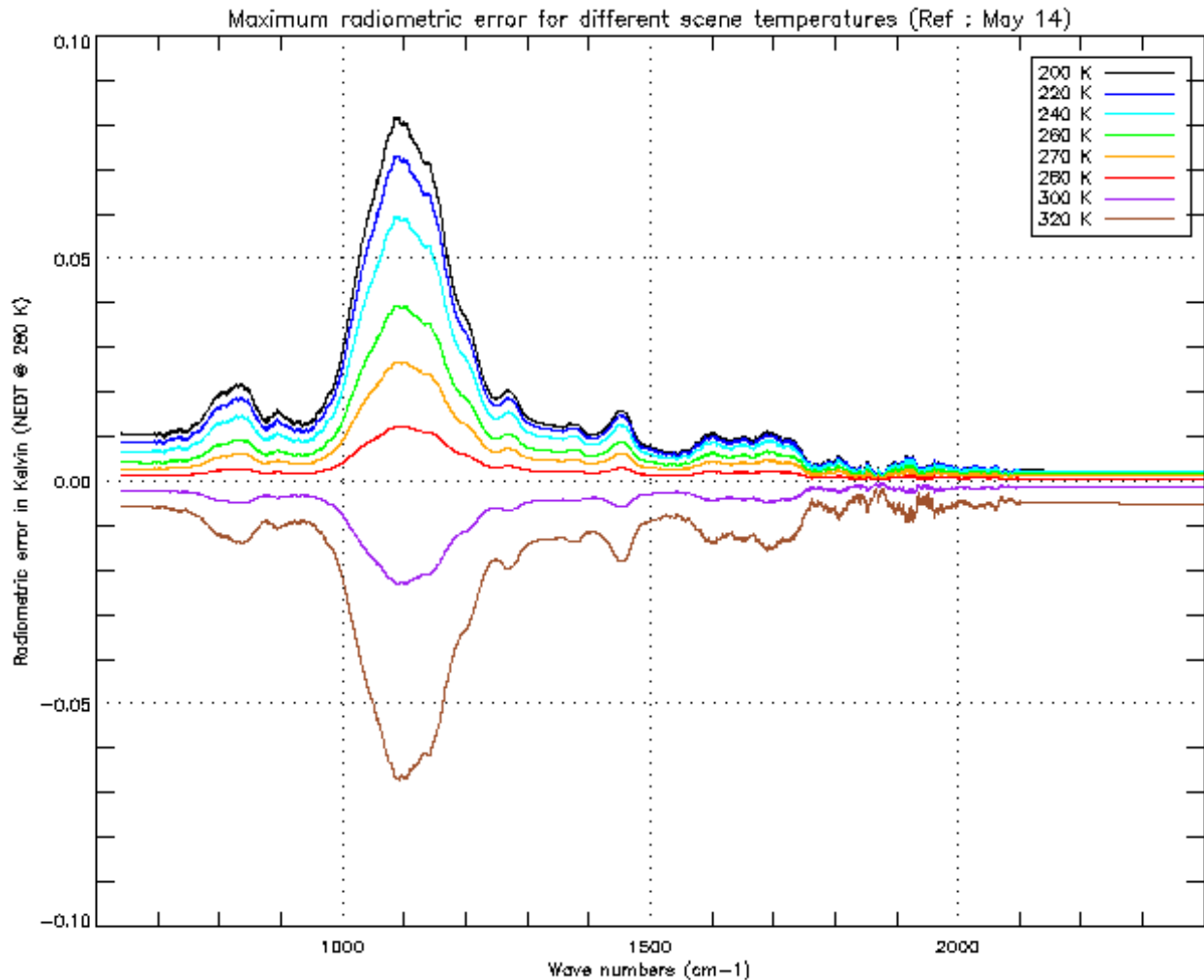


Figure 22 : Scan mirror reflectivity evolution

The reference reflectivity (in black) is the one computed on data from May 2<sup>nd</sup> 2014. We see a slight evolution within [1000-1100 cm<sup>-1</sup>] band. Values for wavenumbers greater than 2400 cm<sup>-1</sup> are not significant because of instrument noise.

The next figure shows the translation of scan mirror reflectivity in terms of maximum radiometric calibration error for different scene temperatures.



*Figure 23 : Radiometric calibration error due to scan mirror reflectivity dependency with viewing angle Maximum effect on SN1 for different scene temperature.  
Done with the period May 2014 / May 2015*

In any cases radiometric calibration maximum error is lower than the specification (0.1K). The scan mirror reflectivity law (on ground configuration) will be updated in the operational ground segment in June 2015 with May 2015 routine External Calibration data.

Internal black body

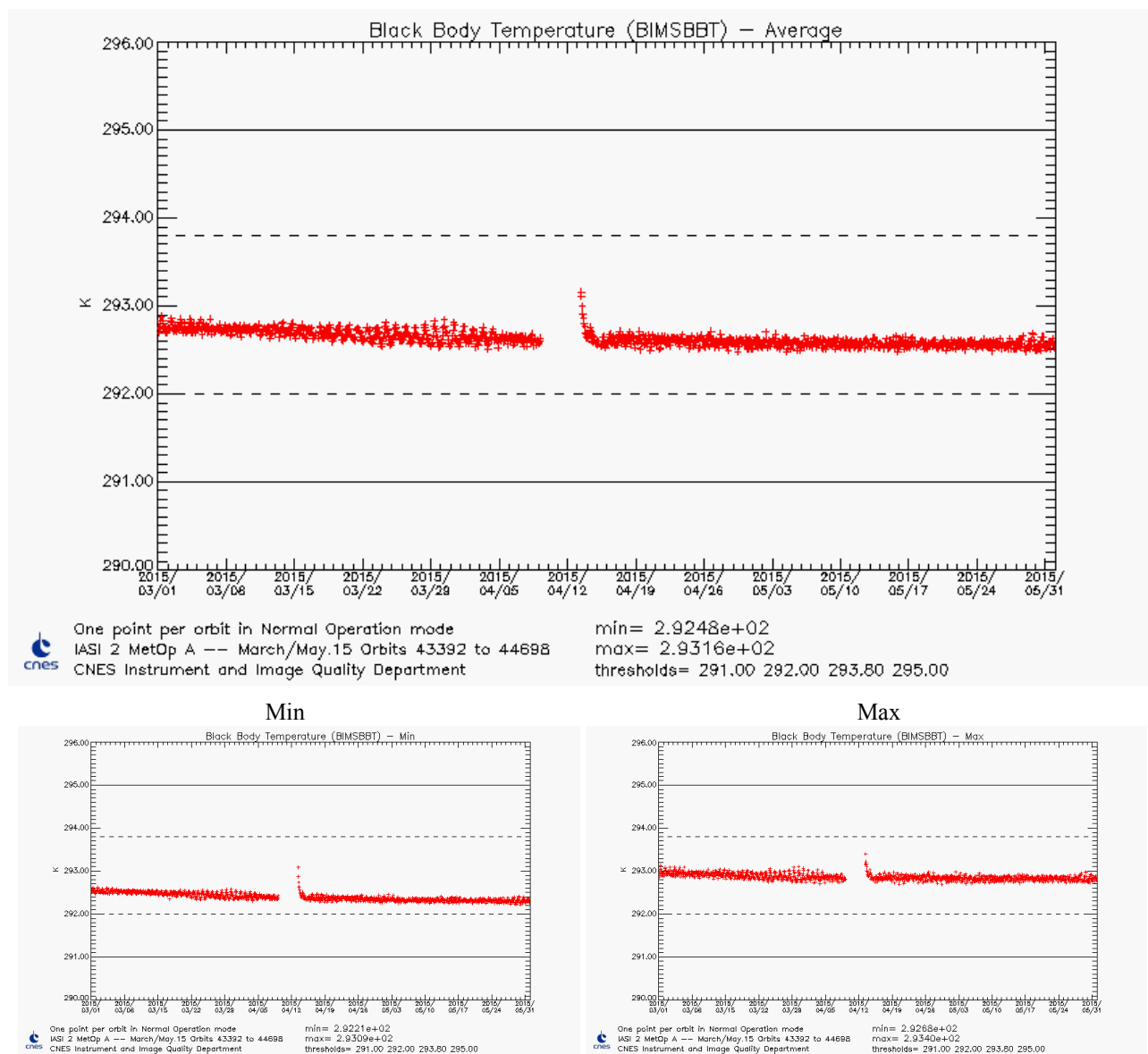




Figure 24 : Black Body Temperature

		Doc n°: IA-RP-2000-4225-CNE Issue: 1.0 Date: 2017-09-27 Sheet: 36 Of: 63
--	--	---

### Non linearity of the detection chains

Non-linearity tables of the detection chains are still nominal as long as sounder focal plane temperature variation amplitude is lower than 1K.

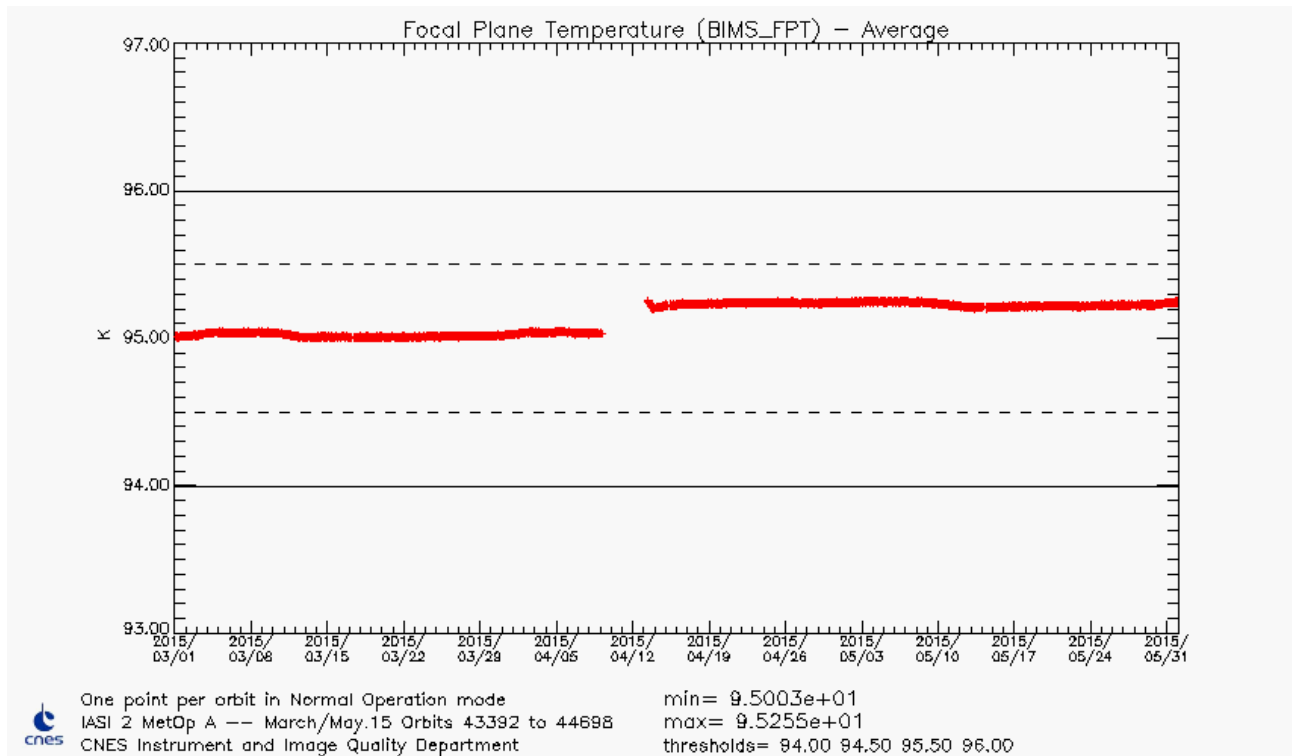




Figure 25 : Focal Plane Temperature

Since the IMS B-side switch (9 to 13th April), we observe an increase of the focal plane temperature due to the change of temperature probe (uncertainty on its transfer function).

		Doc n°: IA-RP-2000-4225-CNE Issue: 1.0 Date: 2017-09-27 Sheet: 37 Of: 63
---	---	---

### 4.5.3 Delay of detection chains

Long term stability and values lower than 400 ns are required in order to properly take into account cube corner velocity fluctuations.

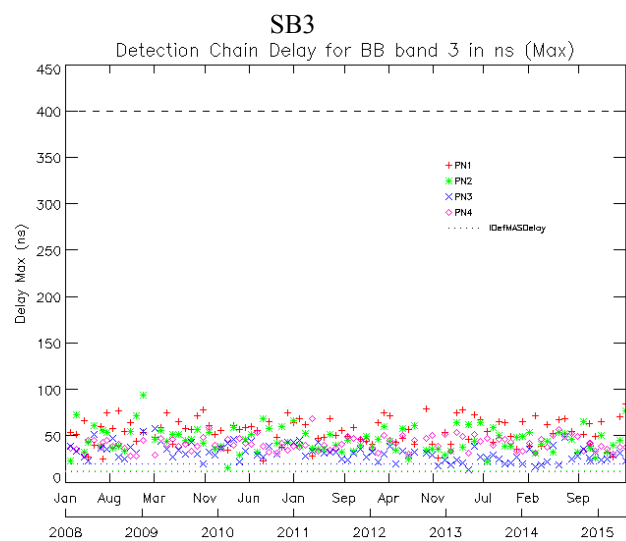
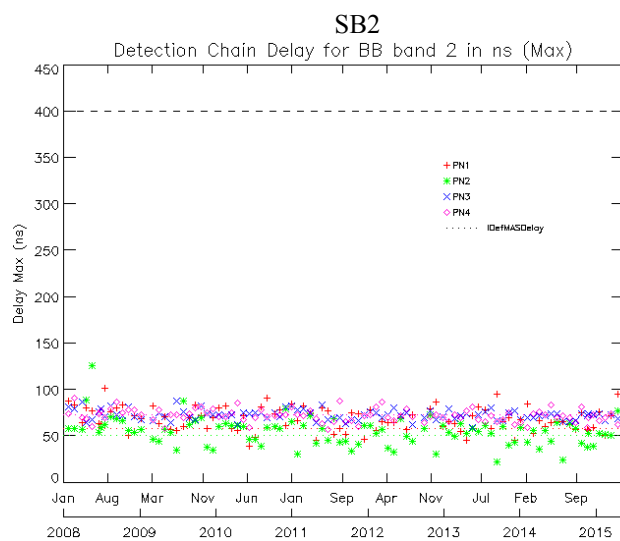
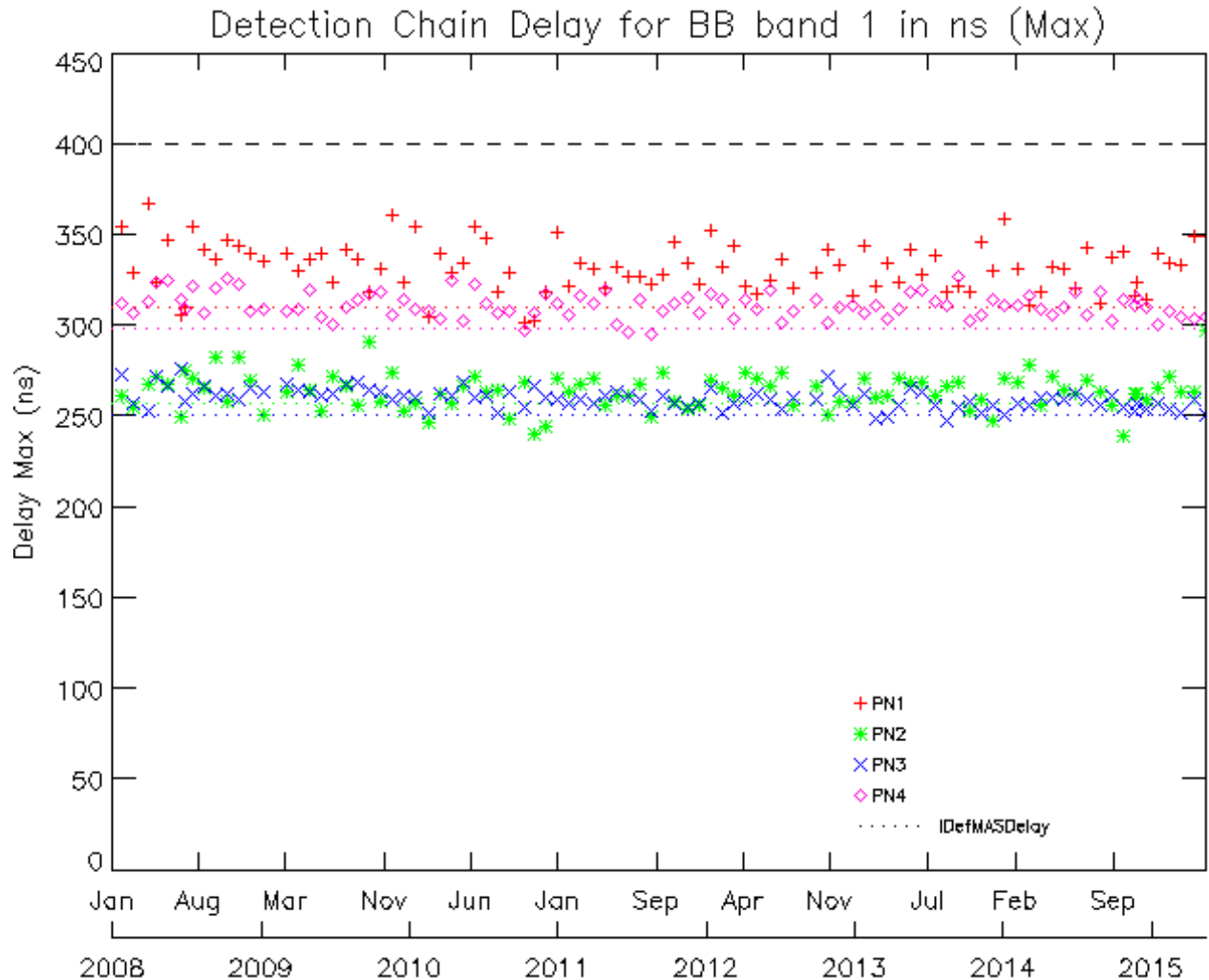




Figure 26 : Monitoring of detection chain maximum delays for all bands

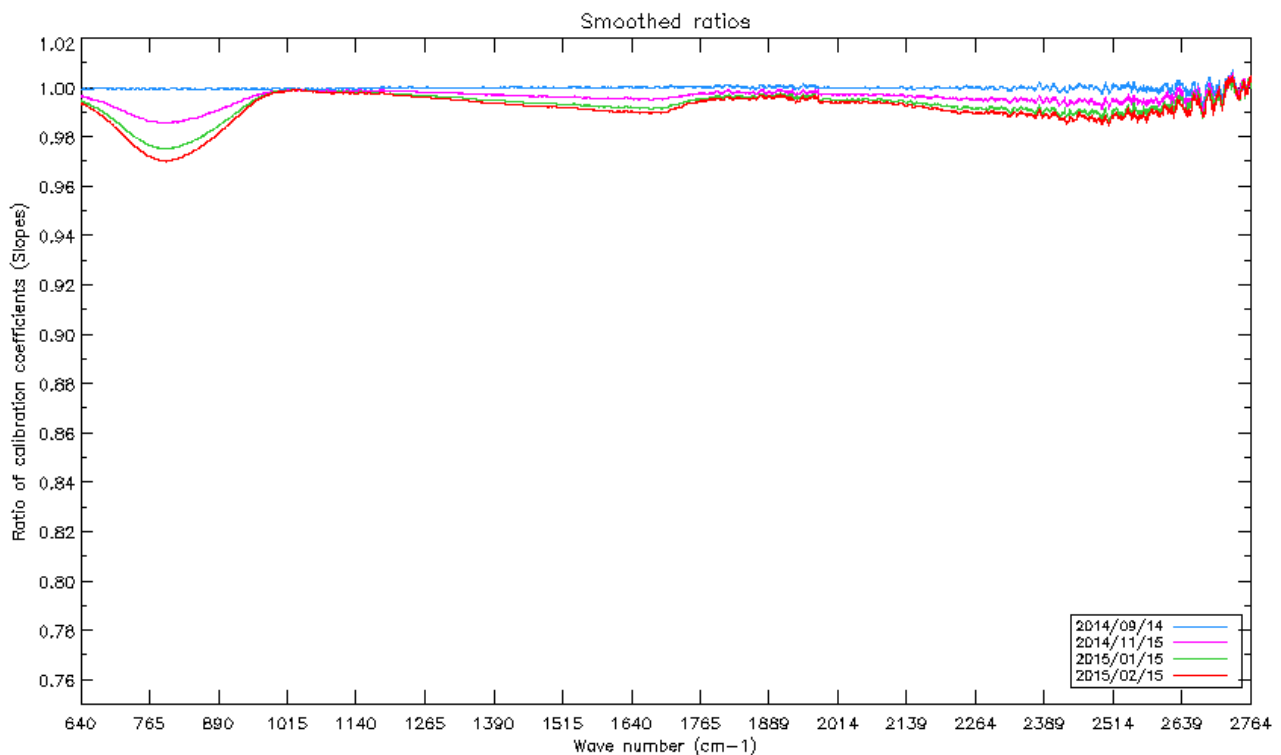
		Doc n°: IA-RP-2000-4225-CNE Issue: 1.0 Date: 2017-09-27 Sheet: 38 Of: 63
---	---	---

#### 4.5.4 Optical Transmission



##### 4.5.4.1 Ice

The IASI interferometer and optical bench are regulated at 20°C temperature, while the cold box containing cold optics and detection subsystem is at about -180°C. Water desorption from the instrument causes ice formation on the field lens at the entrance of IASI cold box. This desorption phenomenon is particularly important at the beginning of the instrument in-orbit life. That's why one of the very first activities of IASI in-orbit commissioning was an outgassing phase consisting in heating the cold box up to 300 K during 20 days. This operation allows removing most of the initial contaminants coming from IASI and other MetOp instruments. A routine outgassing is then needed from time to time to remove ice contamination, but less and less frequently as the desorption process becomes slower. A first run of this routine outgassing procedure (shorter duration and at 200 K), was done for validation purpose during commissioning phase in December 2006. The second one, which was actually the first in routine phase, was done in March 2008. The third one was done in August 2010 and the last was done on September 2014.

The maximum acceptable degradation of transmission is about 20% loss at 850 cm<sup>-1</sup> (which corresponds to an ice deposit thickness of about 0.5 µm).



*Figure 27 : Ratio of calibration coefficient slopes as a function of wave number and time after the last decontamination*

		Doc n°: IA-RP-2000-4225-CNE Issue: 1.0 Date: 2017-09-27 Sheet: 39 Of: 63
---	---	---

#### 4.5.4.2 Prediction of decontamination date

The transmission degradation rate is regularly monitored by CNES TEC through gain measurements given by calibration coefficients ratios.

The decontamination that occurred from 8<sup>th</sup> to 13<sup>th</sup> September is the last one.

#### 4.5.5 Interferometric Contrast

The interferometric contrast is defined as the interferogram fringe discrimination power. Figure 28 shows temporal evolution of instrument contrast on the quarter for all pixels and all CCD.

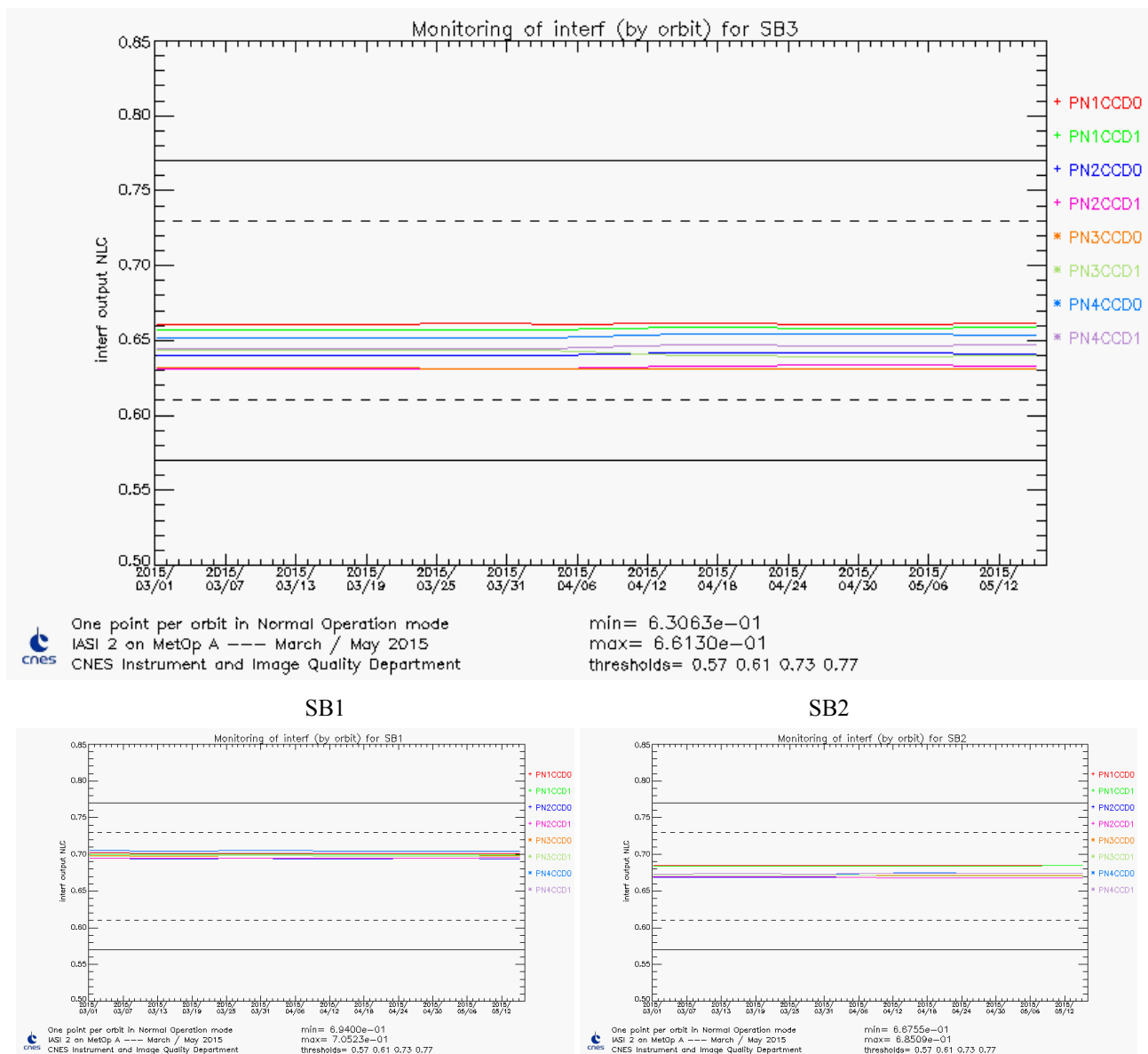


Figure 28 : Contrast Monitoring

#### 4.5.6 Interferogram baseline

The interferogram baseline is the mean value of the interferogram. Figure 29 shows temporal evolution of the baseline of the raw interferograms on calibration targets (BB and CS). The values are raw values, they are not physical, but the evolution is interesting: as the values are proportional to the energy received from a target and calibration targets are stable, the evolution can show the decrease of instrument transmission or events due to energetic particles.

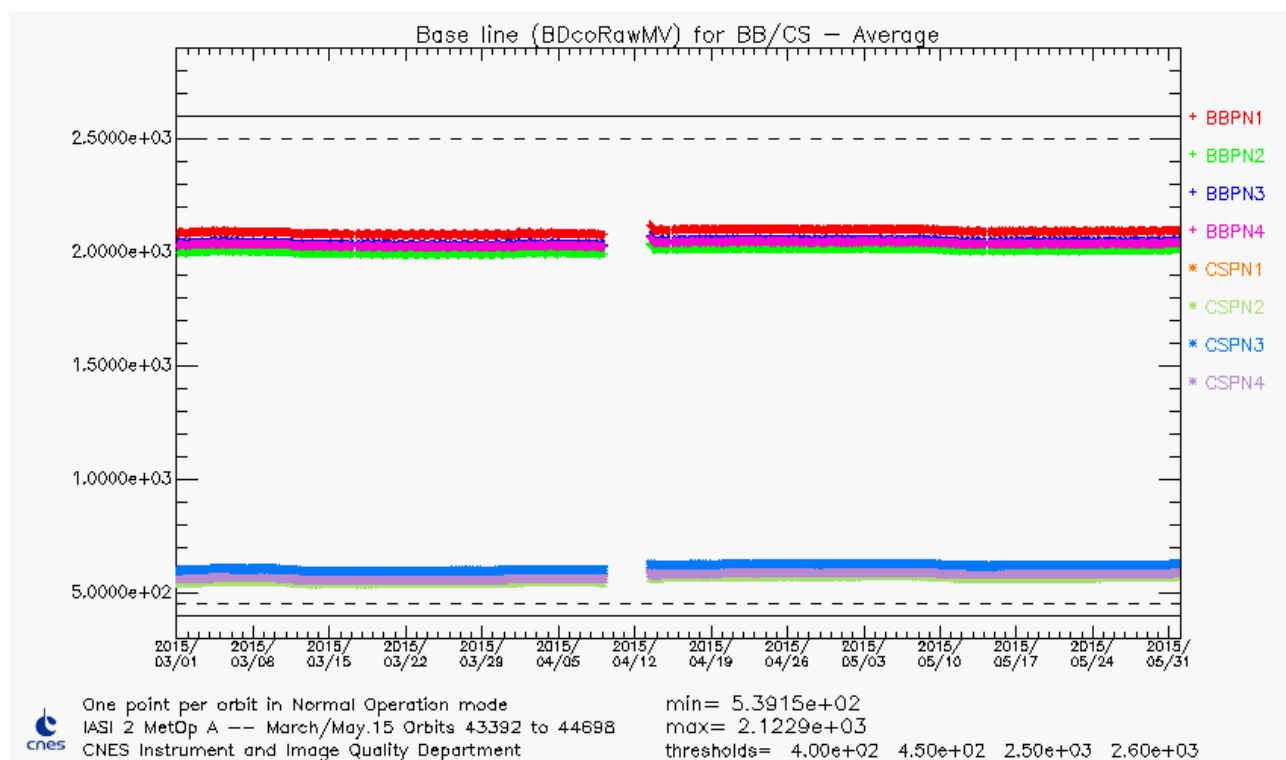


Figure 29 : Monitoring of interferogram baseline



#### 4.5.7 Detection Chain

Detection chains are tuned in gain and offset via telecommand. The goal is to avoid saturation while conserving the maximum dynamic to limit digitalization noise.

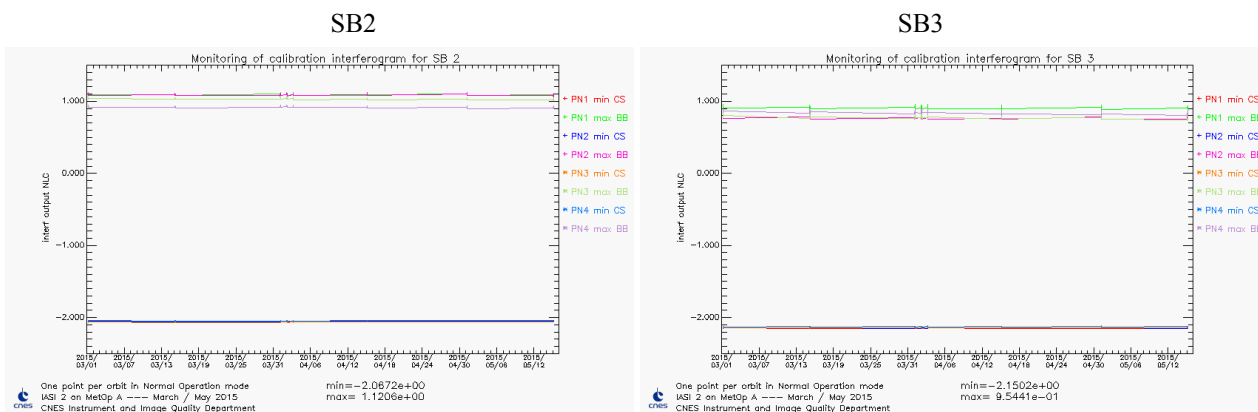
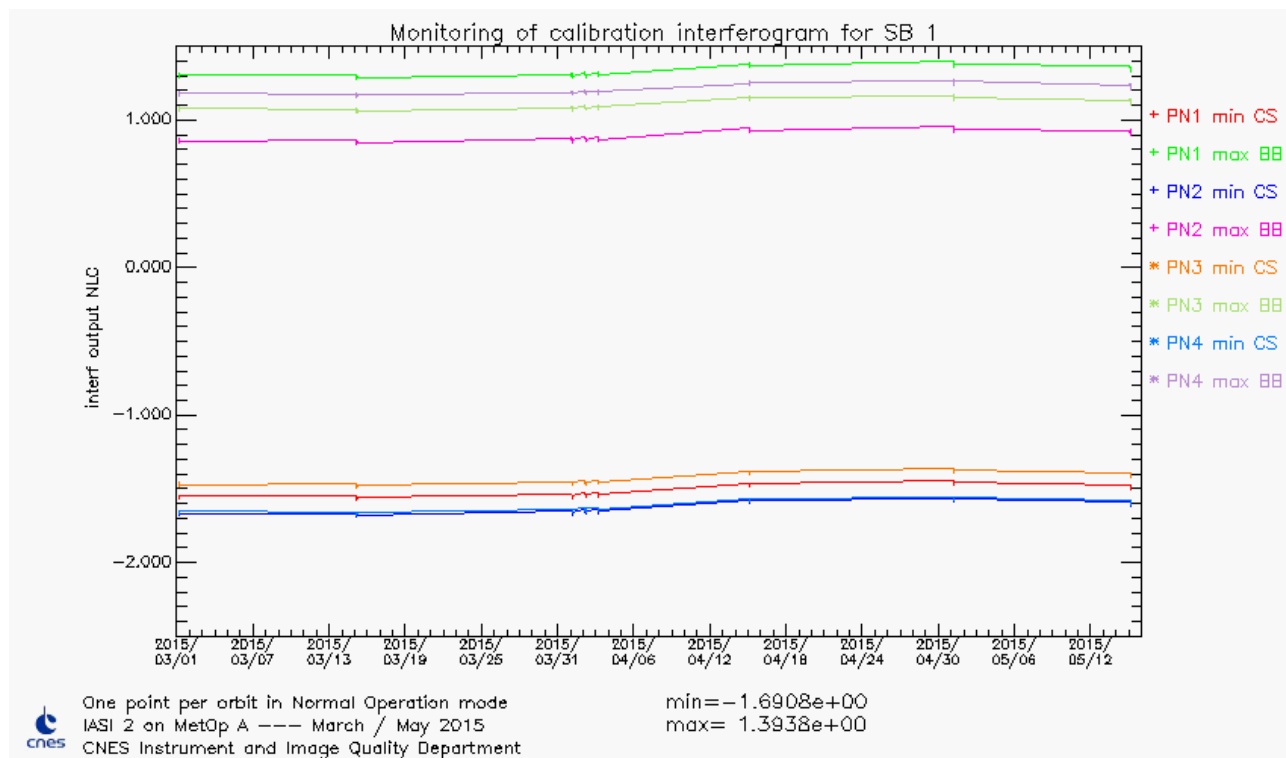




Figure 30 : Monitoring of detection chain margins

Margins are sufficient for the moment. The slight decreasing slope in SB1 (BB) for all pixels is linked to the instrument transmission evolution already mentioned in §4.5.4.1.

#### 4.5.8 Conclusion

The radiometric performances of IASI are nominal and stable. The last decontamination was performed in September 2014. Scan mirror reflectivity was updated in June 2014 with May 2014 data. The next update has been done with May 2015 data and should be updated in the operational ground segment in June 2015.

		Doc n°: IA-RP-2000-4225-CNE Issue: 1.0 Date: 2017-09-27 Sheet: 42 Of: 63
---	---	---

## 4.6 SOUNDER SPECTRAL PERFORMANCES

The goal of the spectral calibration is to provide the best estimates of spectral position of the 8461 IASI channels.

The large sensitivity of infrared spectrum to spectral calibration errors has led to stringent specifications:

- A prior knowledge of spectral position better than of  $2.10^{-4}$  (design)
- A posterior maximum spectral calibration relative error of  $2.10^{-6}$  (after calibration by OPS)

In order to reach the specification of  $2.10^{-6}$ , we need an accurate Instrument Spectral Response Function (ISRF) model. This model have been done and validated in the early time of IASI development.

For sake of operational time constrain, complete ISRF calculation is not done in real-time by OPS software but pre-calculated and stored in a database called “spectral database”. OPS processing determine on-line the most relevant instrument function to be used by OPS with respect to current values of a set of parameters (interferometric axis, cube corner offset...).

The approach to monitor IASI spectral performances is very similar to the one used for radiometric calibration. Spectral calibration fine characterization has been done during ground testing and Cal/Val. All parameters likely to cause a failure in spectral calibration process have been identified and are continuously monitored. As long as they remain stable, there is no problem with IASI spectral calibration.

In addition, a spectral calibration assessment is done over homogeneous scenes when IASI is in external calibration, nadir view.

### 4.6.1 Monitoring of the ISRF inputs

#### 4.6.1.1 Position of the interferometric axis

The interferometric axis is the cube corner displacement direction. Its value was around ( $Y = -160\mu\text{rad}$ ;  $Z = -450\mu\text{rad}$ ) since the beginning of the life of IASI-A. Since the change of IPSF positions in 2013/05/16, its value has changed and is now stable around ( $Y = 445\mu\text{rad}$ ;  $Z = 195\mu\text{rad}$ ). The central position used in the “spectral database” generation, are  $400\mu\text{rad}$  and  $200\mu\text{rad}$ , respectively for Y and Z axis.

Since the drift of the interferometer axis is lower than  $300\mu\text{rad}$ , there is no need to update the “spectral database”.

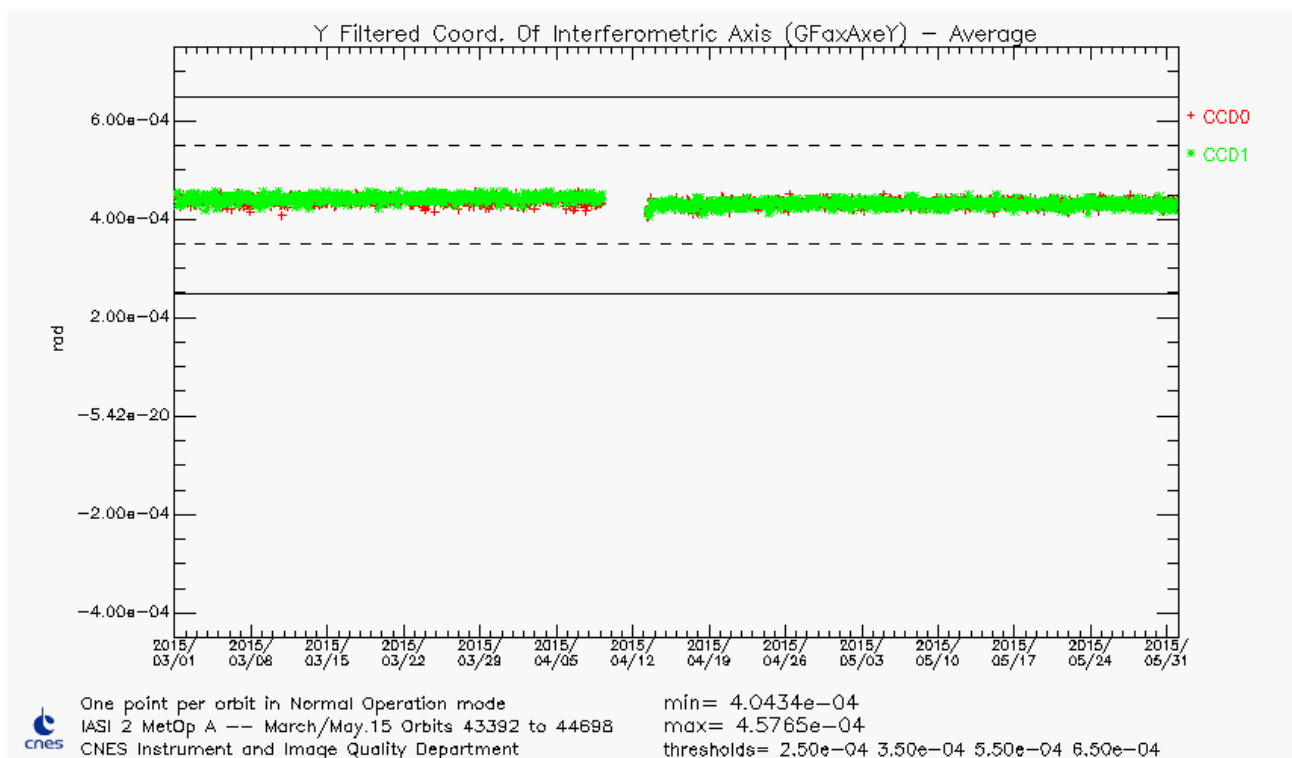
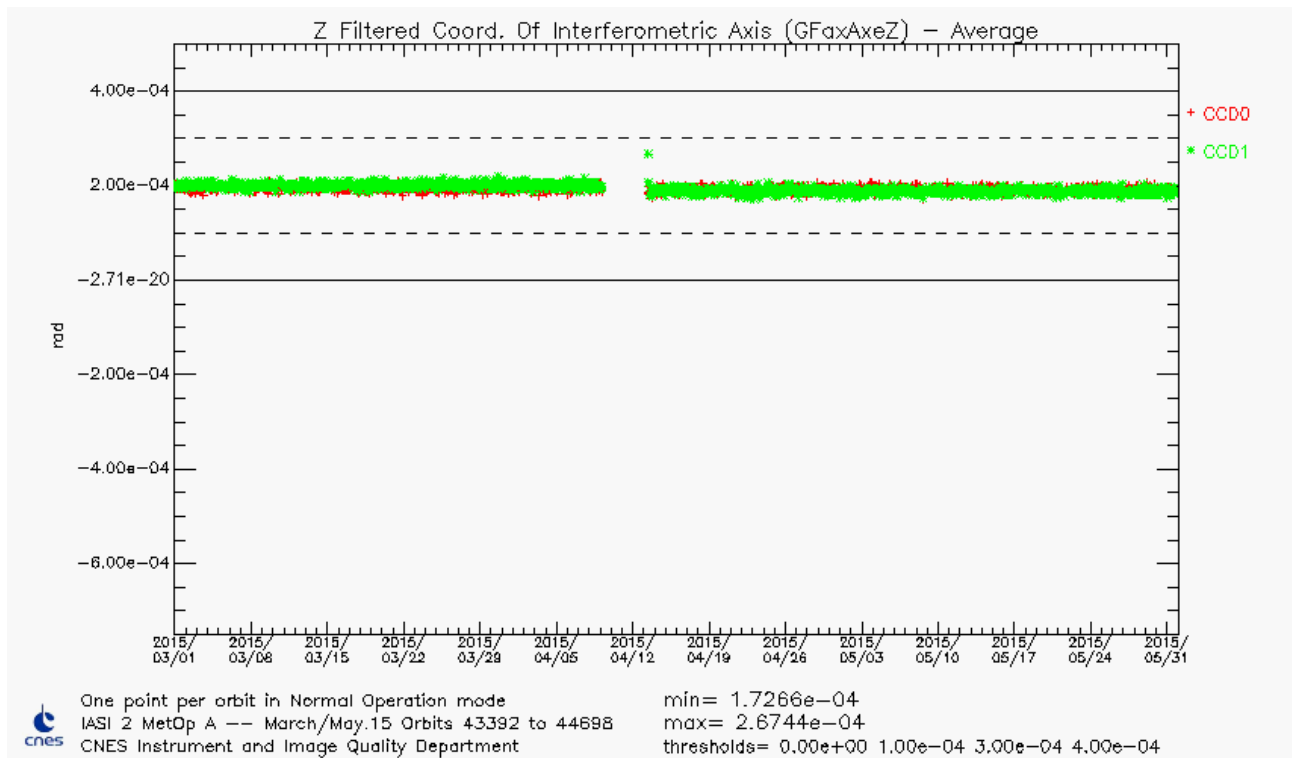
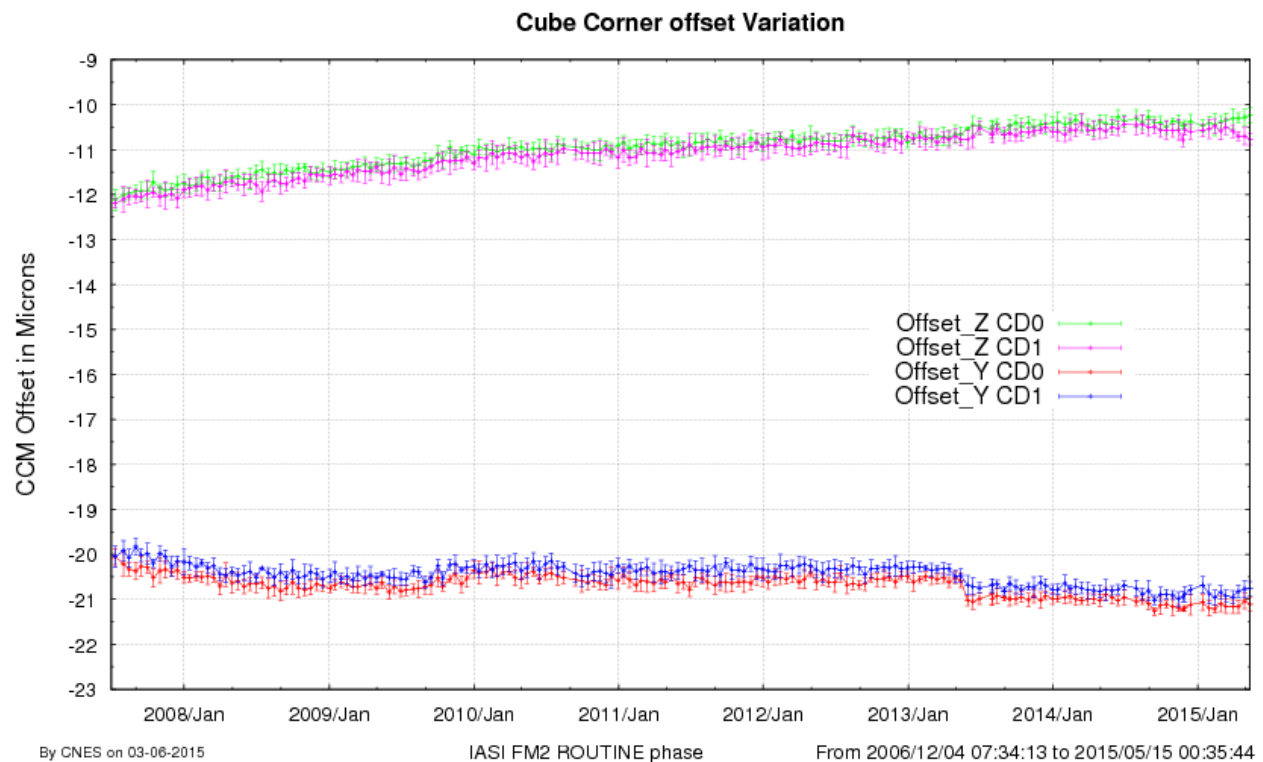




Figure 31 : GFaxAxeY average (Y filtered coordinates of sounder interferometric axis)



#### 4.6.1.2 Cube Corner constant offset



Reference cube corner offsets, used in the spectral database of the period (ODB14), are -21.08  $\mu\text{m}$ , -20.69  $\mu\text{m}$ , -10.49  $\mu\text{m}$  and -10.77  $\mu\text{m}$ , respectively for Y CD0, Y CD1, Z CD0 and Z CD1.

		Doc n°: IA-RP-2000-4225-CNE Issue: 1.0 Date: 2017-09-27 Sheet: 44 Of: 63
--	---	---

The slight change of the cube corner constant offset that happened in May 2013 is due to the update of the IPSF positions in the ground configuration.

Since the drift of cube corner offset is lower than 4  $\mu\text{m}$ , there is no need to update the “spectral database”.

#### 4.6.1.3 Cube corner velocity

Refer to REVEX, paragraph 5.5.

#### 4.6.1.4 Interferometer optical bench temperature

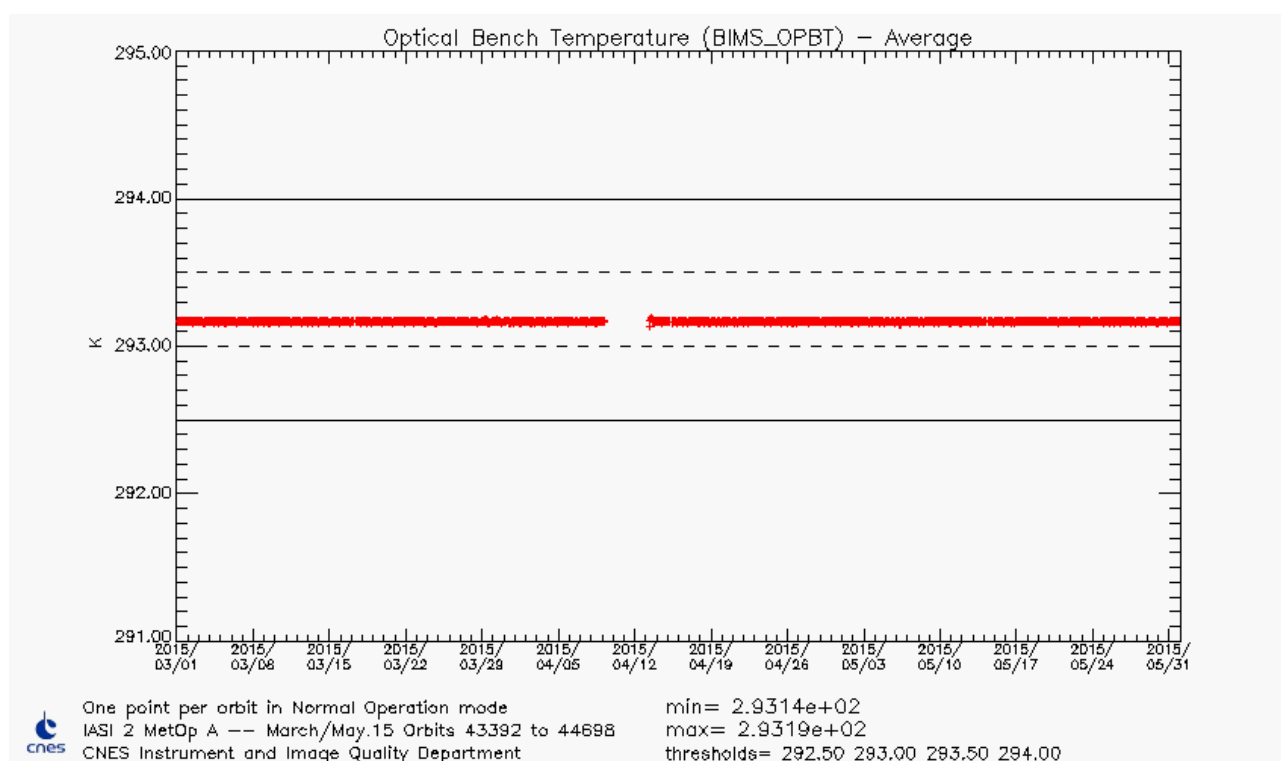


Figure 34 : Optical bench Temperature

### 4.6.2 Spectral calibration assessment

This assessment is performed during routine External Calibration on Earth views at nadir (SP 15).

#### 4.6.2.1 Absolute spectral calibration assessment

IASI LIC spectra are compared with simulated spectra over homogeneous scenes, warm and clear.

The spectra are simulated with 4AOP radiative transfer model with collocated input profiles: temperature and water vapor profiles are extracted from meteorological analysis from ECMWF, the others gazes like CO<sub>2</sub>, O<sub>3</sub>, CO, N<sub>2</sub>O and CH<sub>4</sub> profiles are extracted from a climatological data base.

The IASI spectra are selected using the pseudo channel Variance of the IIS radiance. The variance must be lower than 0.65 Kelvin, that is very close to the IIS noise level. This criterion insures a quasi-perfect homogeneity of the scenes (but not necessarily clear). The minimum of the pseudo channel IIS brightness temperature is 286K, which insures to have a hot scene, rejecting the areas where there is a lack of dynamic in the atmospheric spectral lines and rejecting the majority of cloudy scenes (which are not simulated). Then only contiguous selected scenes are kept (20 lines maximum, 1000 km).

The 4AOP spectra are simulated using the coordinates of the center of each sequence.

The comparison is done by using the correlation method in spectral windows (using the derivative of the spectrum). The position of the maximum of the correlation coefficient gives us the spectral shift. The result is expressed in terms of relative spectral shift error between L1C simulated and measured spectra for each pixel.

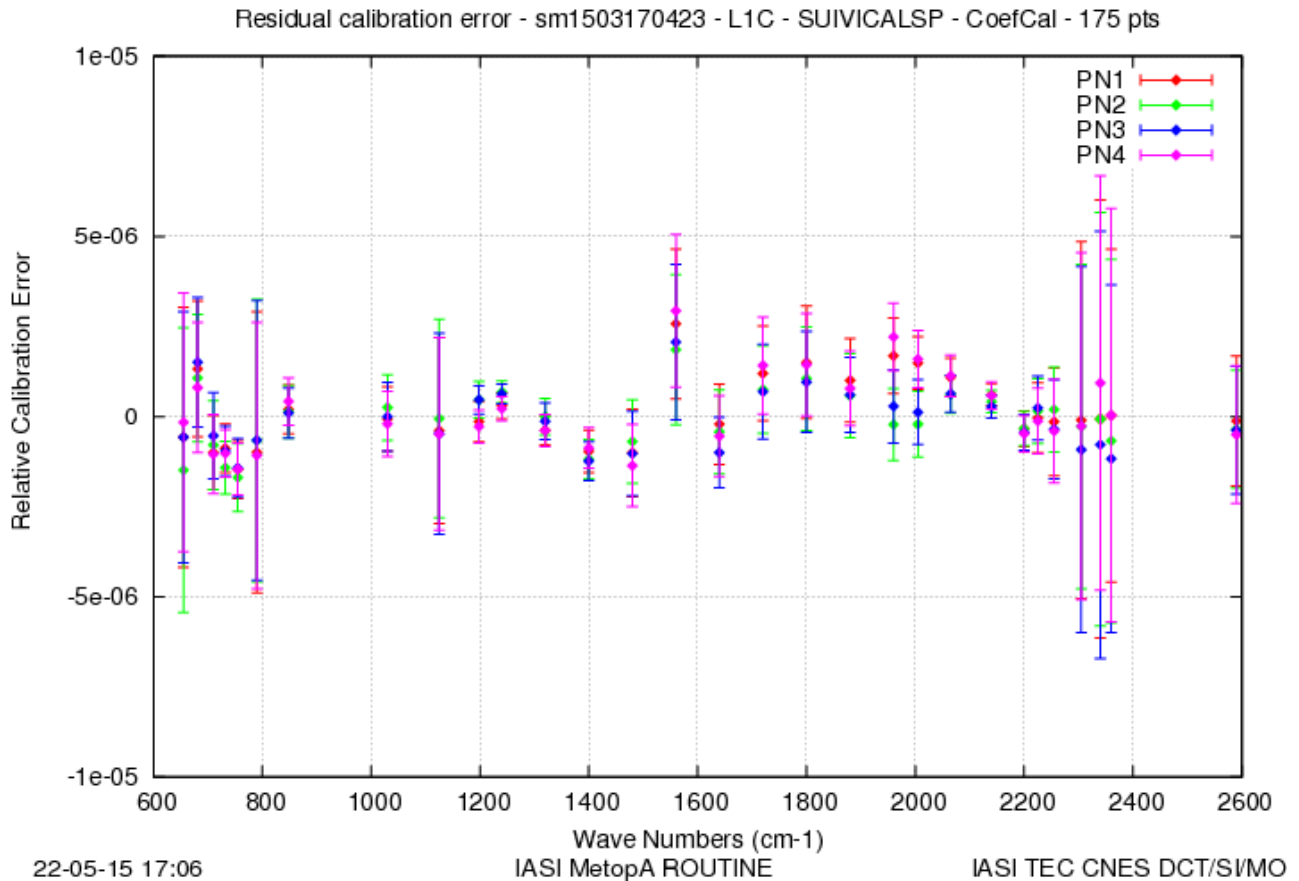


Figure 35 : Spectral shift error between L1C IASI and simulated L1C with A4/OP + ECMWF

The absolute spectral calibration assessment by comparison with a model is fully satisfactory on spectral bands that permits this exercise, the specification of  $2.10^{-6}$  is reached.

We can note that the spectral shift in the inter-band is not good because of a sharp gradient of the spectral filters (transmission function) at the edge of spectral bands. So, the energy in a line is not the same in every channel included in the line, the barycenter of the line changes, that induces a spectral shift. For B1/B2, the inter-band limit is around  $1169 \text{ cm}^{-1}$ , and for B2/B3 it is around  $1953 \text{ cm}^{-1}$ .

The model has its limits : it is not true everywhere in the spectrum, because the geophysical conditions are not well known. For example, in B2 a bad knowledge of the water vapor content leads to a bad simulation and thus to a spectral shift in B2 only due to the variability of the water vapor. There are still improvements to make on spectroscopy and the radiative transfer models.

#### 4.6.2.2 Interpixel spectral calibration assessment

Over the same homogeneous scenes used for absolute spectral calibration assessment, IASI L1C spectra of each pixel are compared with the average spectra of all pixels. The result is expressed in terms of interpixel relative spectral shift error.

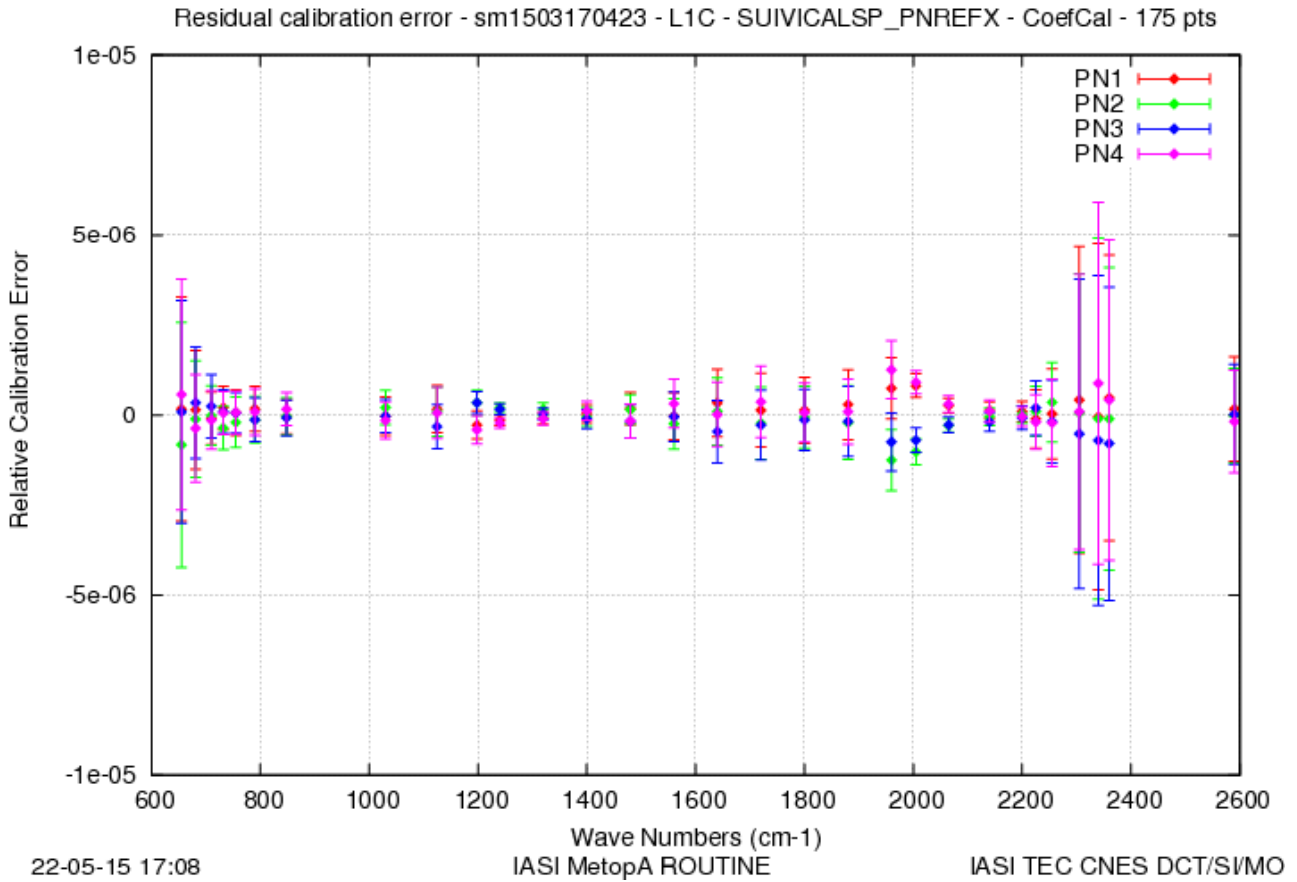


Figure 36 : Inter pixel spectral shift error for L1C IASI

The interpixel spectral calibration is better than 0.2ppm.

The results in the interband region are higher for the same reasons exposed in paragraph 4.6.2.1 . The error bars are high in B3 because of the noise that is higher at the end of B3.

In conclusion, the IASI pixels are spectrally independent.

#### 4.6.3 Ghost evolution monitoring

On-ground test of the instrument has shown a perturbation in the ISRF mainly caused by micro-vibrations of the interferometer separator blade induced by the compensation device.

Ghost origin is understood to be due to micro-vibrations of the beam-splitter. It is therefore stronger for the FOVs which project onto the top part of the beam-splitter (which vibrates more), and weaker for the FOVs which project onto the bottom part of the beam-splitter as it is attached to the optical bench.

The micro-vibrations of the beam-splitter lead to a sampling jitter of the interferogram. The perturbed interferogram  $I(t)$  is expressed as:

$$I(t) = \frac{I_0}{2} \cdot \cos(2 \cdot \pi \cdot \nu_0 (x_{nom} + \delta x(t)))$$

with  $\delta x(t) = U_0 \cdot \cos(2 \cdot \pi \cdot f \cdot t + \psi)$  the part added by the ghost

The phase  $\psi$  is random, the frequency is  $f = 380\text{Hz}$ , and the amplitude is difficult to quantify in flight.

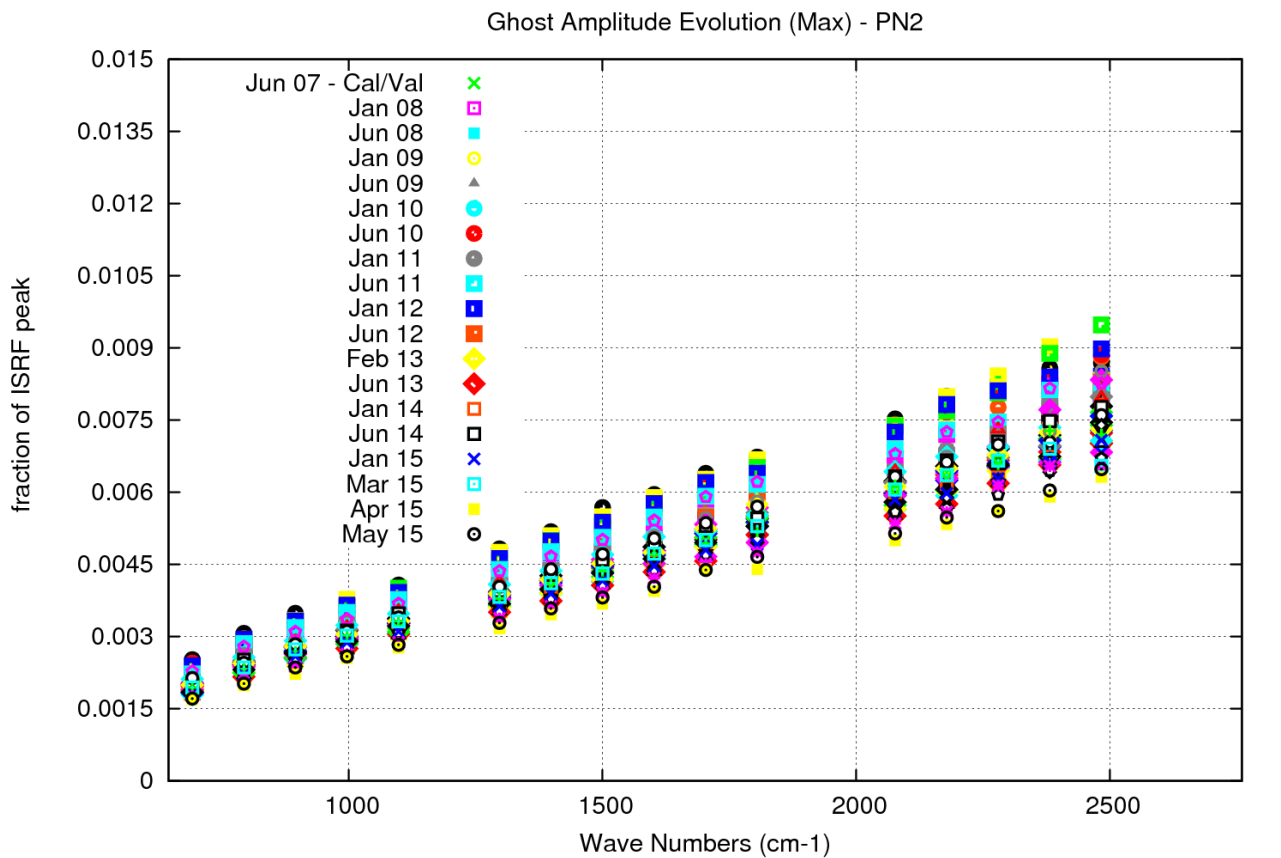
The ghost affects the ISRF by replicating it at about  $\pm 14\text{cm}^{-1}$ . The amplitude of these replications is very low with respect to ISRF maximum value. The amplitude and the central wave number of ISRF replications are function of: cube corner velocity, frequency and mechanical amplitude of the beam-splitter vibration and wave number.

The ghost is monitored at TEC using monthly external calibration (BB views), by computing the ratio between the maximum of the residuals of the imaginary part of the spectrum after on board calibration and the Planck function at the black body temperature:

$$fractionISRF_{peak} = \frac{\max(BArcImagMean)}{Planck(T_{BB})}$$

This ratio understood to be proportional to the ratio between the replicated ISRF due to the ghost with respect to  $ISRF_{max}$ .

The evolution over time of ghost amplitude with respect to  $ISRF_{max}$  amplitude is shown below for the 4 IASI pixels.



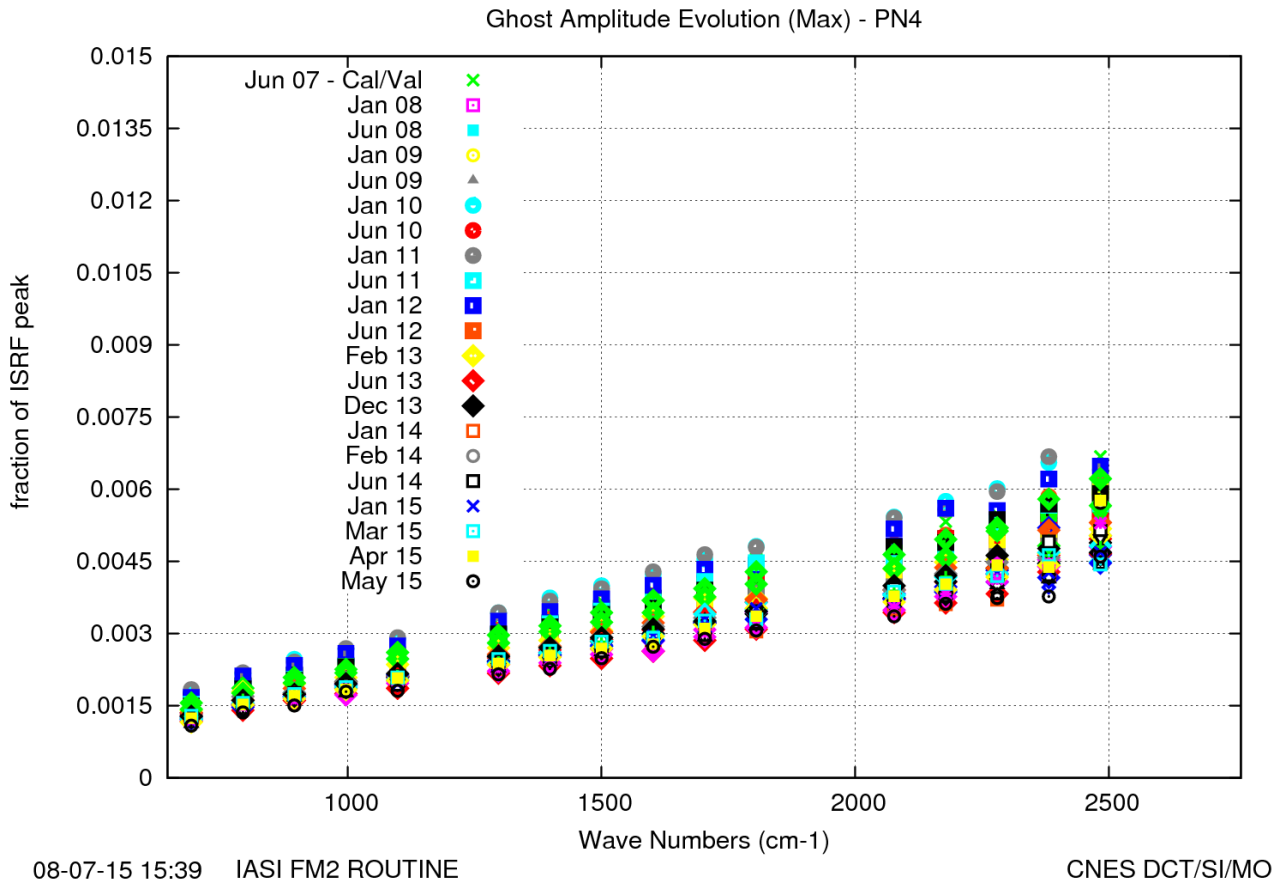


Figure 37 : Ghost amplitude as a function of wave number for different time (Top: pixel 2, bottom: pixel 4)

Maximum values of fraction of  $\text{ISRF}_{\text{max}}$  (@2760  $\text{cm}^{-1}$ ) are proportional to wavenumber; they are similar for the couples pixel 1-2 and pixel 3-4, due to the position of the beam splitter wrt the FOV.

The ghost has an effect on the radiometric calibration and leads to an imaginary residual because the phase at Zpd of the micro-vibration is random and changes each time the mobile cube corner changes its direction. So the phase added by the ghost is not the same on the black body view and on the cold space view of the line LN, and on the black body view of the line LN+1.

As the ghost is not the only effect included in this variable (for example, there is also the noise), we have to be careful in the interpretation of these plots: it is not the exact amplitude of the ghost.

#### 4.6.4 Conclusion

All parameters impacting IASI spectral calibration are stable and within specifications.

IASI has a fully satisfactory spectral calibration. The L1B processing, consisting in the spectral shift correction, and the L1C processing, consisting in the ISRF removal, are working very well.



## 4.7 GEOMETRIC PERFORMANCES

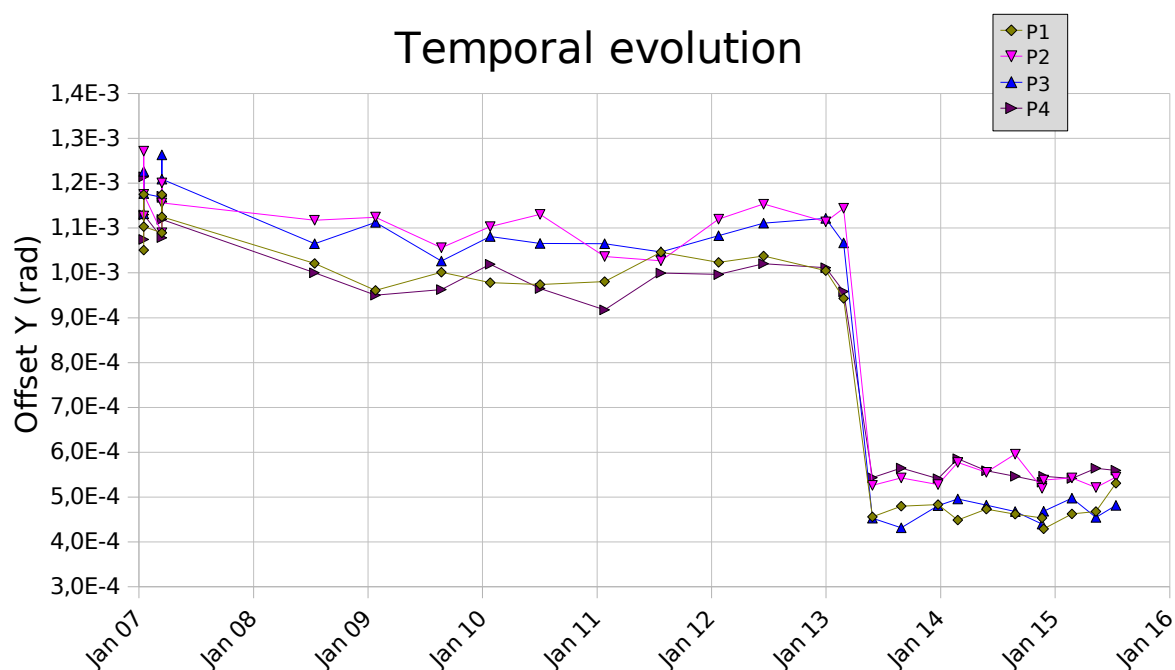
The geometric calibration is performed on ground (level 1 processing). Most of the analyses of geometric performances require being in external calibration mode.

Specifications are the following: the IIS/AVHRR co-registration has to be better than 0.3AVHRR pixel while the IIS/sounder co-registration has to be better than 0.8mrad.

### 4.7.1 Sounder / IIS co-registration monitoring

This monitoring is performed one time a year, generally around September for REVEX and march for mid-REVEX.

The sounder/IIS co-registration has been checked after the switch to IMS the redundant side. There is no change, the sonder/IIS coregistration error is lower than 100 $\mu$ rad (eq. 100m on ground).



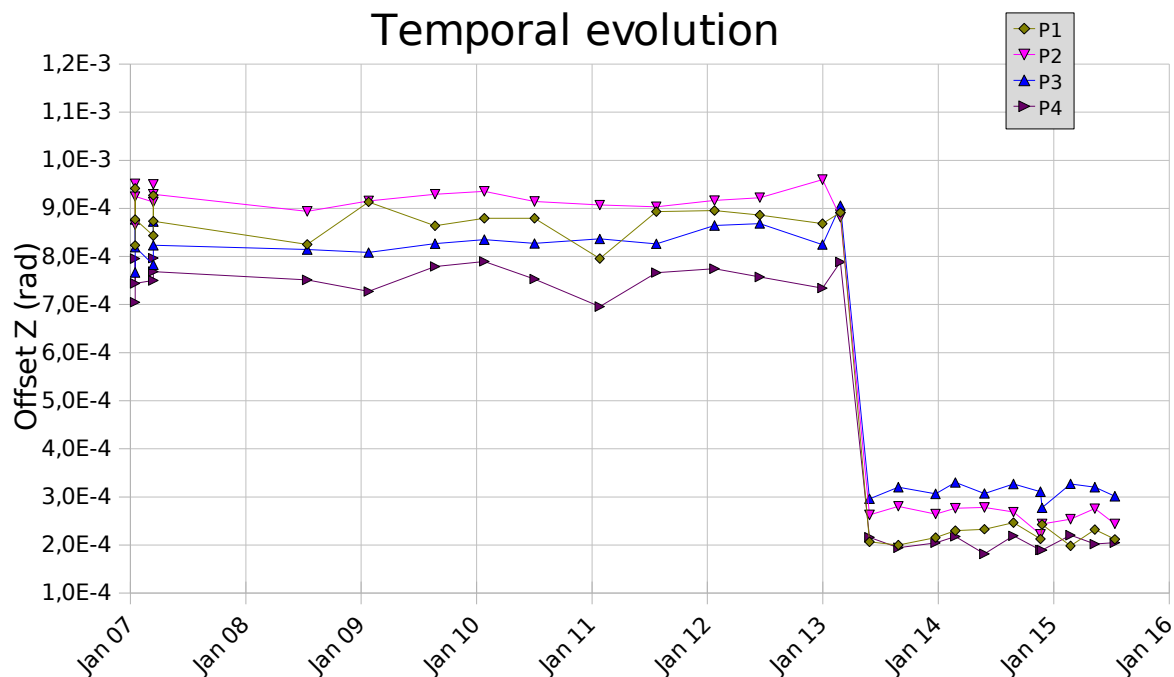


Figure 38 : Temporal evolution of the IIS/sounder co-registration for each sounder pixel.  
The offsets are reported in radian, Y and Z define an orthogonal referential linked to IIS

#### 4.7.2 IIS / AVHRR co-registration

The IIS/AVHRR co-registration is permanently estimated by the L1 processing chain.

Note that AVHRR channels 4 and 5 are within the IIS spectral filter. The spatial resolution of the IIS (0,7km) is close to AVHRR (1km).

The IIS/AVHRR offset guess in the ground segment configuration is used when the algorithm of correlation between IIS and AVHRR does not converge (typically over homogeneous scenes).

The following figures show a comparison of IIS-AVHRR offsets (GiacOffsetIISAvhrr) mean profiles.

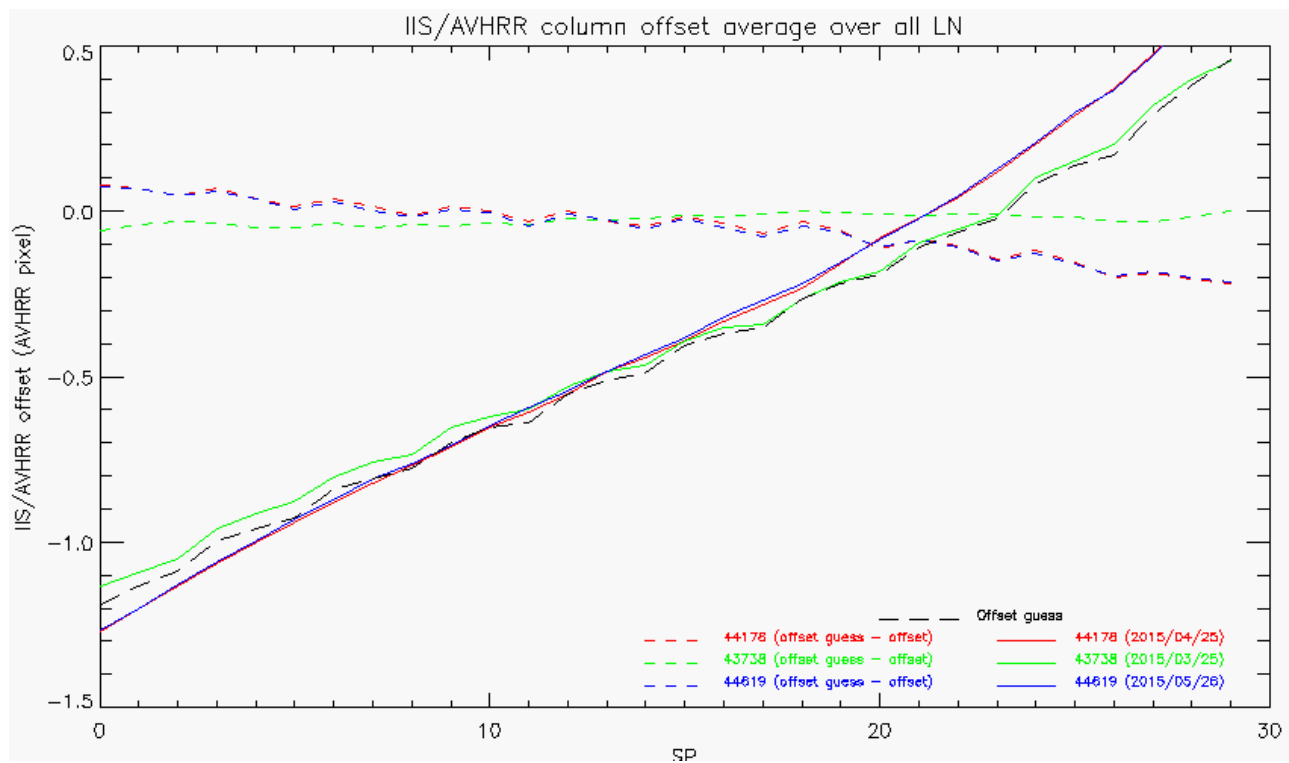


Figure 39 : Column offset (black) guess vs. column offset averaged over all lines (LN) as a function of the scan position (SP=SN), and orbit number

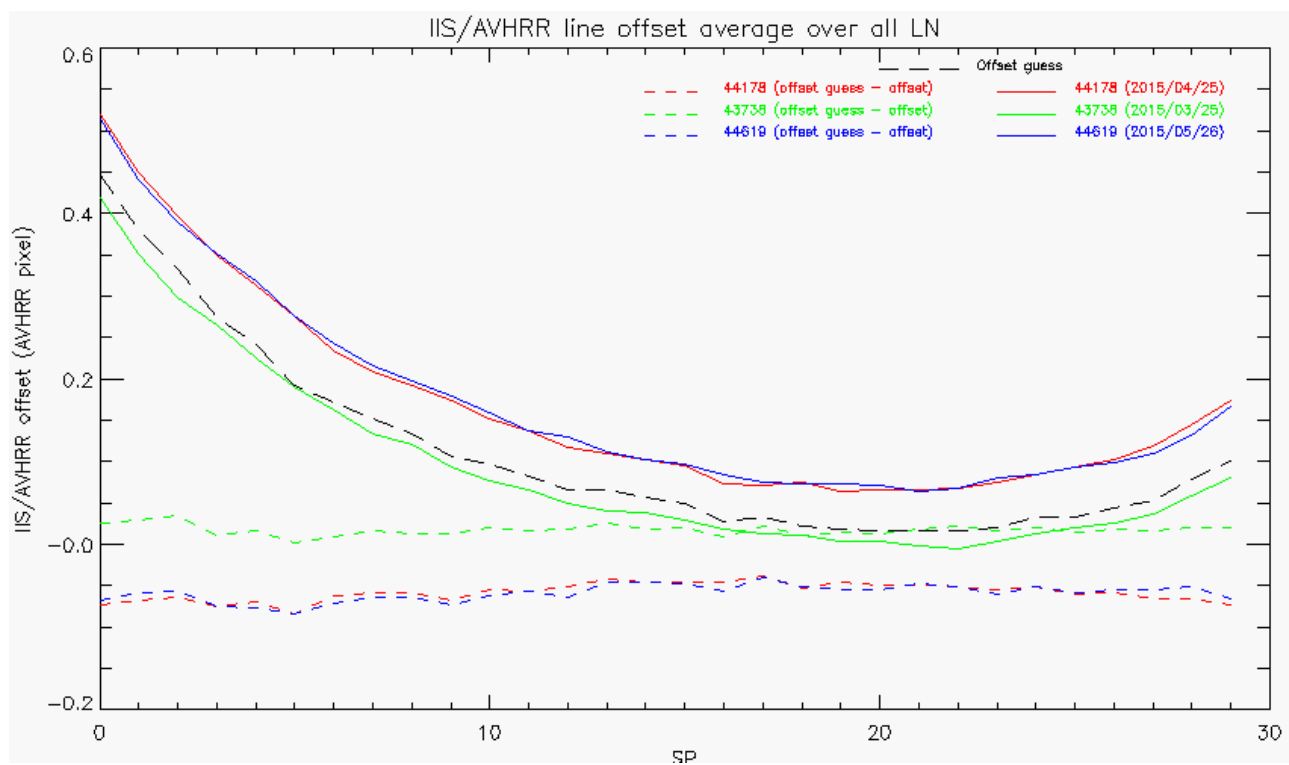




Figure 40 : Line offset guess (black) vs. line offset averaged over all lines (LN) as a function of the scan position (SP=SN), and the orbit number

Since the switch to IMS the redundant side, the commanding of the scan position has changed a bit, leading to a change of the IIS/AVHRR offset. For both across track and along track, the residuals between measured and IIS/AVHRR offset guess in the

		Doc n°: IA-RP-2000-4225-CNE Issue: 1.0 Date: 2017-09-27 Sheet: 52 Of: 63
--	---	---

ground segment configuration are lower than 0.2 AVHRR pixel for all viewing angles. This offset guess in the ground configuration will be updated in autumn 2015.



#### 4.7.3 Conclusion

The positions of IASI pixel are considered stable (apart from the change due to the switch to IMS redundant side) and well within specification.

IIS-sounder co-registration is stable at about 100 $\mu$ rad which is equivalent to 100m on ground (specification : < 0.8 mrad).

IIS-AVHRR offset is lower than two pixels and stable since the switch to IMS redundant side: less than 0.2 AVHRR pixels over three months (specification < 0.3 AVHRR pixel). The IIS-AVHRR offset guess in the ground configuration will be updated with his new value nevertheless.

IASI pixel centre location accuracy in AVHRR raster is around 300m. The geolocation of IASI pixels are thus considered well within specification (5 km).

		Doc n°: IA-RP-2000-4225-CNE Issue: 1.0 Date: 2017-09-27 Sheet: 53 Of: 63
---	---	---

## 4.8 IASI-A INTER-CALIBRATION WITH CRIS AND AIRS

The objective of the radiometric inter-calibration between IASI-A and CRIS and AIRS is to perform an external monitoring of the IASI performances and to ensure the consistency of the hyperspectral TIR sensors. A radiometric and spectral inter-calibration of IASI-B versus IASI-A is given in the IASI-B quarterly performance report. We aim here at checking the performance of the radiometric absolute calibration accuracy of 0.5K per IASI channel.

The inter-calibration is performed with the SIC software. The methodology is described in the SIC algorithm description [DA.2]. Roughly, the methodology is based on the construction of a database in which each data is the difference IASI-A - CRIS or IASI-A - AIRS over a common observation made by both sounders. “Common” means same place, same time and same viewing conditions so that the only difference is not geophysical but due to a calibration bias. Statistics over this database emphasize the radiometric biases. For IASI and CRIS or AIRS, the database is built with Simultaneous Nadir Overpasses, occurring at high latitudes. Each scene is a regional averaging of the soundings, with a spectral reduction in broad pseudo-bands.

### 4.8.1 IASI-A inter-calibration with CRIS

Figure 41 shows the mean and standard deviation of IASI-A - CRIS for one year of data. We see that IASI-A and CRIS are very well cross-calibrated, with biases lower or equal to 0.1K in absolute value (except for one pseudo-band).

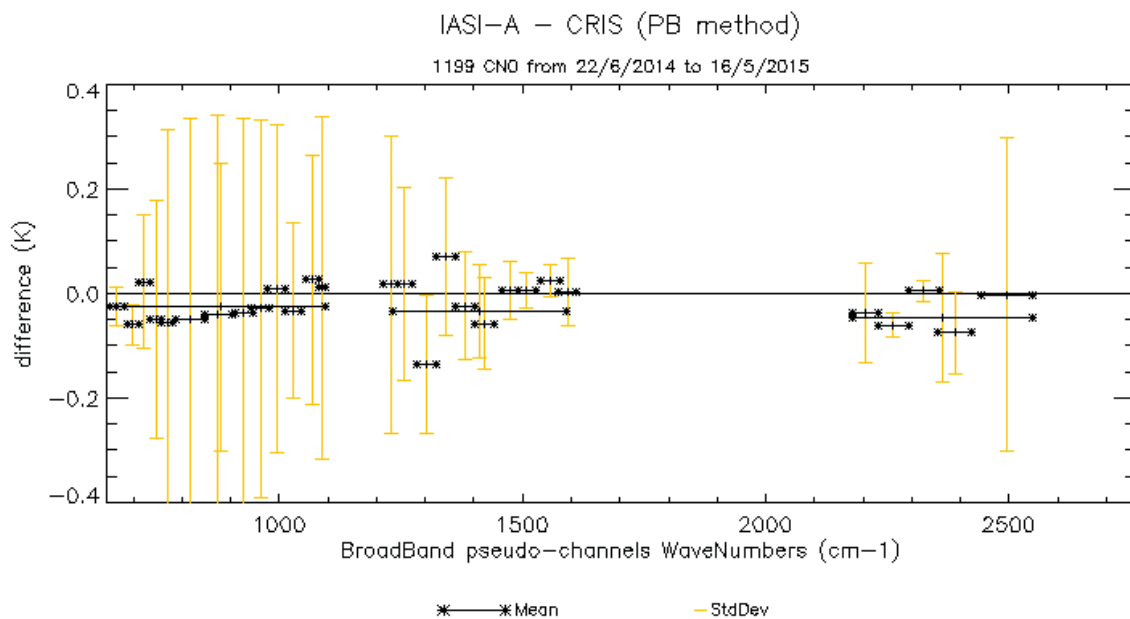


Figure 41 : Mean (black curve) and standard deviation (yellow) of the difference in brightness temperature IASI-A – CRIS

Figure 42 shows the temporal evolution of the three broadest pseudo-channels, corresponding approximately to the IASI bands 1, 2 and 3 (more precisely, to their overlapping with the CRIS coverage). We see that the difference between IASI-A and CRIS is stable with time, with slight variations in IASI B1. Note that some large temporal gaps may be encountered for IASI-A / CRIS, due to the orbital configuration and the tolerance in simultaneity, making some monthly means meaningless.

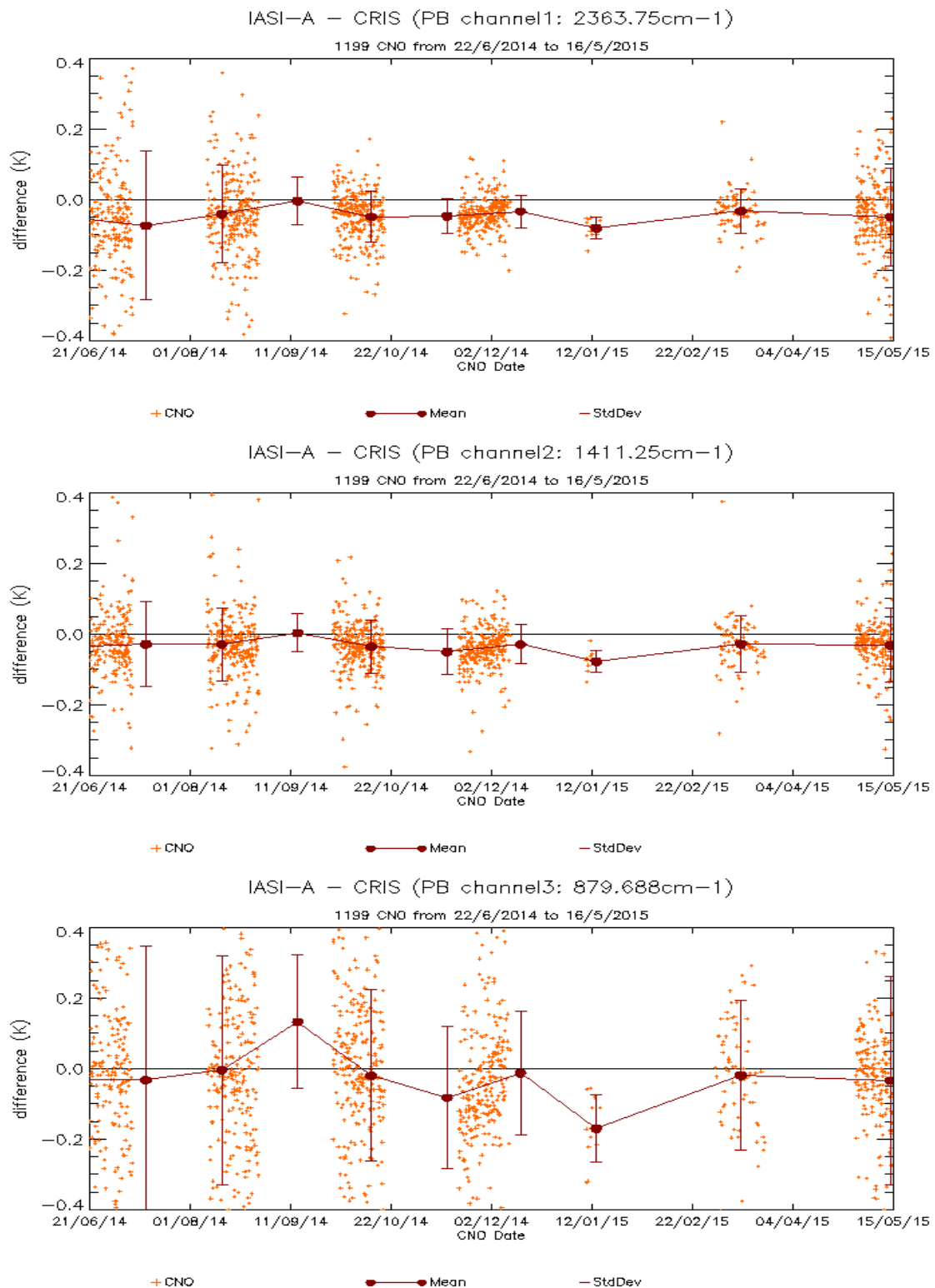


Figure 42 : Temporal evolution of the differences IASI-A – CRIS in brightness temperature over the approximate three IASI bands, with monthly means

#### 4.8.2 IASI-A inter-calibration with AIRS

Figure 43 shows the mean and standard deviation of IASI-A - AIRS for one year of data. We see that IASI-A and AIRS are very well cross-calibrated, with biases lower or equal to 0.1K in absolute value (except for one pseudo-band).

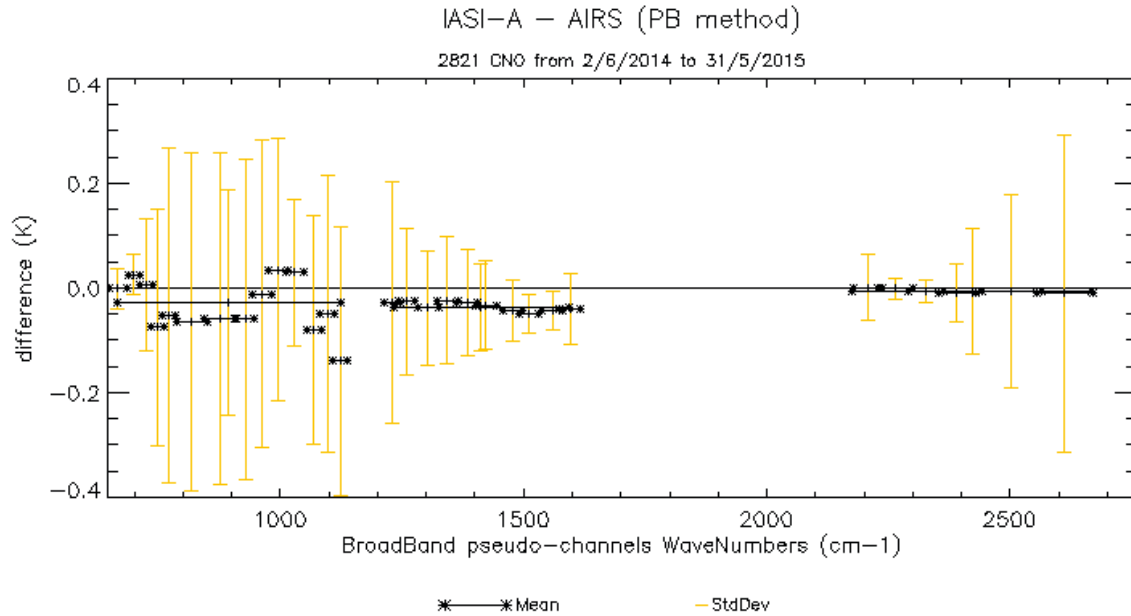
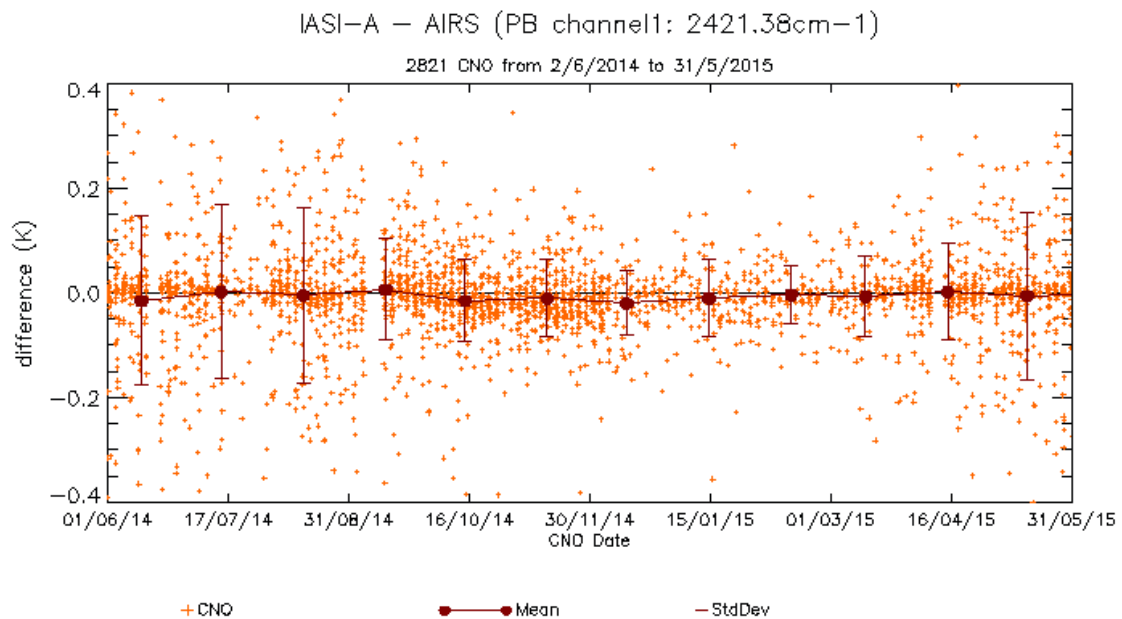


Figure 43 : Mean (black curve) and standard deviation (yellow) of the difference in brightness temperature IASI-A - AIRS.

Figure 44 shows the temporal evolution of the three broadest pseudo-channels, corresponding approximately to the IASI bands 1, 2 and 3 (more precisely, to their overlapping with the AIRS coverage). We see that the difference between IASI-A and AIRS is very stable with time, even more than IASI-A - CRIS. For IASI-A / AIRS no large temporal gaps are observed.



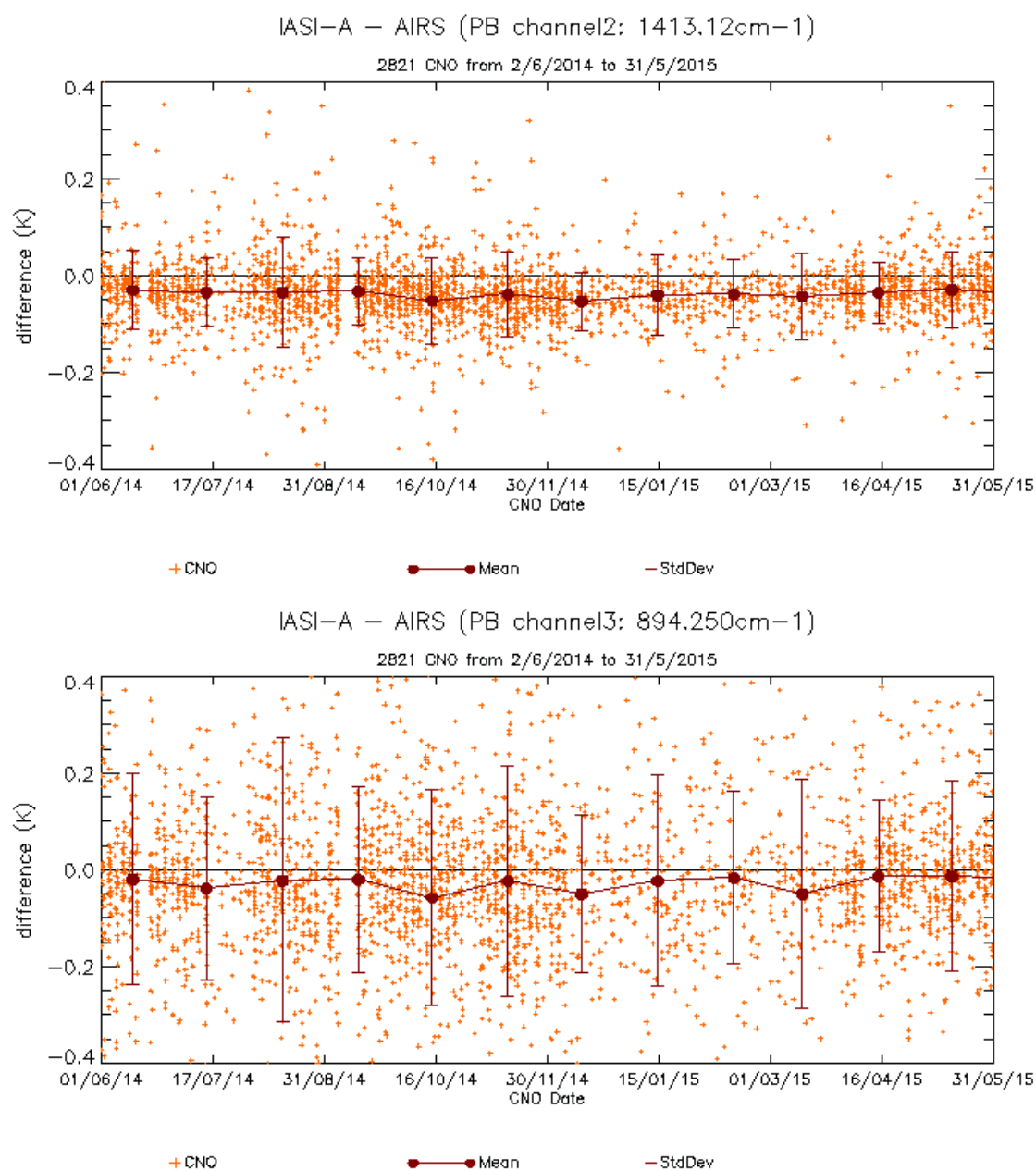


Figure 44 : Temporal evolution of the differences IASI-A – AIRS in brightness temperature over the approximate three IASI bands, with monthly means



## 4.9 IIS RADIOMETRIC PERFORMANCES

The main task of IIS is to insure a good relative positioning of IASI sounder pixels with respect to AVHRR. Its performances are studied each month using routine External Calibration data.

### 4.9.1 IIS Radiometric Noise Monitoring

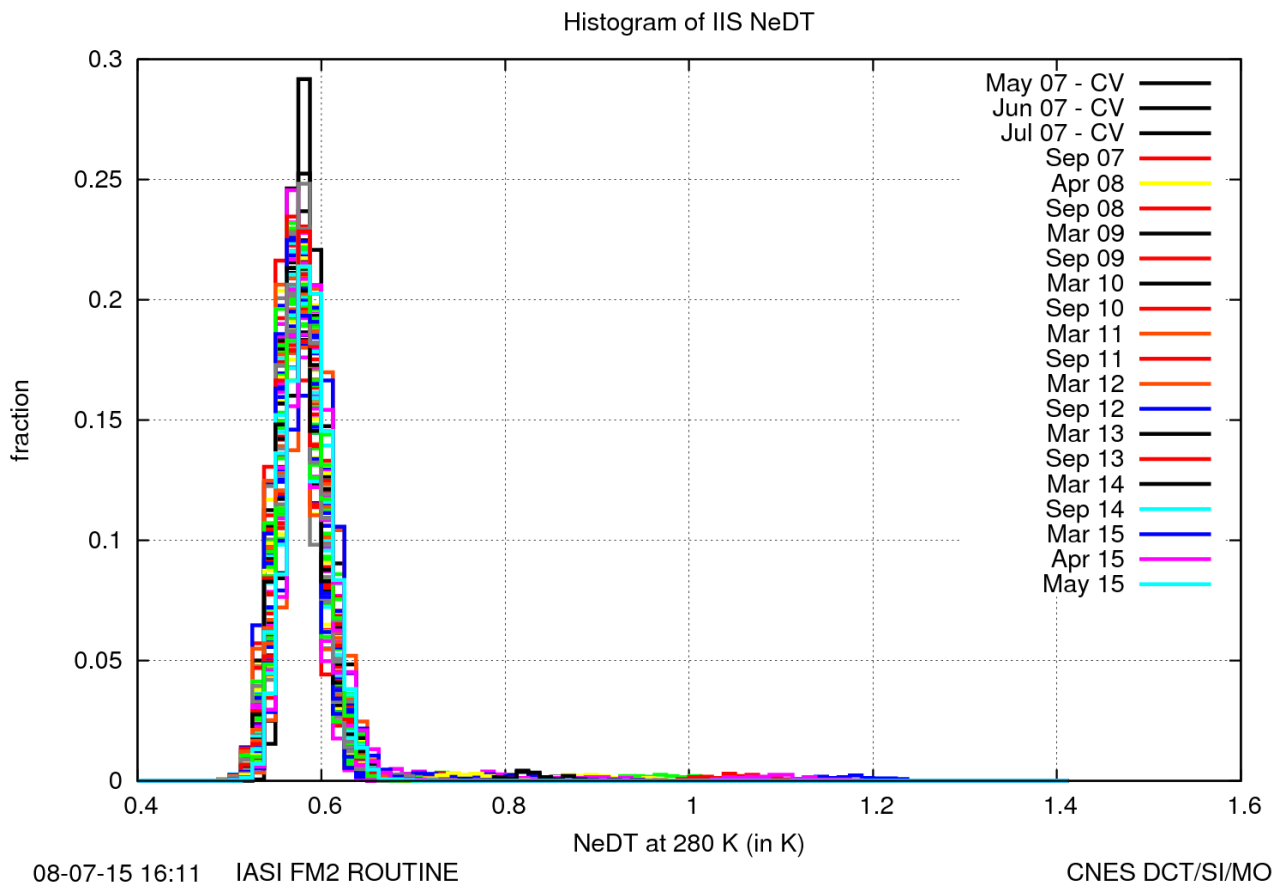




Figure 45 : Temporal evolution of the noise between start and end of the period

Radiometric noise of the IIS is very stable and lower than the specification of 0.8K.

		Doc n°: IA-RP-2000-4225-CNE Issue: 1.0 Date: 2017-09-27 Sheet: 58 Of: 63
--	--	---

#### 4.9.2 IIS Radiometric Calibration Monitoring

In order to assess the stability of IIS radiometric calibration, we follow the time evolution of slope and offset coefficients. Figure 46 shows a comparison of slope and offset coefficients matrix between start and end of the period.

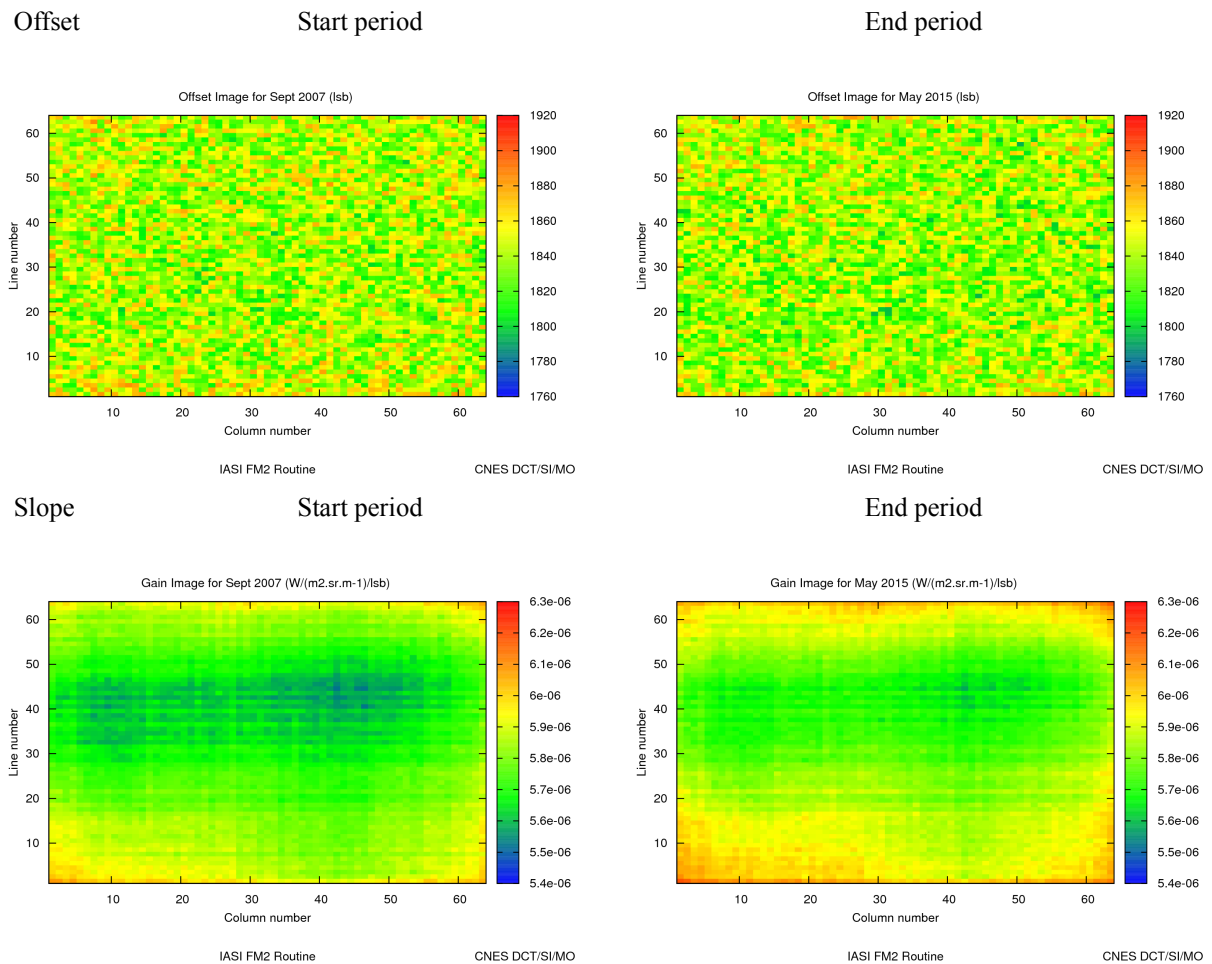
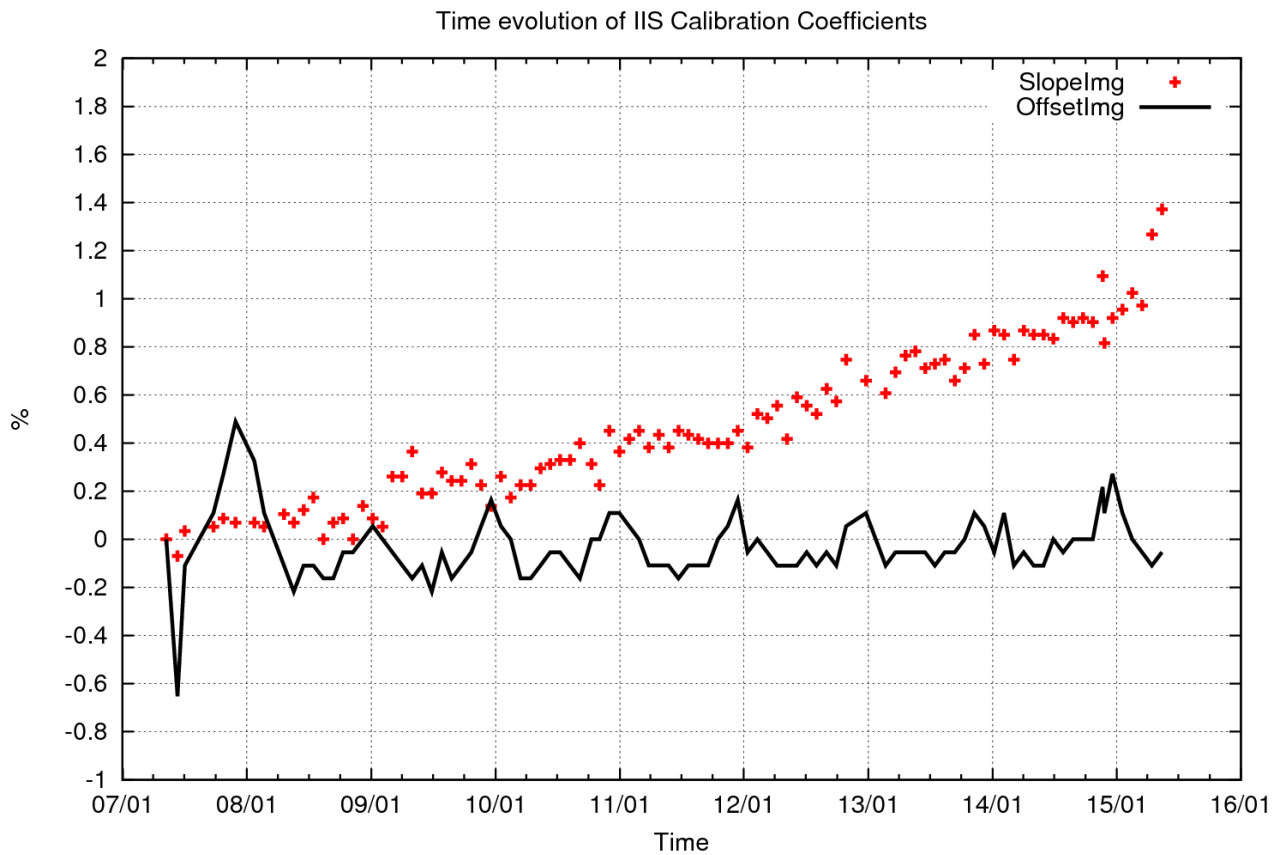


Figure 46 : Slope and offset coefficients matrix

The complete time series of average slope and offset coefficients is given in Figure 47.



08-07-15 16:11 IASI FM2 ROUTINE

CNES DCT/SI/MO

Figure 47 : Relative evolution in % of average of slope (red curve) and offset (black curve) coefficients

The offset coefficient is stable. The slope is slightly evolving (1,5% in 8 years). This evolution is likely to be linked with the slight evolution of IIS focal plan temperature.

The slope coefficient has increased a bit due to the switch to IMS redundant side.

The performances are nominal.

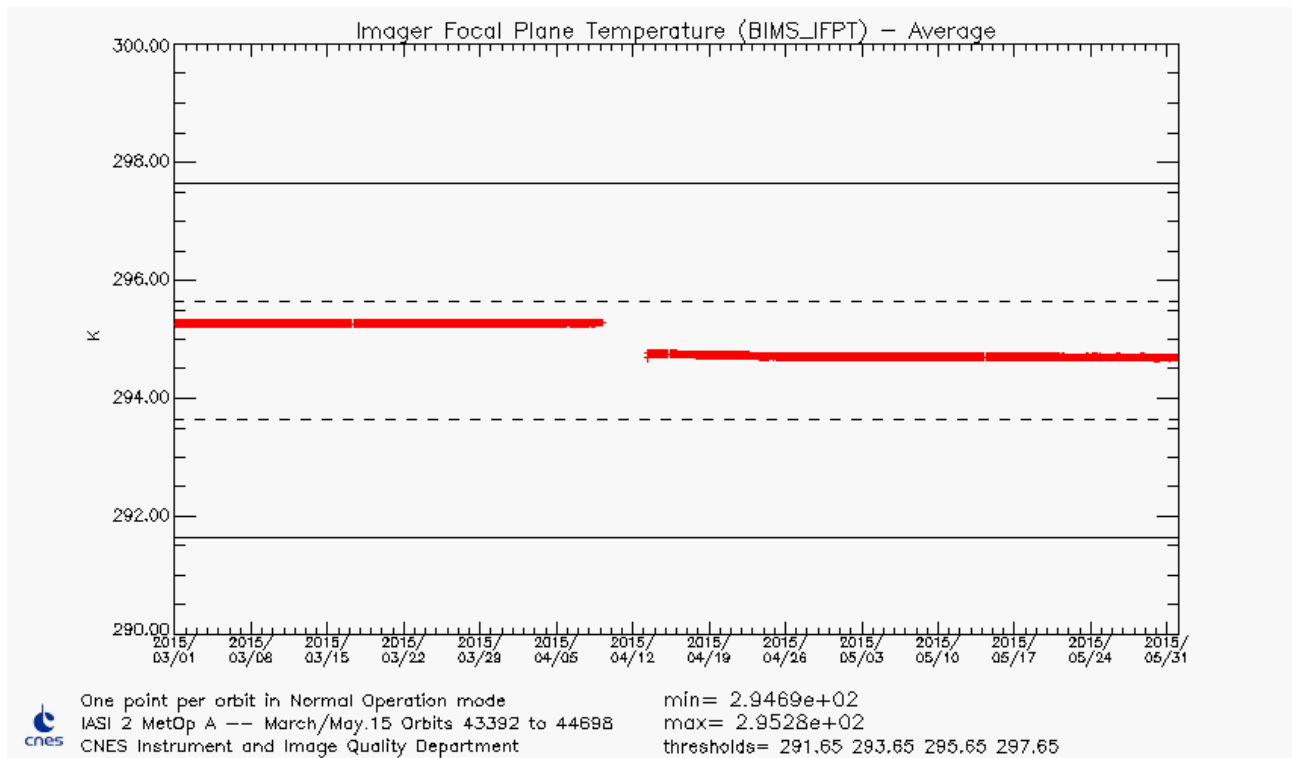




Figure 48 : IIS Focal Plane Temperature

Since the IMS B-side switch (9 to 13th April), we observe an increase of the imager focal plane temperature, maybe due to the change of temperature probe (uncertainty on its transfer function).

#### 4.9.3 Conclusion

The radiometric performance of IIS is well within specification. Since the IMS B-side switch (9 to 13th April), we observe a decrease of the imager focal plane temperature maybe due to the change of temperature probe, and the slope calibration coefficient has increased a bit but still within specification.

		Doc n°: IA-RP-2000-4225-CNE Issue: 1.0 Date: 2017-09-27 Sheet: 61 Of: 63
--	---	---

## 5 IASI TEC SOFTWARE AND INTERFACES

### 5.1 *IASI TEC EVOLUTION*

No evolution within the period.

Table 19 lists previous software evolutions.

IASI TEC software version	implementation	Comments
8.1	06 October 2011	Automatic downloads of L0 products from EUMETSAT FTP
8.2	12 April 2012	New version of product browser (handling IASI L0, L1C products and board configuration).
8.3	22 August 2012	Regularization version before IASI-B CAL/VAL CCAT replaced by CBST in TEC's logs
8.4	19 December 2013	New parameter SP_NV in SLT files Integration of board configuration generation tool (UTOPIE) Integration of LBR products management tool
8.5	19 November 2014	Monitoring of offset voltages from equalization images

*Table 19: IASI TEC at CNES Toulouse*



### 5.2 *SIC EVOLUTION*

A new version “3.3” of the software “SIC” was installed

This Table lists the recent evolutions of the software:

SIC software version	implementation	Comments
3.2	04/2014	Add of spectral inter-calibration, synthesis tool processed per days, new methods for CNO pre-selection, add of preselection for IASI/AIRS and IASI/CRIS, intercalibration with convolution method for IASI/CRIS
3.3	04/2015	New functionalities for data transfer. Improvement of CNO prediction and pre-selection. New parametrization for the synthesis tool. Automation of the software installation and deployment, IDL upgrade, correction of NCR

*Table 20: SIC at CNES Toulouse*

		Doc n°: IA-RP-2000-4225-CNE Issue: 1.0 Date: 2017-09-27 Sheet: 62 Of: 63
--	--	---

### 5.3 EUMETCAST INTERFACE

EUMETCast dissemination is used for Near Real Time data reception by IASI TEC at CNES, Toulouse. Each orbit, L1 ENG, L1 VER, and AVHRR 1B products are received under continuous series of 3 minutes PDU. Full dumps are reconstructed by the EUMETCAST terminal and pushed to a IASI TEC server. Since August 2012, NPP/CrIS PDU are also received to perform inter-comparison with IASI.

In case of failure of the prime EUMETCAST station, products remain available several days on a redundant station.

The behaviour of the EUMETCAST reception is nominal.

The following table lists the recent modifications in the EUMETCAST configuration:



Date	EUMETCAST configuration
29/03/2011	End of IASI L0 dissemination via EUMETCAST
03/08/2011	Hardware and software upgrade of the prime station
04/12/2011	Hardware and software upgrade of the back-up station
13/07/2012	Software patch to correct an anomaly concerning AVHRR files (reception of 0 byte files from EUMETCAST)
24/08/2012	Modification of EUMETCAST configuration to receive NPP/CrIS data
03/2013	“PARALLEL_RECONSTRUCTIONS” set to 3 to avoid missing PDU problems
09/2013	“RECONSTRUCTION TIME-OUT” set to 90 to avoid missing PDU problems
09/12/2014	Antenna repointing and update of reception parameters

*Table 21: EUMETCAST configuration at CNES Toulouse*

### 5.4 FTP INTERFACE

Since March 29<sup>th</sup> of 2011, IASI L0 full dumps are available in Near Real Time on a EUMETSAT FTP server. The IASI TEC software automatically downloads products from the EUMETSAT FTP server.

The reception of L0 products at IASI TEC is nominal.

		Doc n°: IA-RP-2000-4225-CNE Issue: 1.0 Date: 2017-09-27 Sheet: 63 Of: 63
--	---	---

## 6 **CONCLUSION AND OPERATIONS FORESEEN**

Please visit <http://smc.cnes.fr/IASI/> to get IASI news.

### 6.1 ***SUMMARY***

The IASI FM2 instrument is fully operational.

The instrument configuration is the nominal one.

The main events are :

- IP manoeuvre #35 on 28 April 2015
- IASI Instrument Management System switch to B side from 9 to 13 April 2015
- Auto-recovery after DMC checksum error on 2 April 2015

### 6.2 ***SHORT-TERM EVENTS***

- Update of scan mirror reflectivity in the operational ground segment in June 2015
- Update of IIS/AVHRR offset guess in the operational ground segment in autumn 2015
- Moon avoidance on 2-3 September, 1 October and on 30 November 2015

### 6.3 ***OPERATIONS FORESEEN***

- IP Manoeuvre #36 on 15 July 2015
- Out of Plane Manoeuvre (Double Burn) #37 - #38 on 14 and 28 October 2015

*End of document*